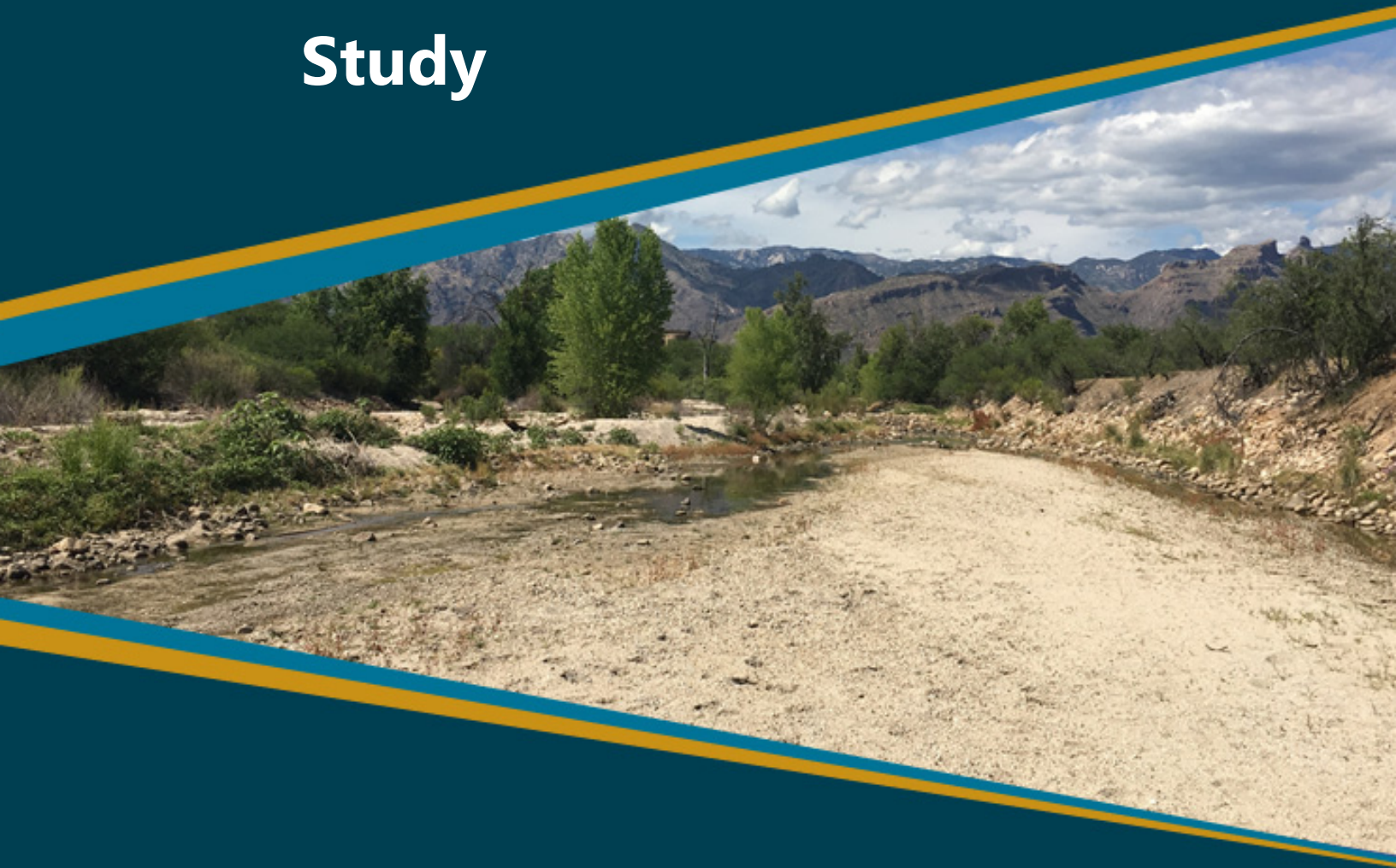




— BUREAU OF —
RECLAMATION

Technical Memorandum No ENV-2020-056

Hydroclimate Analysis Lower Santa Cruz River Basin Study



Mission Statements

The mission of the Department of the Interior is to conserve and manage the Nation's natural resources and cultural heritage for the benefit and enjoyment of the American people, provide scientific and other information about natural resources and natural hazards to address societal challenges and create opportunities for the American people, and honor the Nation's trust responsibilities or special commitments to American Indians, Alaska Natives, and affiliated island communities to help them prosper.

The mission of the Bureau of Reclamation is to manage, develop, and protect water and related resources in an environmentally and economically sound manner in the interest of the American public.

Acknowledgements

The authors gratefully acknowledge the input and review of members of the Lower Santa Cruz River Basin Study Project Team, led by Eve Halper of Reclamation and Kathy Chavez of Pima County. Christopher Castro and Hsin-I Chang at the University of Arizona contributed dynamically downscaled climate analysis and expert review. Tom Pruitt with Reclamation provided Sac-SMA modeling and technical support.

Cover Photo: Sabino Creek in May (Reclamation/Bearup)

BUREAU OF RECLAMATION
Technical Service Center, Denver, Colorado
Technical Memorandum No. ENV-2021-35

Lower Santa Cruz River Basin Study Hydroclimate Analysis

Prepared for:

Phoenix Area Office
Lower Colorado Region
Bureau of Reclamation

Prepared by:

Water, Environmental and Ecosystems Division
Water Resources Engineering and Management Group (86-68210)

Lindsay Bearup, PhD, PE - Civil Engineer

Subhrendu Gangopadhyay, PhD, PE - Civil Engineer

Peer reviewed by:

Kristin Mikkelsen, PhD – Civil Engineer

Abbreviations and Acronyms

°F	degrees Fahrenheit
ADWR	Arizona Department of Water Resources
AR5	5 th Assessment Report
AZMET	Arizona Meteorological Network
CAP	Central Arizona Project
CBRFC	Colorado Basin River Forecast Center
CMIP5	Coupled Model Intercomparison Project phase 5
ET	evapotranspiration
GCM	Global Climate Model
IPCC	Intergovernmental Panel on Climate Change
km	kilometer
LOCA	Localized Constructed Analogs
LR	low resolution
LSCR	Lower Santa Cruz River
MAP	mean areal precipitation
MAT	mean areal temperature
MPI-ESM	Max-Planck-Institute Earth System Model
MR	mid resolution
NA CORDEX	North American Coordinated Regional Downscaling Experiment
NAM	North American Monsoon
NOAA	National Oceanic and Atmospheric Administration
NWS	National Weather Service
PET	Potential Evapotranspiration
PRISM	Parameter-elevation Regressions on Independent Slopes Model
RCM	Regional Climate Model
RCP	Representative Concentration Pathway
RSD	relative standard deviation
Sac-SMA	Sacramento Soil Moisture Accounting
Study	Lower Santa Cruz River Basin Study
TAMA	Tucson Active Management Area
WGIII	Working Group III
WRF	Weather Research and Forecasting Model
WRF-MPI	Max-Planck-Institute Earth System Model downscaled using WRF

Contents

	Page
Executive Summary	vii
Study Formulation.....	vii
Downscaling	ix
Weather Generator	x
Summary: Temperature and Precipitation Change by Season.....	x
Surface Hydrologic Modeling.....	xii
Surface Hydrology Results:.....	xii
1. Introduction	1
2. Climate Analysis.....	3
2.1. Current Climate.....	3
2.2. Climate Scenarios.....	5
2.2.1. Downscaling Methods.....	7
2.2.2. Future Climate Scenarios.....	8
2.3. Projected Changes in Annual Precipitation and Temperature Climatology	12
2.4. Climate Metrics	15
2.4.1. Climate Metric 1: Changes in Intensity and Frequency of Future Precipitation and Temperature.....	16
2.4.2. Climate Metrics 2 and 3: Changes in Seasonality.....	16
2.4.3. Seasonality Results	19
2.5. Climate Summary for Stakeholders	23
3. Weather Generator.....	25
3.1. Development and methodology.....	25
3.2. Validation	27
3.3. Results	27
4. Surface Water Modeling.....	35
4.1. Sac-SMA Model.....	35
4.1.1. Description	35
4.1.2. Input Development	37
4.2. Future Surface Water Discharge	37
4.2.1. Change in Seasonal Streamflow	37
4.2.2. Change in Dry Days.....	42
4.3. Soil Moisture.....	44
4.4. Evapotranspiration.....	48
5. Summary.....	50
5.1. Results	50
5.1.1. Seasonal Length and Timing.....	51
5.1.2. Surface Hydrology—Changes in 30-Year Median Streamflow.....	51
5.2. Conclusion	52
6. References	53
Appendix A—Supporting Climate Figures.....	56
Appendix B—Weather Generator Validation Figures.....	57
Appendix C—Supporting Surface Water Modeling Figures.....	59

Figures

Figure 1 – Lower Santa Cruz River Basin study area and modeling boundaries. 2

Figure 2 – July PRISM temperature and precipitation 30-year (1981-2010) normals..... 4

Figure 3 – Rainy day and total monthly precipitation at the Tucson Airport station
 from 1981-2010..... 5

Figure 4 – Emissions of carbon dioxide (CO₂) alone in the RCPs and the associated scenario
 categories used in the IPCC Working Group III..... 6

Figure 5 – PRISM gridded precipitation scaled to the approximate resolution of
 A) LOCA and B) a sample GCM..... 7

Figure 6 – Historical (1970-1999) daily rainy day precipitation averaged over the
 surface water model boundary area for the Sac-SMA calibration dataset,
 best-case scenario simulation, and worse-case scenario simulation..... 11

Figure 7 – Timeseries of the change in total annual precipitation (inches) and average
 annual temperature (°F) relative to the respective 30-year average of
 simulated historical values for the best- and worse-case climate scenarios. 13

Figure 8 – Change in total annual precipitation averaged over the surface water
 model boundary area (inches per year) and average annual temperature (°F)
 for the best- (and worse-case averaged over the case scenarios for the
 2030s and 2060s. 14

Figure 9 – Conceptual diagram of seasonality in the LSCR basin. 16

Figure 10 – Historical (1950-2009) dry spell statistics by month of start date from the
 Tucson Airport weather station..... 19

Figure 11 – Distribution of seasonal onset day of the year for the best- and worse-case
 scenarios..... 21

Figure 12 – Distribution and statistics of monsoon season lengths (in days) by period
 for the best-case and worse-case climate scenarios..... 22

Figure 13 – Same as Figure 12 but for the winter season lengths..... 22

Figure 14 – Same as Figure 12 but for the dry season lengths..... 22

Figure 15 – Seasonality for each year of simulation for the Sac-SMA calibration
 dataset, and the best-case, and worse-case climate scenarios..... 23

Figure 16 – Model simulated temperature averaged over the surface water model
 boundary area presented as a 30-year averaged seasonal mean and
 averaged precipitation for the same area presented as a 30-year averaged
 seasonal total for each period (colors), season (x-axis), and climate scenario. 28

Figure 17 – Distributions of extreme daily temperatures, averaged over the surface water
 model boundary area, by period and season..... 30

Figure 18 – Boxplot of extreme daily precipitation by season, period, and climate scenario.. 31

Figure 19 – Distribution of extreme daily precipitation by season, period, and climate
 scenario..... 33

Figure 20 – Sac-SMA elevations by elevation zone for each labeled subbasin..... 36

Figure 21 – Median of the ensemble 30-year average dry season total streamflow
 from the modeled historical period for each scenario, and projected change
 from historical in streamflow for the best- and worse-case climate scenarios. 38

Figure 22 – Similar to Figure 21 but for the monsoon season..... 39

Figure 23 – Similar to Figure 21 but for the winter season..... 40

Figure 24 – The number of modeled historical dry days per month under the worse-case scenario for each Sac-SMA subbasin.....43

Figure 25 – Change in the number of dry days per month in the near future for each subbasin under the worse-case climate scenario.....43

Figure 26 – Change in the number of dry days per month in the far future for each subbasin under the worse-case scenario.....44

Figure 27 – Monthly averaged worse-case scenario soil moisture (inches) in each compartment of the Sac-SMA Cienega Creek lower elevation zone.....46

Figure 27 – Ensemble median, monthly average of the total tension water (sum of upper and lower soil zones) under the worse-case climate scenario for: a) modeled historical tension water in inches, b) near future change, and c) far future change as a percent relative to the historical period.....47

Figure 28 – Evapotranspiration (ET) under the worse-case climate scenario for a) modeled historical ET in inches, b) near future change, and c) far future change in ET as a percentage.....49

Tables

Table 1 – Summary of Datasets Used to Define Climate Scenarios 9

Table 2 – Statistics of Rainy-Day Precipitation by Season, Scenario, and Period, 11

Table 3 – Median Date of Seasonal Transition Defined by Climate Metrics.....20

Table 4 – Summary of Projected Basin-Averaged Future Precipitation and Temperature Relative to the its Respective Simulated Historical Period (1970 – 1999).....24

Table 5 – Statistics of the Weather Generated Ensemble of Averaged Temperature for the surface water model boundary area.....29

Table 6 – Statistics of Extreme Precipitation from the Weather Generator Ensemble.....32

Table 7 – Statistics of Period-Averaged Seasonal Total Streamflow Ensembles for Each Scenario, Period, Season, and Selected Subbasins.....41

Executive Summary

This Technical Memorandum covers the climate change and surface water modeling elements of the Lower Santa Cruz River Basin Study (Study). The Study’s goal is to identify where physical water resources are needed to mitigate supply-demand imbalances and to develop strategies to improve water reliability for the municipal, industrial, agricultural and environmental sectors within the Tucson Active Management Area (TAMA) (see Figure ES-1). However, for the purposes of evaluating changes to runoff and streamflow, this analysis focused on the extent of the surface watershed area contributing flow to the TAMA, as delineated by the Sacramento Soil Moisture Accounting Model. We refer this area, which is shaded blue in Figure ES-1, as the “surface water model boundary area” throughout the report. For reference, summary climate change statistics are provided for the area of the TAMA and the Tucson Metro Area Public Forecast Zone, as defined by the National Weather Service (see Figure ES-1).

Study Formulation

The Study’s Project Team, which represents the cost-share partners, made several key decisions that shaped this hydroclimate analysis. First, it chose to simplify the analysis and concentrate on the range of risks to water users by examining two climate scenarios. This approach contrasts with similar Reclamation Basin Studies that have analyzed three to five separate climate scenarios.

For this Study, the Project Team requested a “best-case” future climate, a scenario in which action is taken to reduce the rate of worldwide greenhouse gas emissions and thus represents conditions under which a minimum of adaptation would be necessary. On the opposite end of the range, they requested a “worse-case” climate scenario, where greenhouse gas emissions continued to increase, and the impacts would be on the high end of the range. The use of the term “worse-case” emphasizes that while this scenario represents greater impacts than the “best-case,” it does not describe the most extreme possible outcomes of climate change. More detail on the emissions scenarios used in this Study is provided in Section 2.2. Climate Scenarios.

**Lower Santa Cruz River Basin Study
Hydroclimate Analysis**

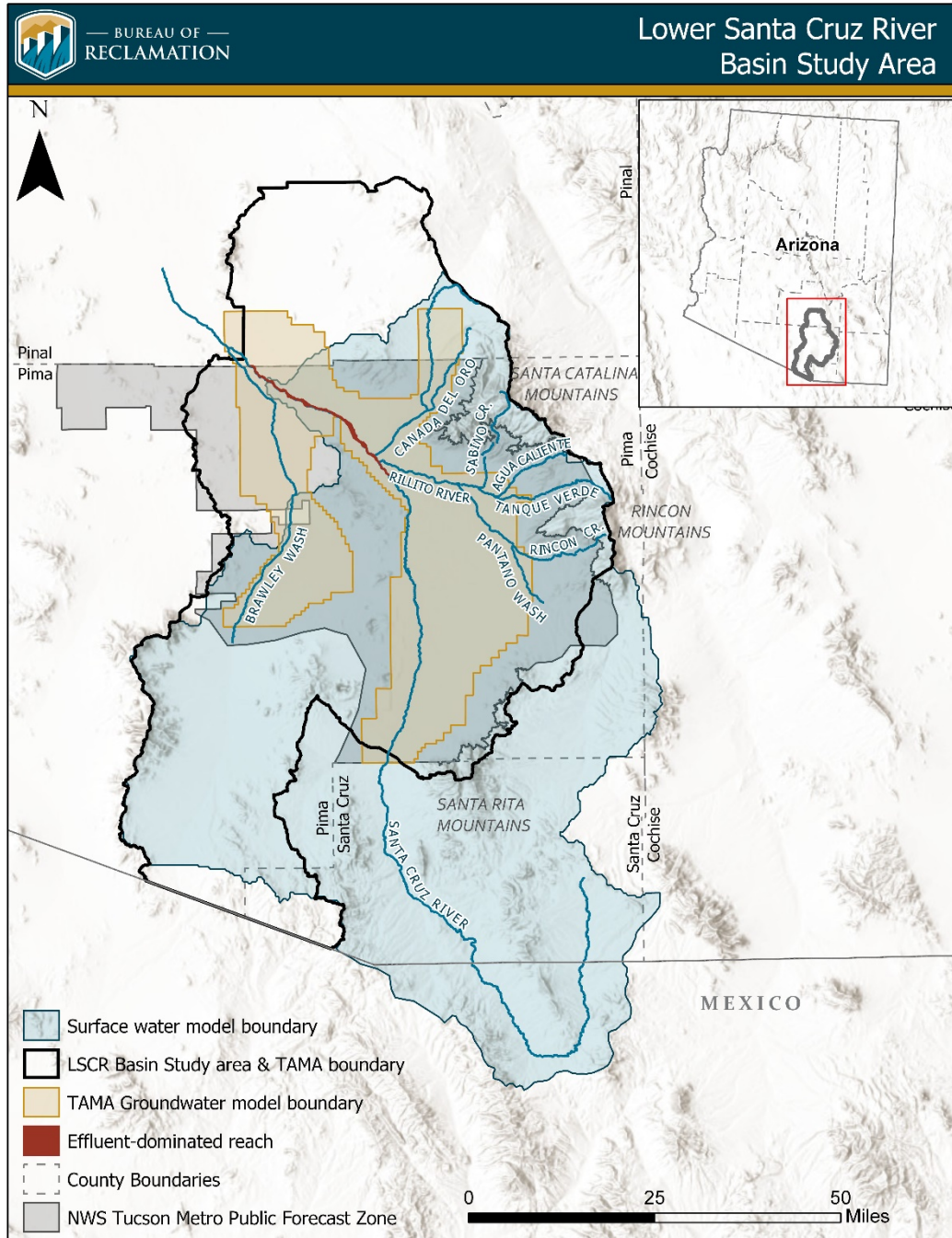


Figure ES-1. Lower Santa Cruz River Basin study area and modeling boundaries.

Downscaling

The output of Global Climate Models (GCM) is too coarse to use in an analysis of basin-scale hydrology. A process called “downscaling” must be applied to the GCM output to infer additional spatial detail. Statistical downscaling is a commonly used technique, and the statistically downscaled output of many GCMs, using a variety of emissions scenarios, are readily available to researchers. To date, all Reclamation Basin Studies have employed statistically downscaled climate projections.

While statistically downscaled climate projections are computationally straightforward and readily available, they are constrained by their reliance on historical observations to project the future. In other words, this technique assumes that the range and distribution of hydrologic events that have occurred in the past will be maintained in the future. In fact, climate scientists have observed that the future variability of hydrologic processes may be fundamentally different from the past (Milly et al., 2008).

To account for this risk, the Project Team requested the inclusion of a climate projection that used a physically based method of downscaling, called dynamical downscaling. Dynamical downscaling uses the GCM output as the input to a Regional Climate Model (RCM) that simulates atmospheric processes that take place at a finer scale (in this case, 25 kilometers). Thus, it can project conditions outside of the historical climate record.

The southeastern Arizona climate is highly seasonal, with two distinct precipitation regimes. The monsoon season is characterized by short, intense, and highly local precipitation that occurs in the late summer and early fall. Precipitation events in the fall and winter are more sustained and widespread, but less intense. After the winter rains, the region experiences a period of low to no precipitation in the dry season before the start of the next monsoon season.

A review of available dynamically downscaled GCMs showed that the best simulated monsoon timing in the study area was from the low resolution (LR) Max-Planck-Institute Earth System Model (MPI-ESM-LR; Giorgetta et al., 2013), run downscaled using the Weather Research and Forecasting Model (WRF). We refer to this downscaled simulation as “WRF-MPI” throughout this report. From a local water resource manager’s perspective, the onset date of the monsoon is a critical consideration. Only the higher emissions scenario was available for this GCM/RCM combination.

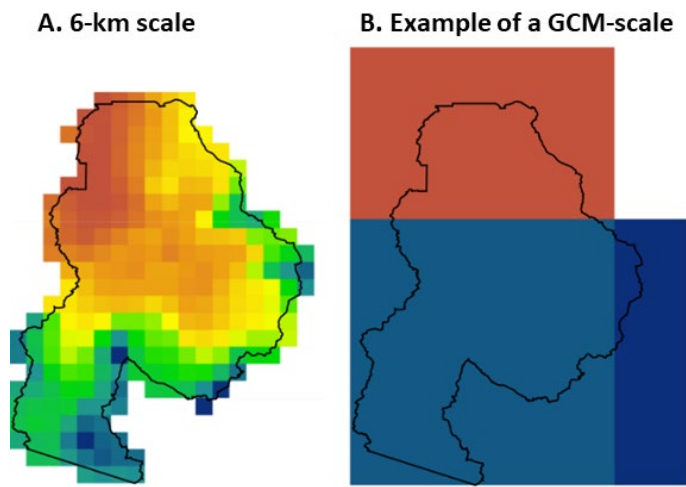


Figure ES-2. Example of resolutions from a downscaled projection (left) and a global climate model projection (right). These use the same data.

Lower Santa Cruz River Basin Study Hydroclimate Analysis

Without a WRF-MPI simulation available for the best-case climate scenario, the Study uses a statistically downscaled MPI-ESM medium resolution GCM output. This GCM is the same model used for the worse-case scenario, but using the run identified as mid resolution (MR). This projection predicts a future that is wetter and cooler than the worse-case scenario.

Due to the natural variability of the climate, it was necessary to compare time periods, rather than individual years, to detect changes in precipitation and temperature. The National Weather Service uses a period of thirty years to calculate a “climate normal.” Similarly, this analysis compares simulations of a base historical period (1970- 1999), to a “near future” period of 2020-2049, also referred to as the “2030s”, and a “far future” period of 2050-2079, or “2060s”. While the groundwater modeling in the Study extends to 2060 to align with the conditions in Reclamation’s Colorado River Basin Study, the hydroclimate analysis was not restricted by assumptions on Colorado River operations. See Table 1 for a summary of the emissions scenarios, downscaling techniques and model specifications used in this analysis.

Weather Generator

In addition to accounting for a range of risks, Project Team members supported an analysis that could simulate the considerable variability and seasonality characteristic of the southeastern Arizona climate. For this analysis, staff from Reclamation’s Technical Service Center developed a three-season “weather generator.” A weather generator is a computer program that produces large numbers (ensembles) of, in this case, precipitation and temperature time series. The distribution of values within the ensemble represents the variability of a system. This weather generator simulated the three distinct seasons: monsoon, winter wet, and dry. The weather-generated ensembles for the best- and worse-case scenarios were used as input to a surface hydrology model to estimate the future distribution of streamflows.

Summary: Temperature and Precipitation Change by Season

Table ES-1 summarizes the climate analysis. Analyses of changes to other key climate metrics, such as the onset and length of the monsoon and winter wet periods, are described in Section 2.4.3. Seasonality Results

Table ES-1. Summary of Projected Basin-Averaged Future Precipitation and Temperature Relative to its Respective Simulated Historical Period (1970 – 1999).

Geography	Statistic	Best- Case 2030s	Best- Case 2060s	Worse- Case 2030s	Worse- Case 2060s
Tucson Active Management Area	Change in Total Annual Precipitation	0.40"	-0.50"	-4.44"	-3.73"
Tucson Metro Public Forecast Zone	Change in Total Annual Precipitation	0.28"	-0.44"	-4.47"	-3.77"
Surface Water Model Boundary Area	Change in Total Annual Precipitation	0.32"	-0.85"	-4.34"	-3.90"
	Change in Average Monsoon Precipitation	0.80"	-0.87"	-2.38"	-1.57"
	Change in Average Winter Precipitation	-0.21"	0.57"	-2.25"	-2.38"
	Precipitation RSD* compared to Historical: Best = 20.3%, Worse = 17.3%	21.6%	28.5%	18.9%	30.4%
Tucson Active Management Area	Change in Average Annual Temperature	2.92°F	3.81°F	3.36°F	5.07°F
Tucson Metro Public Forecast Zone	Change in Average Annual Temperature	2.88°F	3.77°F	3.34°F	5.05°F
Surface Water Model Boundary Area	Change in Average Annual Temperature	2.94°F	3.83°F	3.41°F	5.12°F
	Change in Average Dry Season Temperature	2.59°F	2.31°F	3.44°F	3.34°F
	Change in Average Monsoon Temperature	1.96°F	3.52°F	4.24°F	5.81°F
	Change in Average Winter Temperature	1.88°F	1.85°F	2.45°F	3.20°F

*Relative standard deviation (RSD) is calculated by normalizing the standard deviation to the mean of the 30-year period and presented as a percentage.

Surface Hydrologic Modeling

Downscaled GCM output is the input to the weather generator, which produced separate ensembles of “best-case” and “worse-case” precipitation and temperature time series. These ensembles then serve as the input to a surface hydrology model called the Sacramento Soil Moisture Accounting Model (Sac-SMA). Sac-SMA simulates the processes of surface runoff, infiltration, and evapotranspiration. It is used by the National Weather Service’s Colorado River Forecast Center to model floods in the Study area. The model was calibrated for the period of 1970-1999, aligning with the base historical period of the climate change analysis.

Use of the Sac-SMA model involved modeling several of the upstream basins outside of the Study area, especially to the south and east (Figure ES-1).

Surface Hydrology Results:

The best-case scenario projects overall streamflow increases in the monsoon and winter seasons through the 2030s and 2060s. The worse-case scenario features large streamflow decreases for the monsoon and winter seasons in the 2030s, which moderate in the 2060s. More detail is provided in Section 4.2. However, even under the best-case scenario, many streams may experience an increase in the number of dry days due to increased temperatures (see Appendix C) and changes in precipitation event characteristics. The worse-case scenario predicts an increase in the number of dry days for almost all streams in the Study area. Figure ES-3 illustrates this by using three charts:

- The number of dry days over the course of the year for each of the streams in the Sac-SMA model domain, for the historical period (1970 – 1999).
- The change in dry days by stream for the worse-case in 2030s, relative to the historical period.
- The change in dry days by stream for the worse-case in 2060s, relative to the historical period.
- Changes in soil moisture generally mirror changes in precipitation under future climate scenarios.

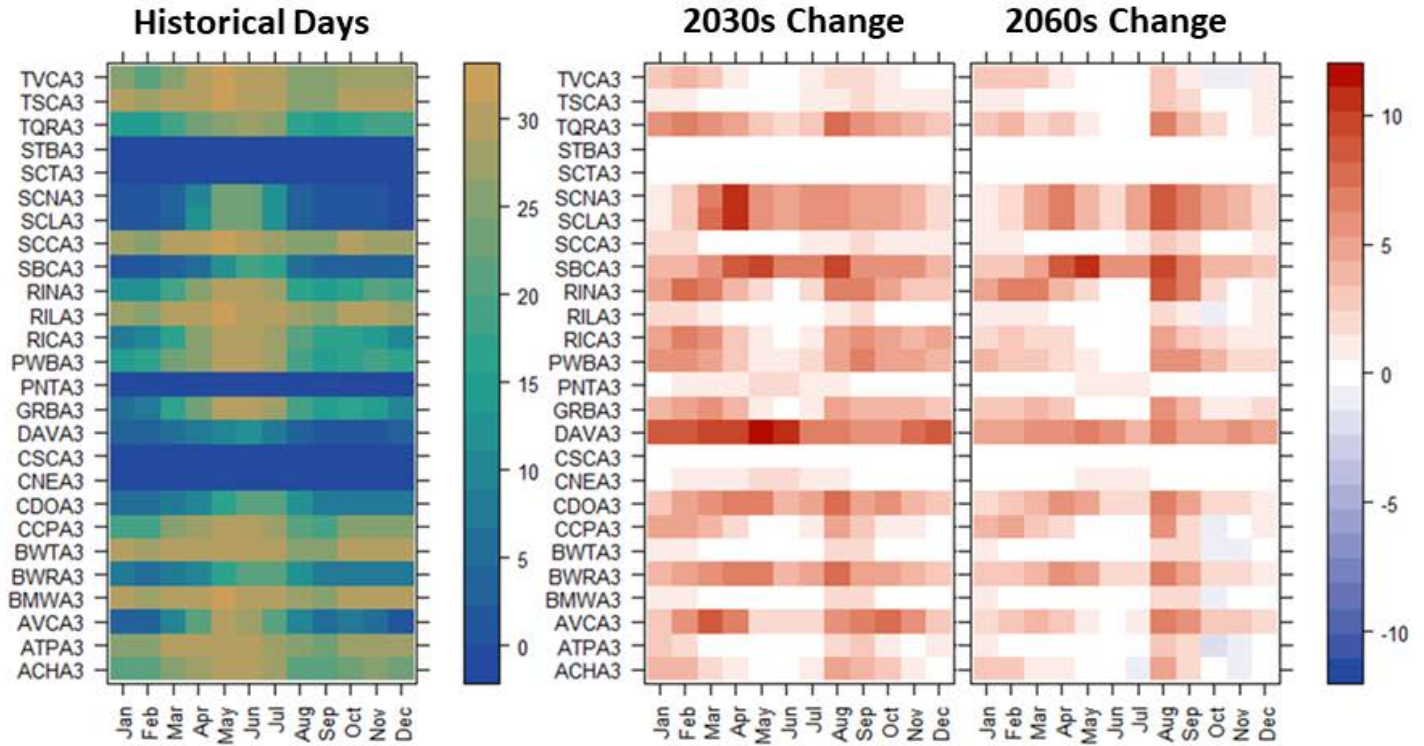


Figure ES-3. Dry days by stream in the simulated historical record and in projections for 2030s and 2060s for the worse-case scenario. See Figure 20 for definitions of the sub-basin abbreviations.

In summary, all models and climate scenarios consistently identify increases in temperature through time. Increases are larger under the worse-case scenario, which represents higher future emissions. Precipitation changes are more variable than temperature. The best-case scenario shows relatively minimal change in seasonal precipitation; in the worse-case scenario, total precipitation decreases in the monsoon and winter wet seasons.

Precipitation also becomes increasingly variable under projected future conditions. In either of these cases, it is likely that the number of dry days for streams will increase, especially in the summer months. The associated impacts include stress to vegetation and wildlife, as well as the potential for reductions in stream infiltration to the local groundwater aquifer, as addressed further in the next phase of the Study.

1. Introduction

The Santa Cruz River flows over 200 miles, originating in the San Rafael Valley in southeastern Arizona. The river crosses the US-Mexico border twice before flowing through Tucson, Arizona's second largest city. During flood events, the Santa Cruz drains to the Gila River, a tributary of the Colorado River. Portions of the main stem of the Santa Cruz River are effluent dependent, relying on the discharge of highly treated wastewater to maintain surface flows between precipitation events or wet seasons. In wet seasons, the river is also fed from tributaries such as the Cañada del Oro Wash and Rillito River, originating from the east of Tucson in the Santa Rita, Rincon, and Santa Catalina Mountains.

Arizona's 1980 Groundwater Code established Active Management Areas in areas of long-term groundwater decline to provide for long-term management and conservation of water supplies. Active Management Areas are primarily based on groundwater basin boundaries but take water use into account as well. The Lower Santa Cruz River (LSCR) Basin Study area is identical to the Tucson Active Management Area¹ (TAMA) within Pima and Pinal Counties, as seen in Figure 1. For the purpose of climate and surface water modeling, the LSCR Study hydroclimate analysis used a model boundary that extends to the south and east as shown in Figure 1. The northwest portion of TAMA was not included in the surface water model because those subbasins drain into the Gila watershed to the north. It is also sparsely populated compared to the rest of the TAMA.

Tucson and the surrounding area rely on groundwater, imported Colorado River water, and treated wastewater effluent to meet water supply needs. Key areas throughout the basin have experienced groundwater table declines, although the use and recharge of imported Colorado River water has helped to offset some of these storage losses. Changes in natural recharge, driven by shifts in precipitation and streamflow regimes, may further impact the local groundwater supply. Colorado River water is conveyed to the Tucson area via the Central Arizona Project (CAP), a 336-mile system of canals and pipelines. Arizona's CAP allocation has junior priority relative to other Colorado River rights holders. This introduces uncertainty to the reliability of the basin's water supply, particularly under projected warmer and potentially drier conditions in the Colorado River Basin (Reclamation 2012).

This report describes the analyses used to assess the impact of projected changes in precipitation and temperature on surface water supplies in the LSCR Basin. The basis of this approach is a pairing of dynamically and statistically downscaled climate projections over the surface water model boundary area, as detailed in Chapter 2 Climate Analysis. To account for the high degree of variability of the southeastern Arizona climate, a statistical "weather generator" was developed for the study, described in Chapter 3. The weather generator creates a large group, or ensemble, of plausible precipitation and temperature time series. Together, these time series simulate the inherent variability of the local climate. The resulting ensemble of climate

¹ <https://new.azwater.gov/ama/management-plan/3>

Lower Santa Cruz River Basin Study Hydroclimate Analysis

information is used with the Sacramento Soil Moisture Accounting (Sac-SMA; Burnash et al. 1973) model to propagate these projected climatic changes to the surface water system as described in Chapter 4. Surface Water Modeling. This study complements ongoing work by the LSCR Basin Study Project Team to evaluate climate change impacts on water supply and demand for agricultural, municipal, industrial, and environmental uses and provides details on the Sac-SMA modeling methodology and output analysis techniques.

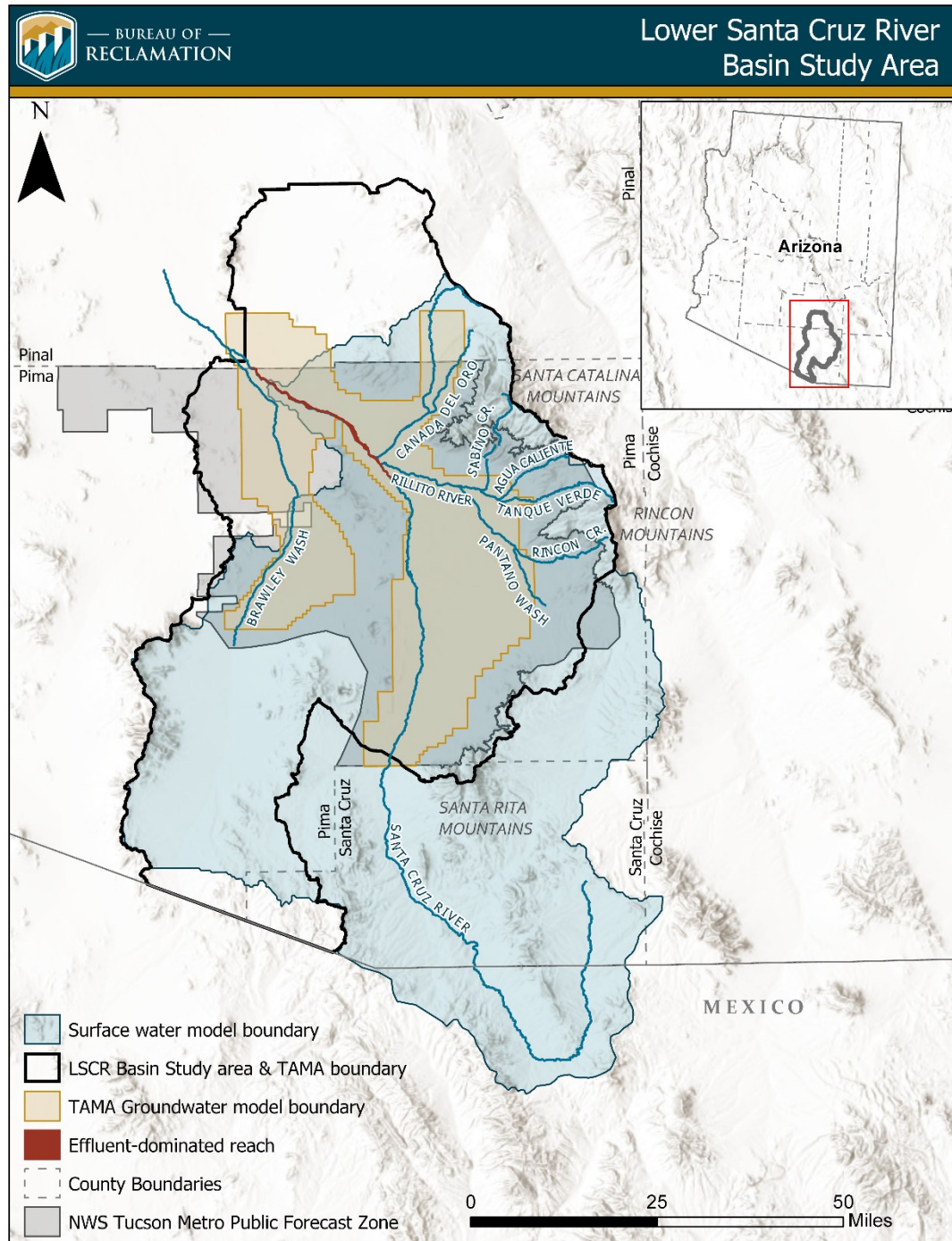


Figure 1 – Lower Santa Cruz River Basin study area and modeling boundaries.

2. Climate Analysis

2.1. Current Climate

This section provides an overview of the Tucson area's climate. Basic climate information is presented for the Tucson Active Management Area, with a focus on weather station data from the Tucson International Airport. Changes in annual temperature and precipitation are provided for the TAMA as well as the National Weather Service's Tucson Metro Area Public Forecast Zone, shown in Figure 1. Beginning in Section 2.2, analysis was performed using the geography of the surface water model boundary area, also shown in Figure 1.

Annual temperatures at the Tucson International Airport² average a minimum of 56 degrees Fahrenheit (°F) and a maximum of 83°F, with large seasonal and diurnal variability typical of mid-latitude steppe and desert climates. June and July have the hottest average monthly maximum temperatures (around 100°F), and December and January have the coolest minimum monthly temperature of approximately 40°F. The Tucson airport station (elevation 2560 feet; Figure 2) receives an average of 11.6 inches of precipitation per year. Precipitation is greater at higher elevations, averaging 33 inches per year in the Santa Catalina Mountains near Mount Lemmon³ (station elevation 7690 feet), often with enough winter precipitation occurring as snow to accumulate snowpack on the ground.

Maximum monthly precipitation typically occurs in July (spatially distributed as shown in Figure 2) and August. Precipitation occurs over two distinct wet periods, one associated with the summer North American Monsoon (NAM) season (mid-June through September) and the other with cyclonic and low-pressure frontal systems in the fall and winter (approximately October-March). Summer monsoon precipitation is characterized by convective events that are typically short, intense, and highly localized. The highest maximum monthly temperatures occur in June and July (see Figure 2), with some cooling associated with the continued monsoon rains in August. Precipitation in the fall and winter produces more sustained and widespread but less intense precipitation events. Following the winter rains, the region experiences a period of low to no precipitation in the dry season preceding the start of the next monsoon season.

²COOP Station #028820 (NCDC 1981-2010 Monthly Normals) - <https://wrcc.dri.edu/cgi-bin/cliMAIN.pl?aztuap>

³COOP Station #025732 (1981-2010 Monthly Climate Summary) - <https://wrcc.dri.edu/cgi-bin/cliMAIN.pl?az5732>

Lower Santa Cruz River Basin Study Hydroclimate Analysis

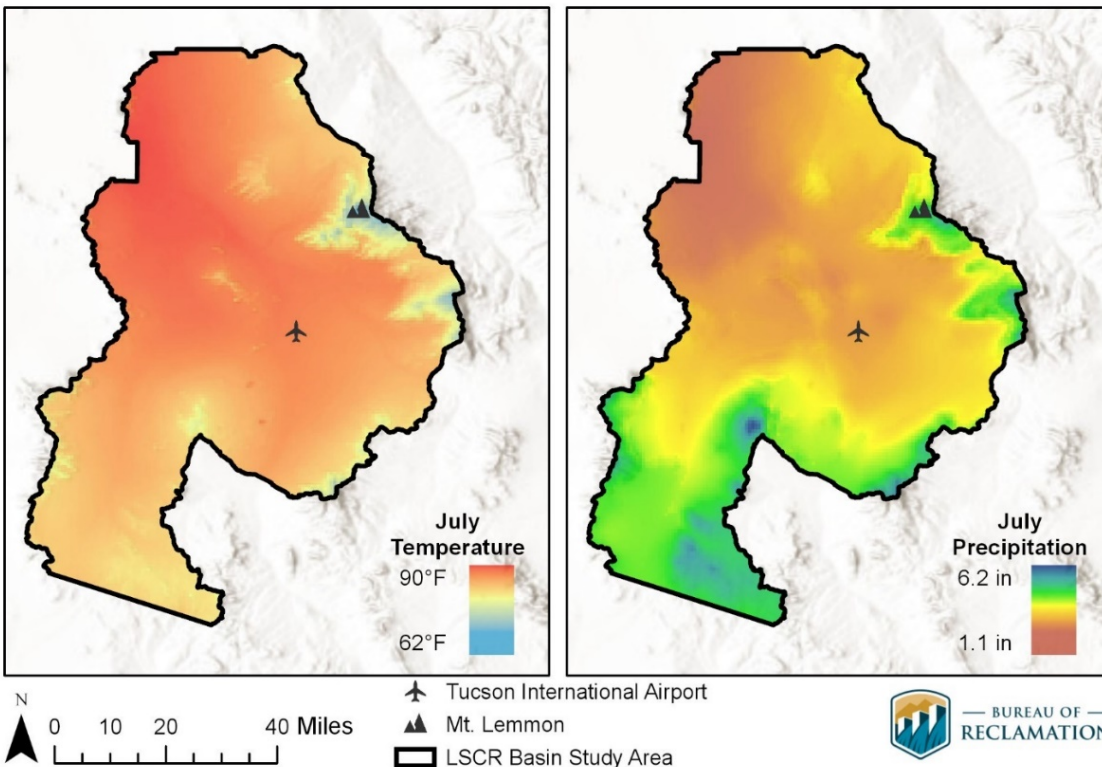


Figure 2 – July PRISM⁴ temperature (left) and precipitation (right) 30-year (1981-2010) normals over the LSCR basin study area.

Precipitation is highly variable across the basin and across days, months, and years (Figure 3), with the variability on the same order of magnitude as the precipitation itself. Over the 30-year period from 1981 to 2010 depicted in Figure 3, some days of the year never received significant rainfall (e.g., June 10th). These consistently dry days tend to occur just before the onset of the monsoon in mid-June or early July (Figure 3, top). In addition to the day-to-day variability during the monsoon season, the start and end of the season can also vary greatly from year to year. The wide range of observed monthly precipitation totals during the monsoon months is depicted by the blue boxplots in the bottom of Figure 3. To represent the distinct seasonality of precipitation in the region, this study takes a dynamic approach to defining the dry, monsoon, and winter seasons, as described in Section 2.4.

⁴ Parameter-elevation Regressions on Independent Slopes Model

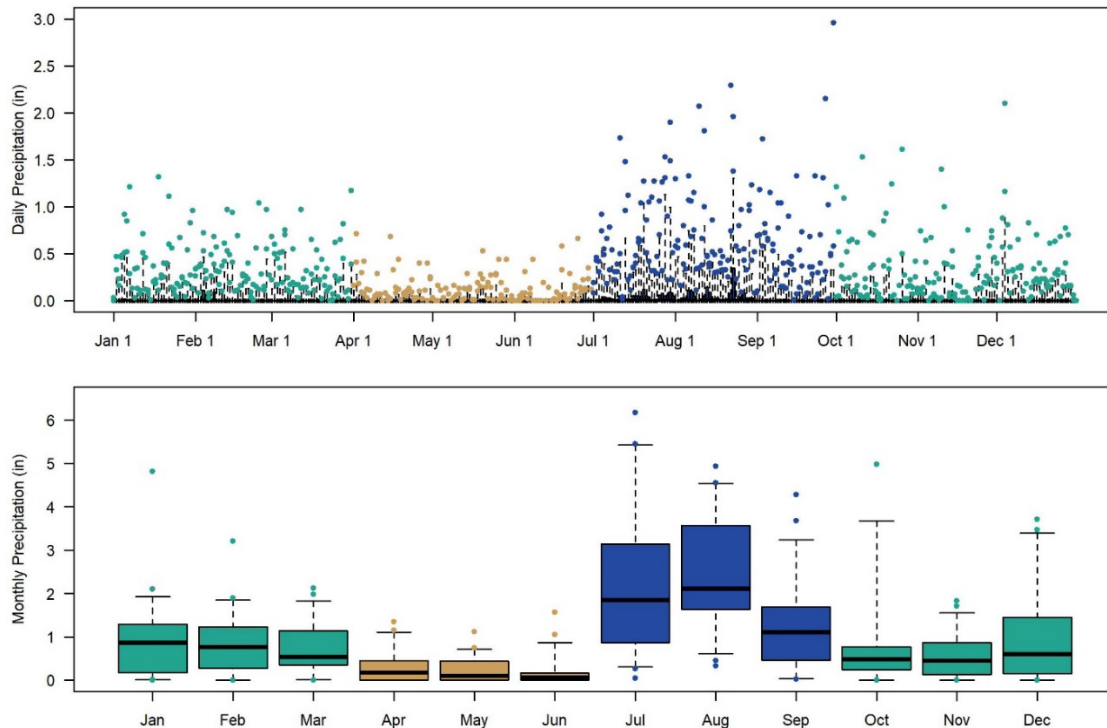


Figure 3 – Rainy day (top) and total monthly (bottom) precipitation at the Tucson Airport station from 1981-2010. Teal boxes indicate months that typically fall in the winter rainy season, tan indicates months that are typically in the dry season, and blue are months typically in the monsoon season. Whiskers represent 5th/95th percentile of interannual variability over the period.

2.2. Climate Scenarios

The formulation of climate scenarios begins by developing assumptions about how the key drivers that impact the Earth’s climate will vary in the future. These factors include the emissions and concentrations of greenhouse gasses and certain aerosols, as well as land use and land cover conditions. While these sets of assumptions contain information besides levels of greenhouse gas emissions, they are commonly referred to as “emissions scenarios”.

The Intergovernmental Panel on Climate Change (IPCC) sponsored the development of standardized emissions scenarios called Representative Concentration Pathways (RCPs) to, “encourage research that will characterize a broad range of possible future climate conditions, taking into account recent climate observations and new information about climate system processes” (Moss et al. 2010). This Study uses two RCPs from the IPCC 5th Assessment Report (AR5) (Taylor et al. 2012 and IPCC 2014) to define future climate outcomes: RCP 4.5 and RCP 8.5 as depicted in Figure 4.

The concept of radiative forcing is key to understanding climate change. National Oceanic and Atmospheric Administration’s (NOAA) Climate.gov website provides a simple description of this process, which is excerpted here:

Lower Santa Cruz River Basin Study
Hydroclimate Analysis

“In accordance with the basic laws of thermodynamics, as Earth absorbs energy from the sun, it must eventually emit an equal amount of energy to space. The difference between incoming and outgoing radiation is known as a planet’s radiative forcing. In the same way as applying a pushing force to a physical object will cause it to become unbalanced and move, a climate forcing factor will change the climate system. When forcings result in incoming energy being greater than outgoing energy, the planet will warm (positive radiative forcing). Conversely, if outgoing energy is greater than incoming energy, the planet will cool.”

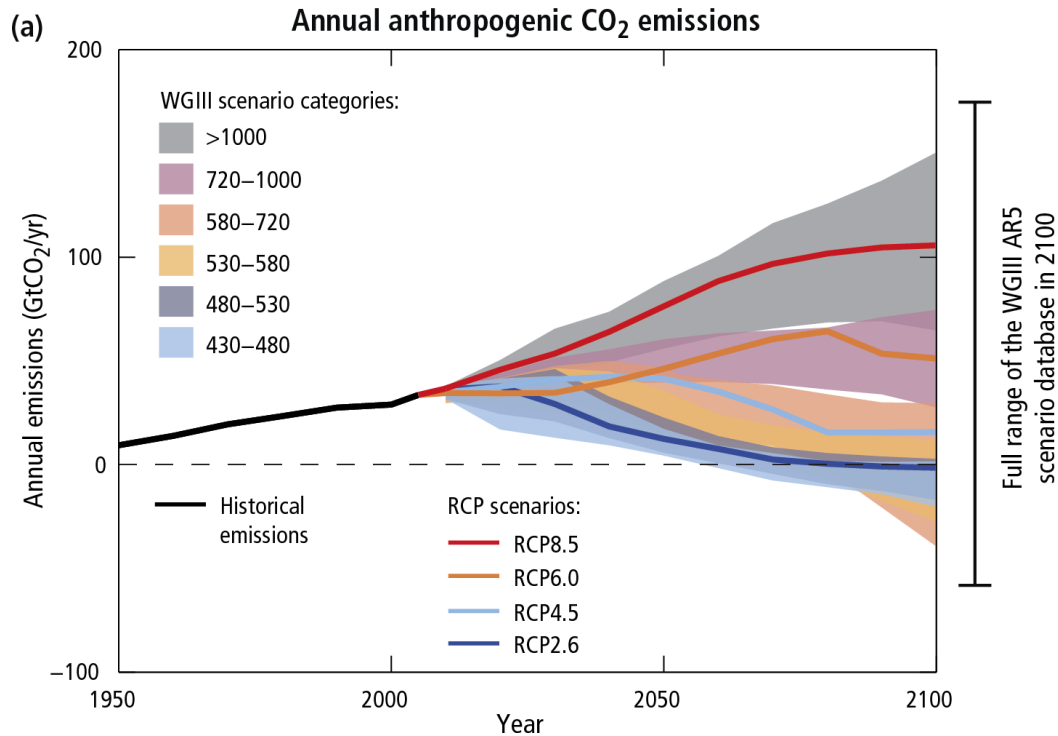


Figure 4 – Emissions of carbon dioxide (CO₂) alone in the RCPs (lines) and the associated scenario categories used in the IPCC Working Group III (WGIII; colored areas show 5 to 95% range). The WGIII scenario categories summarize the wide range of emission scenarios published in the scientific literature and are defined on the basis of CO₂-eq concentration levels (in ppm) in 2100. (Figure and caption from IPCC, 2014).

This Study used the following RCPs:

- **High Risk** (RCP 8.5; Riahi, 2011). Radiative forcing continues to rise through 2100, suggesting minimal improvements from adaptation strategies and continued increases in greenhouse gas emissions. This continued increase most closely reflects the current trajectory of emissions, lending this scenario the “business as usual” label.
- **Low Risk** (RCP 4.5; Thomson et al. 2011). Radiative forcing increases more slowly during the mid-21st century and stabilizes shortly after 2100 from moderate levels of

mitigation of greenhouse gas emissions. At the time of development, RCP 4.5 was considered a more realistically achievable scenario than the lowest RCP (RCP 2.6).

General Circulation Models, also referred to as Global Climate Models (GCM), use RCPs as input to simulate the Earth’s response to changes in incoming and outgoing radiation. This Study uses long-term GCM simulation outputs driven by RCPs from the IPCC’s standardized climate experiments known as the Coupled Model Intercomparison Project phase 5 (CMIP5). GCM outputs represent large-scale atmospheric and oceanic processes, with coarse model grid resolutions, typically on the order of 100 km laterally. Since “climate” refers to the typical weather of an area over a period, often 30 years, long-term simulations are needed to assess how climate may change in the future.

2.2.1. Downscaling Methods

The spatial scale of GCM simulations is typically too coarse to support the type of hydrologic modeling required for local water resource management. The coarse scale of GCMs typically does not capture climate processes such as orographic precipitation, snowfall, and convective storms—processes that are important for water resources planning.

GCM simulations must be spatially downscaled to be used in basin-scale hydrologic modeling. Spatial downscaling methods derive climate information at finer spatial resolution from coarser spatial resolution GCM output. The fundamental basis of spatial downscaling is the assumption that significant relationships exist between local and large-scale climate (USAID, 2014).

The importance of downscaling for basin-scale studies is illustrated in Figure 5, which shows Parameter-elevation Regressions on Independent Slopes Model (PRISM; PRISM Climate Group 2018) precipitation data on a 6 kilometer (km) by 6 km grid (left) versus a 100 km by 100 km grid resolution, typical of a GCM (right). Note how the spatial precipitation patterns are lost at the scale of the GCM. The entire LSCR Basin study area is covered with less than three GCM grid cells, while the 800 meter PRISM precipitation topographic patterns (shown in Figure 2) are still visible at the downscaled 6-km resolution.

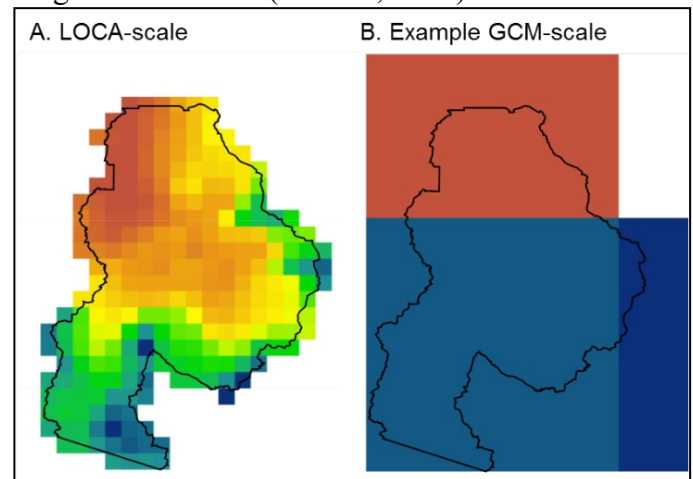


Figure 5 – PRISM gridded precipitation scaled to the approximate resolution of A) LOCA and B) a sample GCM. Both figures use the same data and color scale as Figure 2.

This study uses two approaches for downscaling GCM simulations: *statistical* and *dynamical* downscaling. Statistical downscaling relies on empirical relationships derived between projections and historical observations. This study uses the Localized Constructed Analogs (LOCA) method (Pierce et al. 2014) to downscale CMIP5 GCM simulations to a finer spatial resolution (1/16th degree, or approximately 6 km). The LOCA dataset provides 64 projections of daily precipitation and minimum/maximum temperature from 32 GCMs using two emissions scenarios: RCP 4.5 and RCP 8.5.

Lower Santa Cruz River Basin Study Hydroclimate Analysis

Statistical downscaling methods use observations to map global climate model outputs to a finer scale. LOCA uses the Livneh et al. (2015) gridded dataset over the period from 1950-2005 to select appropriate analog days from observations. While this method relies on the assumption that there is a historical day that captures future patterns, the observation dataset accounts for the systematic effects of local properties such as topography on precipitation and temperature. LOCA uses less temporal averaging than many other statistical downscaling methods to better preserve extreme events, such as hot days or heavy rains (Pierce et al. 2014). This makes it better suited for use in the desert southwest U.S. and for understanding variability in complex topography than other statistical downscaling methods.

Dynamical downscaling uses GCM outputs as input to a higher resolution regional climate model (RCM), such as the Weather Research and Forecasting (WRF) model used in this study. The benefit of this approach is that it simulates physical processes and does not rely on finding a suitable historical analog to provide local climate information. As decision-makers ask increasingly detailed questions regarding future changes in local climate, dynamical downscaling provides a method to look at changes in processes and patterns outside of the observed record.

The computational expense of running an RCM often limits the number of models and scenarios that can be evaluated. Therefore, this approach may not capture the uncertainty associated with model development choices or provide a range of RCPs to quantify uncertainty related to future emissions scenarios. As the available dynamically downscaled projections in this Study were based only on RCP 8.5, a statistically downscaled projection was used to include RCP 4.5 and the uncertainty surrounding the composition of the future atmosphere.

The consequence of downscaling methodology selection on projected water resources was recently evaluated in two Arizona basins by a Reclamation Science and Technology study (Shamir and Halper, 2019). This study concluded that the changes projected by the dynamically downscaled simulations are substantially larger than the statistically downscaled, for both projected wetter and drier future scenarios.

2.2.2. Future Climate Scenarios

The study's cost-share partners, represented by the Project Team, helped to shape the approach to the future climate analysis. Partners indicated that they wanted to model a range of risks to the area's water using sectors, from a "worse-case" scenario (severe but not impossible to adapt to) to a "best-case" scenario (one that would require a minimum amount of adaptation). These scenarios would "bookend" the range of impacts to water users and serve as a basis for future planning activities.

Study partners were aware of recent University of Arizona research that compared the impact of downscaling method on projected streamflows for three Colorado River catchments, the Upper Colorado River at Lees Ferry, the Salt River, and the Verde River (Mukherjee 2016). The study compared two ensembles of CMIP 3 GCMs, downscaled using either statistical or dynamical methods. For all three basins, the mean of the dynamically downscaled ensemble projected lower monsoon and winter precipitation compared to the mean of the statistically downscaled ensemble.

This finding led to a concern that omitting the use of a dynamically downscaled projection could lead to an underestimate of risks to water users. Partners requested that Reclamation work with researchers from the University of Arizona Hydrology and Atmospheric Sciences Department to develop a climate scenario using dynamically downscaled projections as part of the “worse-case” scenario. The limited number of dynamically downscaled datasets necessitated the selection of a statistically downscaled best-case scenario based on the lower risk RCP 4.5 as a counterpart to the high-risk RCP 8.5 dynamically downscaled worse-case scenario (Table 1).

Table 1 – Summary of Datasets Used to Define Climate Scenarios

Scenario	Downscaling	RCP	Downscaled Resolution	Date Range
Historical Best-Case	Statistical (LOCA)	-	6km	1970-1999
Historical Worse-Case	Dynamical (WRF)	-	25km	1970-1999
2030s Best-Case	Statistical (LOCA)	4.5	6km	2020-2049
2030s Worse-Case	Dynamical (WRF)	8.5	25km	2020-2049
2060s Best-Case	Statistical (LOCA)	4.5	6km	2050-2079
2060s Worse-Case	Dynamical (WRF)	8.5	25km	2050-2079

**Note that both the statistically and dynamically downscaled datasets include retrospective (historical) simulations to provide a baseline for evaluating model performance and relative change in climate. Historical years from the modeled dataset were selected to align with the surface water model calibration period.*

The worse-case scenario uses outputs from the low resolution (LR) Max-Planck-Institute Earth System Model (MPI-ESM-LR; Giorgetta et al. 2013) run downscaled using WRF (WRF-MPI) as part of the North American Coordinated Regional Downscaling Experiment (NA-CORDEX) archive. Only RCP 8.5 is currently available for this GCM/RCM combination. While other combinations of GCMs and downscaling models are available as part of NA-CORDEX, University of Arizona analysis determined that WRF-MPI best simulated monsoon timing in the study area (Chang 2018). From a local water resource manager’s perspective, the onset date of the monsoon is a critical consideration. WRF-MPI simulations are available at 25 km lateral resolution and 6-hourly temporal resolution from 1950-2100. Additional details on WRF configuration are provided in Castro et al. (2017).

Without WRF-MPI simulations available for RCP 4.5 in the NA-CORDEX archive, the best-case scenario was created using the LOCA statistically downscaled MPI-ESM-MR GCM output for the RCP 4.5 emission scenario. The GCM for this scenario is the same model used for the worse-case scenario, but using the run identified as mid resolution (MR) to provide a scenario that is wetter and cooler than the worse-case (refer to Figure 8 in Section 2.3. Projected Changes in Annual Precipitation and Temperature Climatology).

As discussed in the introduction to Chapter 2, precipitation in the LSCR basin is extremely variable across a range of temporal scales from days to years. Partners requested an analysis that would preserve the variable nature of the southern Arizona climate, rather than one that focused on average changes. To accomplish this, the analysis describes two future periods that characterize the climatology of two 30-year intervals. The first interval is centered around the 2030s (2020-2049) and the second is centered around the 2060s (2050-2079). These periods are

Lower Santa Cruz River Basin Study Hydroclimate Analysis

also referred to as the “near future” and “far future” in this report. The 2060s time horizon was selected to align with the demands and external supply projections for the Lower Colorado River Basin. The historical period (calendar years 1970-1999) aligns with the surface water model calibration period.

We compared simulations of the historical period using the two GCM/downscaling method combinations with the observed data used to calibrate the Sac-SMA model. The Sac-SMA model calibration data over this historical period are derived from hourly gauges and radar data aggregated to elevation bands to drive the surface water model. The surface water model and forcing dataset are described further in Section 4.1 and used throughout this study as a historical dataset for comparison. Each historic period climate simulation (LOCA and WRF-MPI) provides retrospective results that are used as a baseline for comparisons and for bias correction.

2.2.2.1. Bias Correction

All model outputs contain biases, or systematic errors, related to the configuration of the model, downscaling method, or input data. To account for these biases, this study compares each future period to its respective historical period simulation with the same model configuration and inputs to identify projected changes. For example, the 2060s worse-case scenario was compared to the WRF dynamically downscaled historic period simulation, while the 2060s best-case scenario was compared to the LOCA statistically downscaled historic period simulation. In other words, to adjust for systematic errors, we present the changes between the simulation of the historic period and the future period using the same emissions scenario, climate model and downscaling method.

Bias correction is often used to account for systematic differences between modeled results and observations. Modeled temperatures are less uncertain than precipitation but required bias correction to ensure that realistic values for potential evapotranspiration calculations would be used in the Sac-SMA hydrology model. Bias correction requires historical observations. This study uses the observed dataset used to calibrate the Sac-SMA model for temperature bias correction. Future temperatures were adjusted (or bias corrected) based on the difference between the cumulative density functions of the observed and modeled historical temperatures within a 15-day window (Thrasher et al., 2012).

Similar correction methods were not applied to precipitation to maintain the important but uncertain nature of the extremes in the precipitation distribution. However, the WRF-MPI dataset developers extensively analyzed the raw WRF output for use in this study (Chang 2018). Modeled precipitation, averaged over the surface water model boundary area, was also reviewed to ensure realistic values, defined here as not exceeding 150% of the annual maximum historical daily averaged precipitation for the same area from the Sac-SMA calibration dataset (Figure 6). The best- and worse-case scenario future daily precipitation data were also subjected to this screening procedure (Table 2). No values (historical or future) exceeded this threshold, a constraint similar to those used in previous studies (Reclamation 2011, Payne et al. 2004, and Maurer et al. 2007).

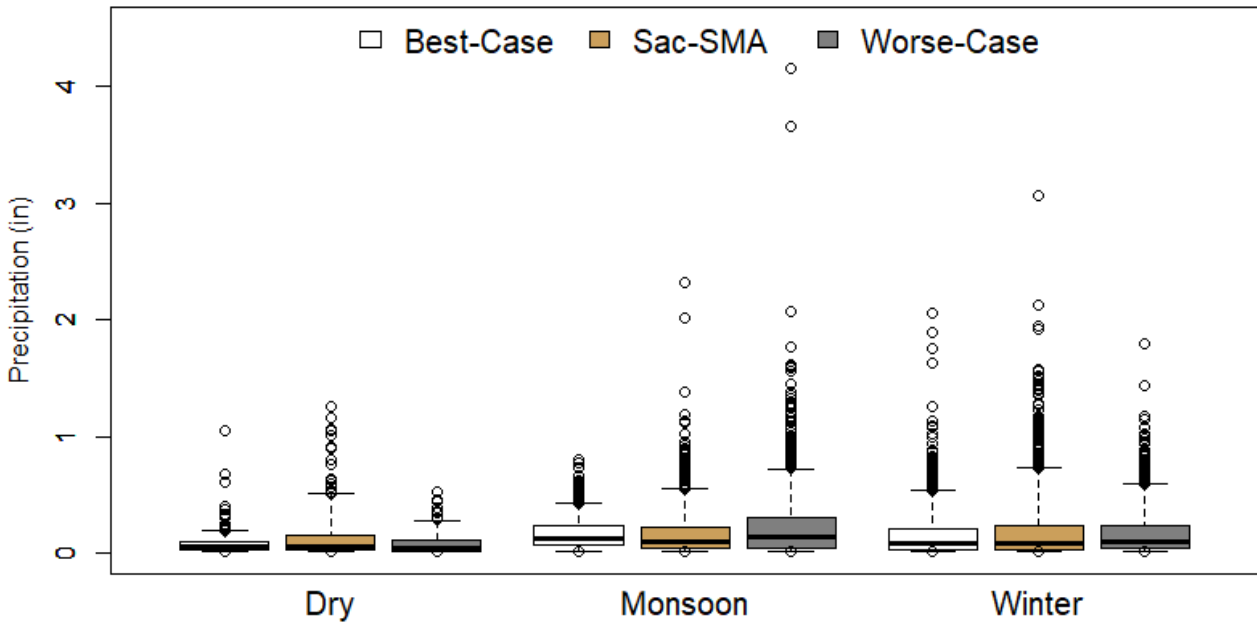


Figure 6 – Historical (1970-1999) daily rainy day precipitation averaged over the surface water model boundary area for the Sac-SMA calibration dataset (tan), best-case scenario simulation (white), and worse-case scenario simulation (gray), presented by season. Here, rainy days are defined as any day with greater than 0.01 inches of rain precipitation, a threshold selected after considering local climatology. Whiskers represent 5th/95th percentile of interannual variability over the historical period.

Table 2 – Statistics of Rainy-Day Precipitation by Season, Scenario, and Period, averaged across the surface water model boundary area.

		Precipitation (inches)							
		<u>Sac-SMA</u>	<u>Best-Case Simulation</u>			<u>Worse-Case Simulation</u>			
		Hist.	Hist.	2030s	2060s	Hist.	2030s	2060s	
Dry	5 th Percentile	0.01	0.01	0.01	0.01	0.01	0.01	0.01	
	Mean	0.13	0.08	0.08	0.08	0.08	0.10	0.09	
	Median	0.06	0.06	0.05	0.04	0.04	0.05	0.05	
	95 th Percentile	0.52	0.19	0.23	0.28	0.28	0.37	0.32	
	Maximum	1.25	1.05	0.47	0.82	0.53	0.75	0.65	
Monsoon	5 th Percentile	0.01	0.02	0.01	0.01	0.01	0.02	0.01	
	Mean	0.17	0.16	0.15	0.13	0.23	0.20	0.20	
	Median	0.09	0.13	0.11	0.08	0.14	0.12	0.11	
	95 th Percentile	0.55	0.43	0.43	0.42	0.73	0.64	0.69	
	Maximum	2.32	0.80	1.00	1.37	4.15	4.09	4.23	
Winter	5 th Percentile	0.01	0.01	0.01	0.01	0.01	0.01	0.01	
	Mean	0.19	0.15	0.16	0.19	0.18	0.16	0.18	
	Median	0.08	0.08	0.07	0.09	0.10	0.08	0.09	
	95 th Percentile	0.73	0.53	0.58	0.68	0.59	0.55	0.57	
	Maximum	3.07	2.05	1.75	2.14	1.80	1.59	2.28	

2.2.2.2. Model Limitations

The dynamically downscaled simulation uses a physically based approach that better captures the monsoon season dynamics important to this study. The LOCA simulation provides a complement to the dynamically downscaled projection and was selected to agree with the WRF-MPI scenario, consistent with the goal of illustrating a range of risks (i.e., best- and worse-case scenarios). The developers of LOCA and its user-community do not typically recommend using single projections for analysis. This is because a single LOCA projection does not reflect the physics of the atmospheric patterns in the same way that dynamical downscaling does. Also, selecting a GCM that is well performing for a region does not guarantee the processes for which it was selected are retained. Individual large extreme precipitation events are often not well represented in statistically downscaled data, which is reflected here in the absence of monsoon season precipitation extremes in the LOCA MPI-ESM dataset, as seen in Figure 6.

While the dynamically downscaled dataset was selected based on the GCM's ability to capture the monsoon season in the region (Chang, 2018), capturing remnant tropical cyclones that recurve into the Southwestern United States, typical of the late summer to early fall period (August – October), is a known weakness of these simulations. With these inherent limitations in mind, the best- and worse-case scenarios are still very useful for planning and adaptation strategy development and fit within the range of change seen from the larger ensemble of statistically downscaled models available from the LOCA dataset, as described in the next section.

2.3. Projected Changes in Annual Precipitation and Temperature Climatology

The statistics provided in this section cover the surface water model boundary area, which includes higher elevation areas that are cooler and rainier than the Study area. Projected changes in annual precipitation and temperature for the Tucson Active Management Area and the National Weather Service's Tucson Metro Forecast Zone are provided in Table 4.

Projected annually averaged temperature over the surface water model boundary area generally increases through time, (Figure 7), with larger increases under the worse-case scenario. Under the best-case scenario, the average annual change in precipitation increases by 0.32 inches in the 2030s and decreases by 0.85 inches in the 2060s, relative to the simulated historical period, which averages 15.8 inches. For the worse-case scenario, the future precipitation decreases more drastically in the near future (4.34 inches) and recovers slightly in the far future with a decrease of 3.90 inches, relative to the simulated historical average of 23.1 inches. The slight improvement in the far future may be caused by abnormally wet years in the far future (Figure 7).

Similar to projected precipitation changes, temperature changes are more severe in the worse-case scenario than in the best-case scenario, with temperatures consistently increasing more in the far future than in the near future. Near future average annual temperature increases range from 2.94°F in the best-case to 3.41°F in the worse-case scenario. Far future increases range from 3.83°F to 5.12°F for the best- and worse-case scenarios, respectively. The larger increase in

temperature in the far future under the worse-case scenario mirrors the continued increase in greenhouse gas emissions under RCP 8.5 relative to a reduction in emissions under RCP 4.5.

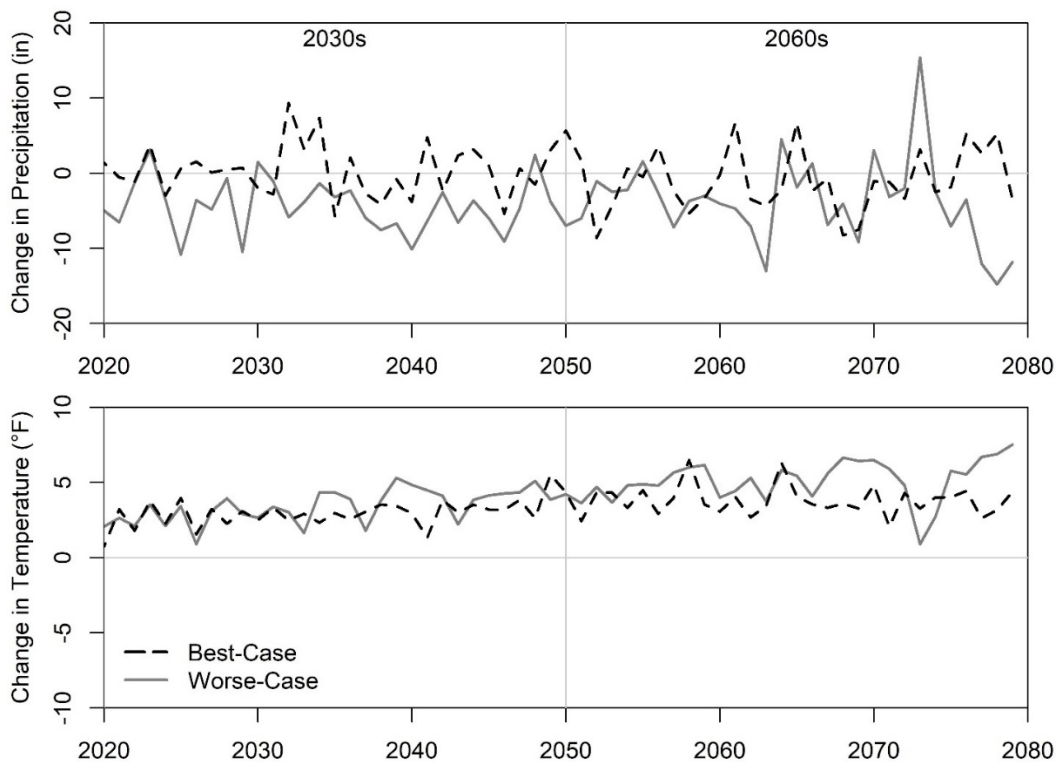


Figure 7 – Timeseries of the change in total annual precipitation (inches) and average annual temperature (°F) relative to the respective 30-year average of simulated historical values for the best- (dashed black line) and worse-case (solid gray line) climate scenarios. The gray vertical line represents the break between the near future (2030s) and far future (2060s). Values above the gray horizontal line at zero indicate future increases in precipitation or temperature and values below indicated decreases.

Figure 8 shows the changes in precipitation and temperature for the best- and worse-case scenarios, relative to the range of changes predicted by the 64 LOCA simulations, for the two future periods. These plots indicate where the selected cases fall within a larger portfolio of climate models. Note that the colors on the y-axis (temperature) go from lighter red at the bottom to darker red at the top. This is due to the fact all scenarios had increases in temperature. In contrast, some LOCA simulations had increases in precipitation while others had decreases, indicated by the transition from blue (wetter) to red (drier) on the x-axis.

In general, the best-case climate scenario (black square) has a wetter and cooler climatology over the two future periods used in this study (Figure 8), relative to the worse-case scenario (black triangle). Statistics of the full LOCA ensemble, reflected by the horizontal and vertical lines in Figure 8, provide context for the severity of the change relative to the range of uncertainty in the ensemble of 64 LOCA-downscaled CMIP5 models. This ensemble includes both RCP 4.5 and RCP 8.5 data, but does not include other emission scenarios, thus better reflecting uncertainty from model selection—not the full range of possible future emissions.

Lower Santa Cruz River Basin Study Hydroclimate Analysis

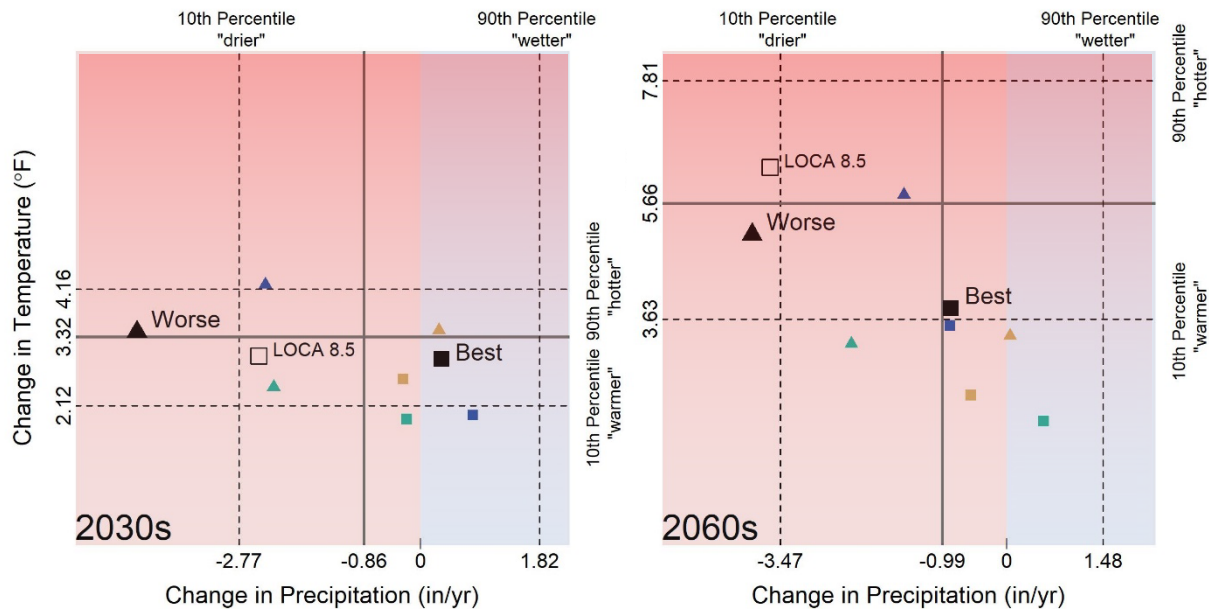


Figure 8 – Change in total annual precipitation averaged over the surface water model boundary area (inches per year) and average annual temperature (°F) for the best- (filled square) and worse-case (filled triangle) averaged over the case scenarios for the 2030s (left panel) and 2060s (right panel). Seasonal changes are also displayed as smaller shapes for the dry (tan), monsoon (blue), and winter (teal) seasons with change in precipitation in units of inches of precipitation per season. The open square is the RCP 8.5 equivalent of the LOCA-downscaled MPI-ESM-MR projection. Dashed lines are the 10th and 90th percentile change from the full LOCA ensemble and solid dark gray lines are the median change. Note the use of consistent scales in the 2030s and 2060s panel plots.

While only two projections were analyzed in detail in this study, these two scenarios fit well within the range of change seen in the larger LOCA model ensemble. Figure 8 includes the 10th, 50th (median), and 90th percentiles of change from the LOCA simulations averaged over the surface water model boundary area. Although the best- and worse- cases were selected based on additional analyses of model performance, in the 2030s the best- and worse-case scenarios also represent warmer/wetter and hotter/drier scenarios, respectively, relative to the range of the full set of LOCA simulations (32 GCMs, 2 RCPs). In the 2060s, the worse-case scenario continues to provide a scenario that is hotter and drier than the best-case. This provides confidence in suitability of the selected cases.

Figure 8 also plots the LOCA MPI-ESM-MR RCP 8.5 scenario as open squares, which is the same emission pathway and GCM used for the worse-case scenario. While downscaling influences the magnitude of annual change in precipitation and temperature, the direction of change is largely consistent between the WRF and LOCA RCP 4.5 datasets, suggesting the WRF-MPI dataset is a reasonable worse-case scenario relative to the best-case LOCA-MPI scenario.

Figure 8 investigates period-averaged annual changes to look at changes in climatology, however precipitation and temperature vary from year to year within these periods. Interannual variability in precipitation is larger than for temperature (Figure 7). Standard deviation provides a measure

of this variability, with low standard deviations indicating that values tend to be closer to the mean and high standard deviations indicating a larger spread of values around the mean. Here, the relative standard deviation (RSD), or coefficient of variation, normalizes the standard deviation to the mean of the 30-year period to indicate the deviation as a percentage of the mean and provide context for high and low variability. The RSD of the Sac-SMA calibration dataset precipitation is approximately 25% and temperature is less than 2%, illustrating that total precipitation varies much more than average temperature from year to year.

Interannual variability in precipitation and temperature across the surface water model boundary area increases into the future under both climate scenarios. These changes are summarized in Section 2.5. Under the best-case scenario, annual precipitation RSD increases slightly (by approximately 1% of the mean) in the near future (2030s) and more (by 8% of the mean) in the far future (2060s). The interannual variability of the worse-case precipitation scenario has even greater increases through time, with a rise of approximately 2% of the mean in the near future and a nearly 12% increase in the far future. The interannual variability in the temperature scenarios increases as well, but the RSD is small relative to that of precipitation.

The distinct seasonality of the LSCR basin necessitates a closer look at changes in sub-annual precipitation and temperature to describe changes in the climate system. Precipitation occurs over two distinct wet periods associated with the summer monsoon season (mid-June through September) and cyclonic and low-pressure frontal systems in the fall and winter (referred to here as the “winter” season). The remaining months are very dry with little to no rainfall. Additional description of these seasons follows in Section 2.4. Climate Metrics. Generally, projected temperature increases are greatest for the worse-case monsoon season (Figure 8). Projected decreases in precipitation are also greatest for the worse-case monsoon and winter seasons, suggesting decreases during important seasons for water supply, recharge, and environmental considerations. These seasonal changes are critical to stakeholder decision making in the basin and ultimately drove the development of the climate metrics used for the hydroclimate analysis.

2.4. Climate Metrics

Stakeholders requested detailed climate information to develop adaptation scenarios. As a result of discussions with the study cost-share partners, the Reclamation team developed three climate metrics of concern to local water users to quantify and analyze. These metrics include:

1. **Extreme events: temperature and precipitation, intensity, and frequency**
Local stakeholders’ concerns related to the intensity of precipitation events extend beyond interest in available water. Flooding, groundwater recharge, and changes in the timing or intensity of extreme temperature (including heat waves and freezes) were of concern across the basin.
2. **Monsoon timing: onset and demise**
The monsoon season in Southern Arizona marks the end of a prolonged dry season with little to no rain. Local water users therefore highly anticipate the start of the monsoon season, and any changes in the timing of onset are of great interest. The importance of

this timing is far reaching, also including supporting native vegetation and signaling the end of fire season.

3. Dry period onset

The onset of the dry season marks the end of winter rains and the start of the dry season. Along with changes in end of the dry season (i.e., monsoon onset), this metric defines the length of the dry period. Changes in these metrics would require water users to develop adaptation strategies to prepare for the extended dry season.

2.4.1. Climate Metric 1: Changes in Intensity and Frequency of Future Precipitation and Temperature

Not only are changes in the amount of rainfall and magnitude of temperature of interest for planning future adaptation measures, but the timing between rain events is of concern. Prolonged dry periods could drive increases in water demand, even if complemented by equal amounts of precipitation during the season from larger intensity events. For a discussion of the changes in extreme temperature and precipitation, see Section 3.3. Weather Generator Results.

2.4.2. Climate Metrics 2 and 3: Changes in Seasonality

Southern Arizona has a desert climate with high evaporation rates and low total annual precipitation. Precipitation falls during the summer monsoon and winter seasons, resulting in three distinct seasons: monsoon, winter wet, and dry (Figure 9). The definition of these seasons is critical to incorporating these metrics in the weather generator development (Section 3). Metrics used to define these seasons require weather variables, either directly or derived, that are common to all three climate datasets (i.e., dynamically downscaled WRF-MPI, statistically downscaled LOCA-MPI and Sac-SMA historical calibration datasets).



Figure 9 – Conceptual diagram of seasonality in the LSCR basin.

2.4.2.1. Determination of Monsoon Onset

Multiple approaches exist to define the North American Monsoon onset timing (#1 in Figure 9) in the southwestern United States, including methods using dewpoint temperature, precipitation, and atmospheric dynamics. In Tucson, the National Weather Service (NWS) previously defined the onset of the monsoon season as the first of three consecutive days reported with a mean daily dewpoint temperature greater than 54°F (Ellis et al., 2004) or 53°F (Chang, 2018).

Since 2008, however, the NWS has defined the monsoon season as June 15 to September 30,⁵ mainly for increasing public awareness and severe weather hazard preparation. The fixed monsoon definition avoids some of the challenges of the dewpoint-based metric, including occasional non-monsoon moisture events that temporarily increases the dewpoint temperature, incorrectly signaling the start of the monsoon season. However, using the June 15 to September 30 date limits the signal of early or late monsoon onset and does not account for monsoon season interannual variability.

⁵ <https://www.wrh.noaa.gov/twc/monsoon/monsoon.php>

To account for possible future shifts in monsoon seasonality, the dewpoint-based metric was adopted to develop the weather generator seasonality. The daily average 53°F threshold was found to capture the start of monsoon precipitation better than 54°F and better match the observed historical monsoon-onset timing reported by Ellis et al. (2004).

Dewpoint temperature is a measure of humidity and reflects the temperature at which a parcel of air becomes saturated with water vapor. Dewpoint, or other humidity measures that could be used to calculate dewpoint directly, are not available for this model as part of the LOCA simulations or from the Sac-SMA calibration data, although it is available from the WRF dataset. Therefore, this study approximated dewpoint for LOCA and Sac-SMA data using the dewpoint depression approach. This approach assumes that the daily minimum temperature approaches the dewpoint temperature and is offset by a depression constant. For LOCA, this approach uses PRISM-based depression constants, consistent with previous applications of LOCA data (Reclamation, 2015) and minimum daily temperature, which is provided in the LOCA dataset.

The 6-hourly temperature data from the Sac-SMA calibration dataset was used alongside the Tucson Arizona Meteorological Network (AZMET⁶) station record to determine daily minimum temperature. AZMET stations began operating in 1987 and are designed to provide meteorological observations for primarily agricultural interests. Measurements include air and soil temperature, humidity, solar radiation, wind speed and direction, and precipitation. The relative humidity observations were needed here to calculate dewpoint temperature. The Tucson AZMET station record was also used to derive dewpoint depression constants for all subbasins in the Sac-SMA dataset. Using the dewpoint relationships at the AZMET station to extrapolate to all elevation zones was not reliable for determining the monsoon timing. Sac-SMA seasonality is provided for reference and was used in Weather Generator development.

Analysis of the WRF-modeled dewpoint temperature revealed an atmospheric dry bias in the dynamically downscaled data, requiring bias correction of the onset threshold. This correction used PRISM dewpoint data (PRISM Climate Group, 2018) for the cell over the local AZMET station to determine the percentile of 1981-2010 June and July dewpoint temperatures that corresponds to the daily average of 53°F. PRISM provided a gridded data product with the expected bimodal distribution of June/July dewpoint temperatures to capture the shift from dry to wet weather regimes. Applying the resulting percentile to the distribution of dynamically downscaled dewpoint temperatures resulted in a bias-corrected threshold of 50.3°F, for use only with the WRF-MPI data (Chang, 2018). That is, for the WRF-MPI data the onset of monsoon season was defined as the first day in a three-day average of mean daily dew point temperature above 50.3°F. For further details, see Appendix D, Dynamically Downscaled Climate Projections in the Lower Santa Cruz Basin Study, Final Report for Cooperative Agreement R17AC00061.

2.4.2.2. Determination of Monsoon Demise

The end of the monsoon season is less well defined beyond the NWS fixed date of September 30. For consistency with the onset metric and literature (Ellis et al., 2004), monsoon demise is defined here as the day after the last three consecutive days above the dewpoint temperature threshold. For LOCA simulations and Sac-SMA historical data used in the best-case scenario,

⁶ <https://cals.arizona.edu/AZMET/>

Lower Santa Cruz River Basin Study Hydroclimate Analysis

monsoon demise is, therefore, the day after the last three consecutive days with dewpoint above 53°F. For WRF-MPI data used in the worse-case scenario, it is the day after the last three consecutive days above 50.3°F. The demise of the monsoon season is not always followed by immediate winter storms, as these could occur any time during the winter season. Here, the winter wet season is considered the period that stratiform rain events can occur, and thus does not experience sustained elevated humidity.

2.4.2.3. Determination of the Start of Dry Season

The dry season in the LSCR basin is characterized by prolonged periods with low to no rainfall. The transition to this season typically occurs between March and May and dry conditions persist until the start of the monsoon season. The NWS reports 1981-2010 averaged precipitation totaling less than 0.75" from April through June.⁷ Over the historical period of this study (1970-1999), the observed average length of dry spells beginning in the months leading into the dry season (March, April, and May) is 15, 21, and 18 days, respectively. Here, a dry spell is defined as consecutive days with no precipitation greater than 0.01 in/day.

Figure 10 depicts these average lengths and number of dry spells grouped by the month in which the spell begins (the dry spell can extend into the next month and the length can therefore be longer than 30 days). The length and number of dry spells are highly dependent. Bars aligning closer to the left of the plot indicate more frequent but shorter dry spells, while bars aligning to the right of the plot indicate longer, less frequent dry spells but also suggest months that approach no rainy days.

The distribution of dry spells in March is skewed toward longer events (median length = 6 days, mean length = 15 days) suggesting some transitions to the dry season occur in March, but that the transition more consistently occurs in April. January and February average 10-day dry spells, suggesting a 14-day period with no rain (≤ 0.01 inch) is sufficient to capture the transition out of the winter rain patterns with shorter dry periods that dominate January and February. The onset of the dry period is therefore based on the first time there is a dry spell of 14 days or more that ends after May 1st and starts before June 15th, in order to constrain the trigger events to the dry fore-summer period.

⁷ <https://www.wrh.noaa.gov/twc/climate/tus.php>

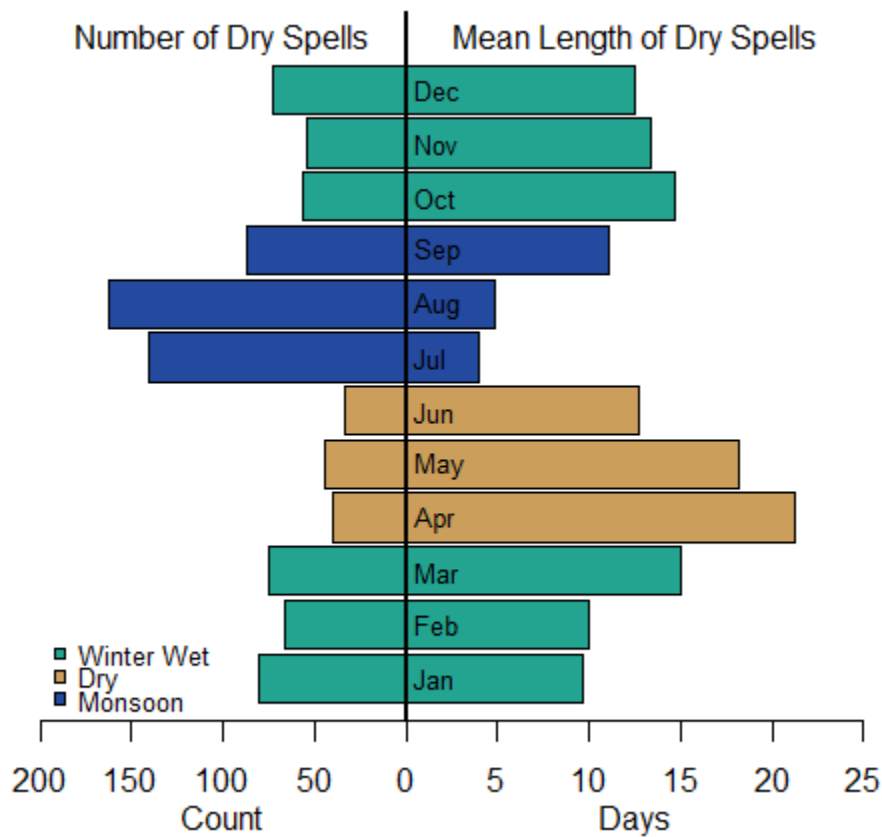


Figure 10 – Historical (1950-2009) dry spell statistics by month of start date from the Tucson Airport weather station compiled by M. Crimmins (personal communication 2018). Color indicates approximate season with teal = winter wet season, tan = dry season, and blue = monsoon season.

2.4.3. Seasonality Results

2.4.3.1. Historical Period

The Tucson NWS reports the median 1948-1997 monsoon onset date as July 3 (Table 3). The median day of monsoon onset for the historical period (1970-1999) simulated using LOCA-MPI (the same model as the best-case scenario) is July 5 (Table 3) and all years have monsoon onset dates within the fixed NWS monsoon period (i.e., onset after June 15) as seen by the position of the best-case monsoon distribution medians within the gray box in Figure 11. For the worse-case scenario based on WRF-MPI retrospective modeling, the simulated historical median onset date is June 22 (Table 3). The historical WRF-MPI simulation has a wider range of possible monsoon onset dates and exhibits more variability in monsoon timing (Figure 11), both onset and demise. This is likely due to the use of dynamical downscaling.

Both the best- and worse- cases have some years when the monsoon season ends after the last day of the NWS monsoon period (September 30). The median monsoon demise (or onset of the winter wet period) over the modeled historical period was September 7 for the best-case and October 2 for the worse-case, which fall on either side of the literature reported median of September 14 (Table 3). The simulated historical median onset of the dry season is April 24 for

**Lower Santa Cruz River Basin Study
Hydroclimate Analysis**

the best-case scenario and May 6 for the worse-case scenario, both occurring later than the date calculated from observations at the Tucson Airport (April 15). The resulting length of the dry season, or the number of days between the dry season and monsoon season onset dates, reflects the larger variability of the worse-case seasonality results (Figure 14). The median historical dry season length for the best-case scenario was 80 days, while the worse-case scenario only had a median length of 49 days, but with more interannual variability. These modeled values provide a baseline to compare future values accounting for some of the inherent model biases.

Table 3 – Median Date of Seasonal Transition Defined by Climate Metrics

	Dry Season Onset	Monsoon Onset	Monsoon Demise
Literature	April 15 ^c	July 3 ^a	September 14 ^b
Sac-SMA Calibration Dataset	April 19	July 7 ^d	September 16 ^d
Best-Case Model, Historical Period	April 24	July 5	September 7
Worse-Case Model, Historical Period	May 6	June 22	October 2

a. Tucson National Weather Service Forecast Office 1948-1997 Median (Ellis et al., 2004)

b. Phoenix National Weather Service Forecast Office 1948-1997 Median, Tucson unavailable (Ellis et al., 2004)

c. Median onset 1950-2009 from metric applied to Crimmins’ (2018) dry day analysis at the Tucson airport weather station

d. Sac-SMA monsoon dates use dewpoint developed at the elevation zone over the Tucson AZMET station.

2.4.3.2. Future Periods

Future periods exhibit small changes in monsoon onset for the best-case scenario with median onset dates advancing by two days for each future period, to July 3 and July 1 for the 2030s and 2060s, respectively. Although small, the shift in the median and the tightening of the range of onset timing, particularly with respect to fewer late onset dates in the future periods, drive an earlier start to the best-case monsoon season (Figure 11). The worse-case scenario does not show a single trend in monsoon onset date for the future periods, with a later median onset date of June 29 in the near future and returning to a median date of June 22 in the far future. The worse-case climate scenario therefore does not provide earlier relief to the dry season, as in the best-case.

A weather typing study using GCM and dynamically downscaled data in New Mexico found a similar minimum in the frequency of monsoon weather types around the middle of the 21st century, followed by an increase in monsoon events after 2050 (Prein et al., 2019 and personal communication). Prein also identified an earlier shift in the start of monsoon events and an increased frequency of monsoonal precipitation events in July and September. Both the best- and worse-case results project a later end of the monsoon period, or onset of the winter wet period (Figure 11), suggesting a general lengthening of the monsoon season in the future periods, particularly in the far future (Figure 12). Figure 13 shows winter season lengths and Figure 14 dry season lengths.

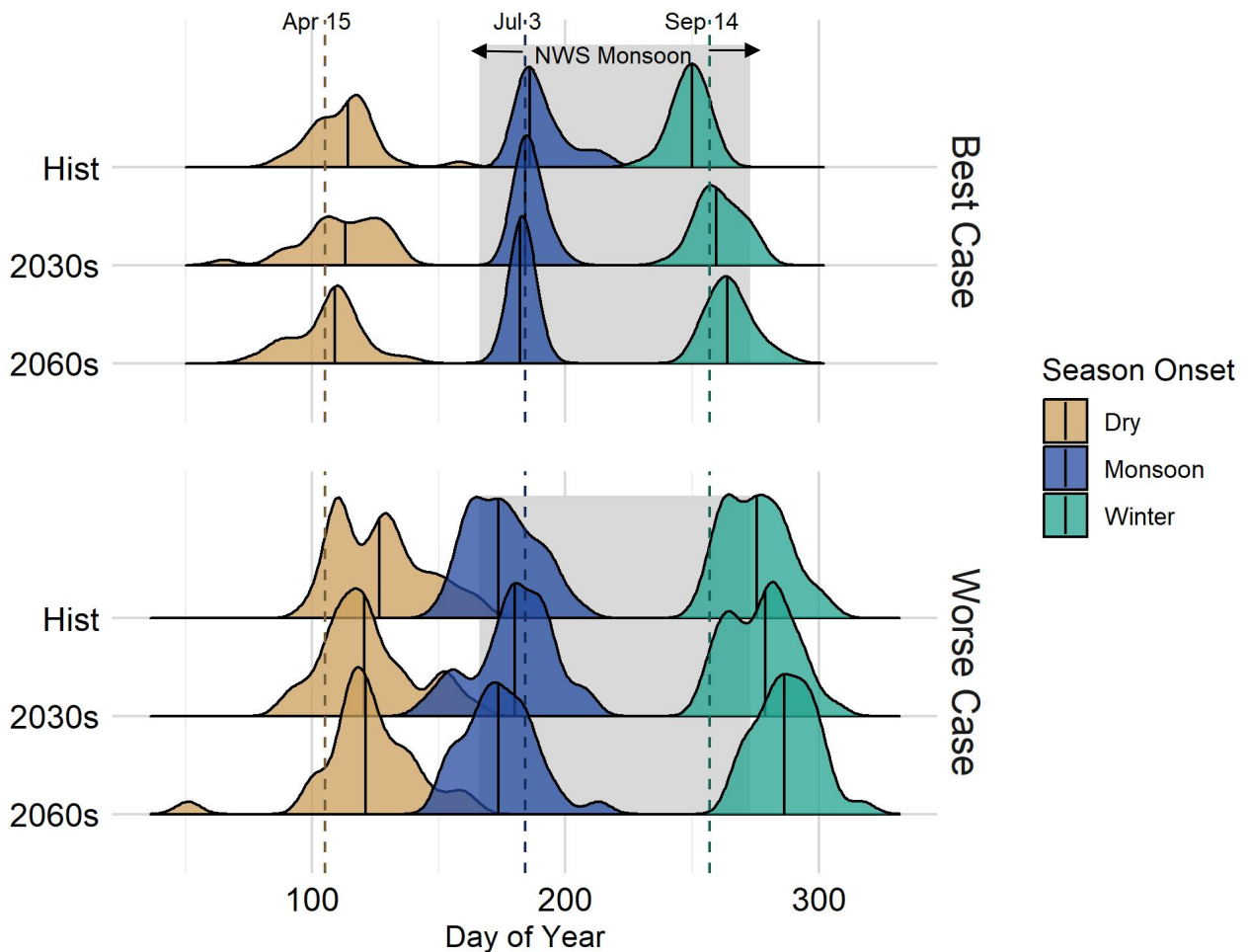
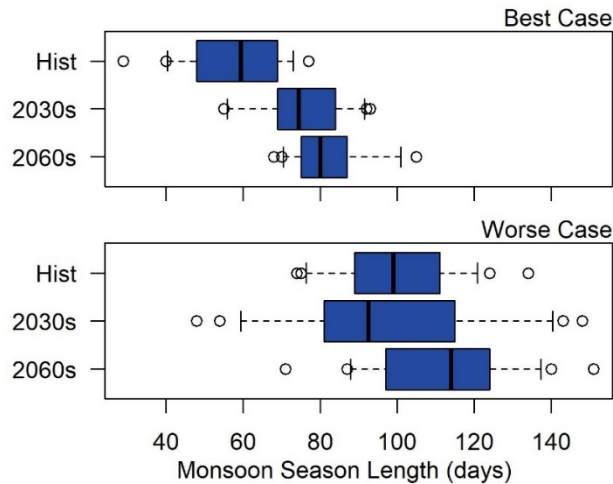


Figure 11 – Distribution of seasonal onset day of the year for the best- (top) and worse- (bottom) case scenarios. Black solid lines represent median onset day for each distribution and labeled, dashed lines represent select literature values given in Table 3. Gray shading indicates the NWS monsoon period of June 15 through September 30.

The lengthening of the monsoon season and changes in the dry season onset result in a consistent shift toward shorter winter wet periods under both scenarios (Figure 13). In both projected futures, the dry season begins slightly earlier in the year (Figure 11). In the best-case scenario, the median onset date of the dry season is one day earlier in the near future and five days earlier in the far future, relative to the historical period. The trend is less consistent in the worse-case scenario. Similar to the monsoon onset date, there is a larger advancement of the dry season onset in the near future (6 days) and a slight rebound to only a 5-day advancement in the far future. The combined changes in the starts of the dry and monsoon seasons result in both increases and decreases in the length of the dry season over time (Figure 14). Generally, the best-case scenario exhibits a shorter dry season in the future than the modeled historical period and the worse-case scenario projects an increase in dry season length.

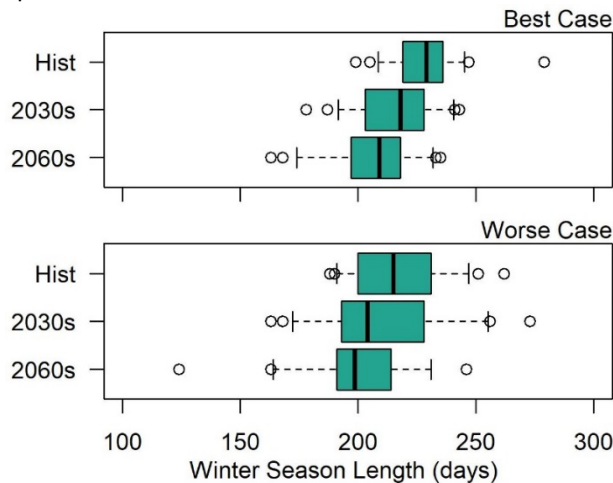
**Lower Santa Cruz River Basin Study
Hydroclimate Analysis**



	5 th perc.	Median	95 th perc.
Hist.	40	60	73
2030s	56	75	92
2060s	70	80	101

	5 th perc.	Median	95 th perc.
Hist.	76	99	121
2030s	59	93	140
2060s	88	114	137

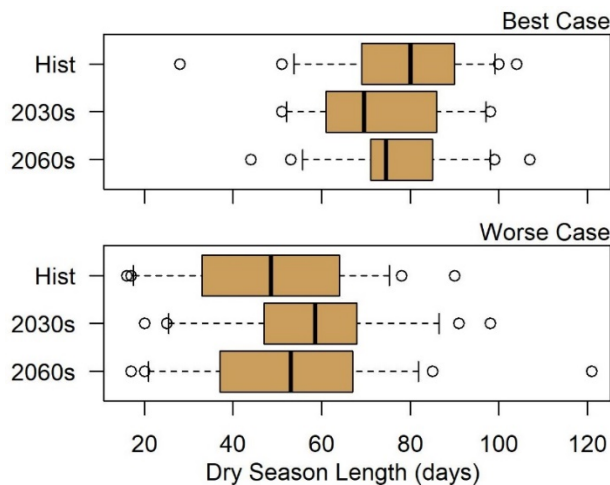
Figure 12 – Distribution and statistics of monsoon season lengths (in days) by period for the best-case (top) and worse-case (bottom) climate scenarios. Whiskers represent 5th/95th percentile of data.



	5 th perc.	Median	95 th perc.
Hist.	209	229	245
2030s	192	218	241
2060s	174	209	232

	5 th perc.	Median	95 th perc.
Hist.	191	215	247
2030s	172	204	255
2060s	164	198	231

Figure 13 – Same as Figure 12 but for the winter season lengths.



	5 th perc.	Median	95 th perc.
Hist.	54	80	99
2030s	52	70	97
2060s	56	75	98

	5 th perc.	Median	95 th perc.
Hist.	18	49	75
2030s	26	59	87
2060s	21	53	82

Figure 14 – Same as Figure 12 but for the dry season lengths.

In general, the worse-case scenario provides a greater range of seasonal lengths from year to year, representing a more variable future (Figure 15). The more variable nature of monsoon onset may be related to changes in the distribution of monsoon rainfall, with precipitation events becoming more intermittent, but more extreme. This change has been documented in the historical record by Luong et al. (2017) and DeMaria et al. (2019). More intense precipitation events are a result of increased moisture and atmospheric instability under future conditions. These events also contribute to increased variability of precipitation under future conditions.

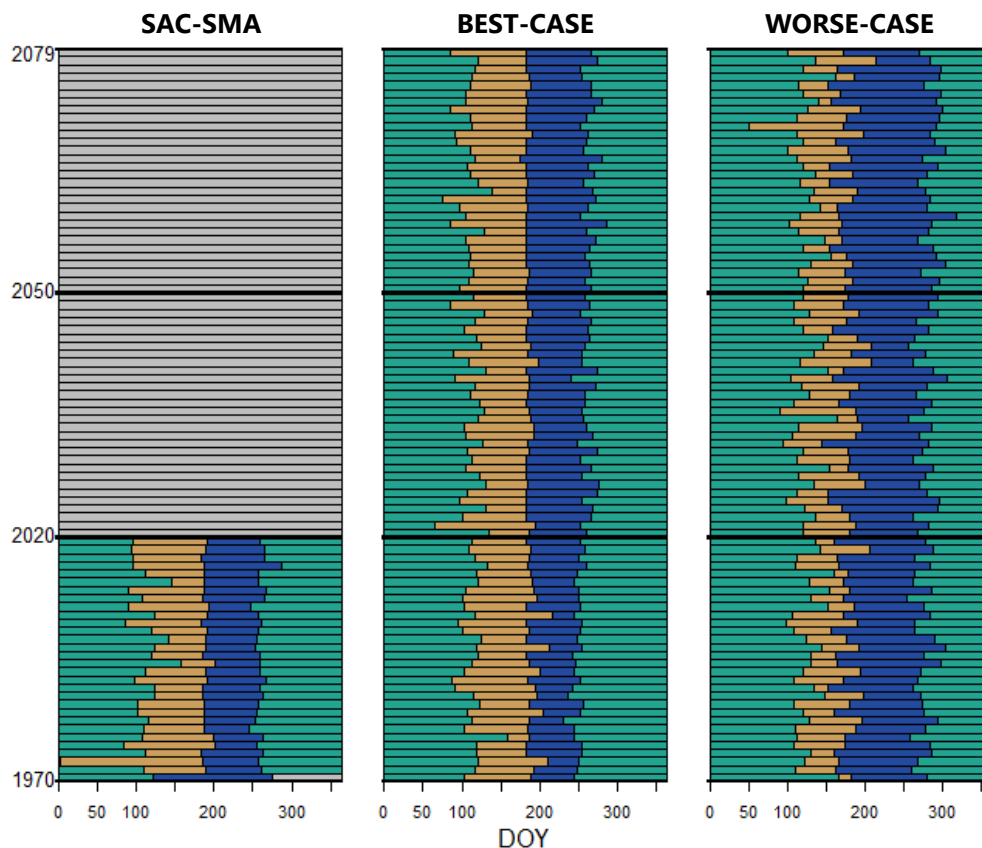


Figure 15 – Seasonality for each year of simulation for the Sac-SMA calibration dataset, and the best-case, and worse-case climate scenarios. Teal indicates days of the year (DOY) falling in the winter wet season, tan indicates days in the dry season, and blue indicates days in the monsoon season.

2.5. Climate Summary for Stakeholders

The historical climate in the Lower Santa Cruz River Basin varies greatly from year to year. Future projections under the scenarios developed here (Table 4) consistently identify increases in annual temperature, from the historical average of 63.3°F over the surface water model boundary area. Increases are larger in the worse-case scenario. The worse-case represents a future with no mitigation strategies to reduce greenhouse gas emissions while the best-case scenario represents a future with mitigation to curb emissions. The best-case scenario suggests relatively minimal change in seasonal precipitation. The worse-case scenario indicates decreases in total annual and seasonal precipitation. Interannual variability in precipitation increases for both scenarios.

**Lower Santa Cruz River Basin Study
Hydroclimate Analysis**

Table 4 – Summary of Projected Basin-Averaged Future Precipitation and Temperature Relative to the its Respective Simulated Historical Period (1970 – 1999). All geographic areas are depicted in Figure 1.

Geography	Statistic	Best-Case 2030s	Best-Case 2060s	Worse- Case 2030s	Worse- Case 2060s
Tucson Active Management Area	Change in Total Annual Precipitation	0.40"	-0.50"	-4.44"	-3.73"
Tucson Metro Public Forecast Zone	Change in Total Annual Precipitation	0.28"	-0.44"	-4.47"	-3.77"
Surface Water Model Boundary Area	Change in Total Annual Precipitation	0.32"	-0.85"	-4.34"	-3.90"
	Change in Average Monsoon Precipitation	0.80"	-0.87"	-2.38"	-1.57"
	Change in Average Winter Precipitation	-0.21"	0.57"	-2.25"	-2.38"
	Precipitation RSD* compared to Historical: Best = 20.3%, Worse = 17.3%	21.6%	28.5%	18.9%	30.4%
Tucson Active Management Area	Change in Average Annual Temperature	2.92°F	3.81°F	3.36°F	5.07°F
Tucson Metro Public Forecast Zone	Change in Average Annual Temperature	2.88°F	3.77°F	3.34°F	5.05°F
Surface Water Model Boundary Area	Change in Average Annual Temperature	2.94°F	3.83°F	3.41°F	5.12°F
	Change in Average Dry Season Temperature	2.59°F	2.31°F	3.44°F	3.34°F
	Change in Average Monsoon Temperature	1.96°F	3.52°F	4.24°F	5.81°F
	Change in Average Winter Temperature	1.88°F	1.85°F	2.45°F	3.20°F

*Relative standard deviation (RSD) is calculated by normalizing the standard deviation to the mean of the 30-year period and presented as a percentage.

For additional climate figures, see Appendix A—Supporting Climate Figures.

3. Weather Generator

Precipitation is particularly variable in southern Arizona. While the best- and worse-case scenarios each provide one possible future precipitation and temperature sequence, there are other patterns of precipitation that are equally likely. To account for this uncertainty in daily patterns of precipitation and temperature, this study developed and applied a “weather generator” to introduce variability around the broader climate projection trends.

A weather generator is a numerical tool that resamples an input timeseries many times, while preserving observed or projected characteristics of importance, such as the statistics of the transition between wet and dry days. The resulting large group, or ensemble, of likely rainfall and temperature timeseries represents a range of possible amounts, daily patterns, and seasonality at a scale appropriate for driving the surface water model to produce a range of possible streamflows.

The weather generator is run using daily precipitation and temperature averaged over the surface water model boundary area, but the Sac-SMA surface hydrology model requires sub-daily information for each elevation zone in a subbasin. Therefore, the weather generator results are disaggregated both spatially and temporally, maintaining the patterns observed in the original climate simulations. From this point on, we use the best- and worse-case scenario to refer to the weather-generated ensembles of future temperature and precipitation. For additional details on the construction and performance of the weather generator, see Gangopadhyay et al., 2019.

3.1. Development and methodology

The weather generator takes in daily timeseries of precipitation, temperature, and season, averaged over the extent of the Sac-SMA basins depicted in Figure 1 in Section 1. Introduction. Three input sources were used for all available time periods: 1) the best-case climate scenario (from LOCA-MPI RCP 4.5); 2) the worse-case climate scenario (from WRF-MPI RCP 8.5); and 3) the Sac-SMA input dataset that was used for calibration of the surface water model. We used these three sets of inputs to generate an array of future weather conditions. Inputs for each of these weather generator runs include time series of the seasons developed using the metrics described in Section 2.4. Each day was numbered either: 1 = dry fore-summer, 2 = monsoon, 3 = winter wet. With these inputs, the weather generator performs the following calculations:

1. *Wet/Dry Day Transition Probabilities*: The probability of transitioning between wet and dry states was computed for each year on a seasonal basis over each study period. The time series of rainy days used to calculate these probabilities were derived from the daily timeseries of precipitation from the dynamically downscaled and statistically downscaled versions of the climate model, for each historical and future period, in order to capture any changes in precipitation frequency in the projections. A rainy day is defined as any day with 0.01 or more inches of rain.

Lower Santa Cruz River Basin Study Hydroclimate Analysis

2. *Weather Generation*: The weather generator process was repeated 100 times, running daily over 28-year-run lengths (used in the historic Sac-SMA runs) or 30 years for the future periods.
 - i. *Initial conditions*: Each simulation begins in January, assuming it is the winter wet season. The antecedent wet/dry state is sampled from all January 1st conditions for a given input timeseries (Sac-SMA historical period or the four future periods).
 - ii. *Wet/Dry State Transitions*: The occurrence of precipitation for a given day is based on the probability of transitioning out of the current state into the other for that season. For example, if the previous day was wet, and a given day in that season in the downscaled wet/dry time series transitioned from wet to dry 30% of the time, then approximately 30 of every 100 simulations results in a dry day and 70 in a wet day.
 - iii. *Precipitation Simulation*: A nonparametric approach to precipitation simulation is taken, wherein non-zero daily precipitation is sampled uniformly from within a window of time from the date being simulated. More specifically, if precipitation occurs for a given day (i.e., it was determined to be a wet day in the previous step), a day is randomly selected from all rainy days in a seven-day window centered on that day of the year from all years in the 28- to 30-year period. The date of the sampled precipitation values is retained for spatial disaggregation.
 - iv. *Temperature Simulation*: Temperature is less variable and simulated using a parametric approach. After determining if the simulated day is wet or dry, the temperature is calculated from an autoregressive linear equation with precipitation occurrence and mean monthly temperature as predictors. The equation includes lag-one persistence and adds variability using a random sample from a normal distribution centered on zero with a standard deviation equal to that of the residuals from the linear model for that month.
3. *Spatial disaggregation*: The outputs of precipitation and temperature averaged over the surface water model boundary area needed to be disaggregated to the elevation zones for surface water modeling. The pattern from the weather generator input timeseries for each scenario was remapped to the Sac-SMA elevation zones prior to averaging. For precipitation, the weather-generated area-wide value was multiplied by the ratios of elevation zone precipitation to the area average on the precipitation day sampled in step 2.iii. For temperature, the weather-generated area-wide value was added to the difference between the elevation zone temperature and the area-averaged temperature for the sampled day. For non-rainy days, the spatial temperature offsets were derived from that date in the Sac-SMA, LOCA, or WRF original inputs. This procedure results in a daily time series of precipitation and temperature at each elevation zone that is consistent with the best- and worse-case climate scenario spatial patterns.

4. *Temporal disaggregation*: Although the LOCA and WRF-MPI input simulations used here provide information for spatial disaggregation, they do not provide 1-hourly data needed for surface water modeling (see Table 1). The sub-daily patterns of precipitation (1-hourly) and temperature (6-hourly) for a given elevation zone are taken from the Sac-SMA historical calibration dataset. Out of the 28 years available in the Sac-SMA dataset, the day with the closest area-averaged precipitation value to the weather generated value for that day of the year was used to calculate the precipitation ratios and temperature offsets from the daily value to create sub-daily timeseries.

3.2. Validation

For additional details regarding the weather generator validation, see Appendix B.

3.3. Results

The resulting weather generated ensembles, depicted in Figure 16 and Table 5, indicate changes in seasonally averaged temperature and seasonal precipitation totals with respect to the historic period that are largely consistent with the changes in the input timeseries summarized in Table 4. Temperature consistently increases from the historical period to each future period. This increase is greater, as expected, for the worse-case scenario and into the far future (Figure 16, top row).

Extreme temperatures also increase in both scenarios, best depicted when looking at the most extreme temperatures (defined in Figure 17 as average daily temperatures that exceed the 99th percentile in that season, from all the years within a weather generated 30-year simulation). Extreme temperatures increase consistently in the future periods in every season, with the largest increases occurring in the dry and monsoon seasons (Figure 17), which are the spring and summer months when extreme temperatures pose the largest public health risk.

In the best-case scenario, the mean of the distribution of extreme dry season temperatures increases by 4.9°F in the 2030s and 4.5°F in the 2060s, relative to the historic period. The mean monsoon extreme temperature increases 3.5°F in the 2030s and 5.0°F in the 2060s. The increases in extreme temperatures are even larger under the worse-case scenario, with the dry season mean increasing by 5.3°F in the 2030s and 6.6°F in the 2060s. Mean monsoon season extreme temperatures increased 4.5°F in the 2030s and 7.1°F in the 2060s. The larger increases in the far future extreme temperatures reflect the emission scenario (RCP 8.5) underlying the worse-case climate, which does not include future emissions mitigation as the best-case does.

Seasonal precipitation changes in the best-case scenario, shown in the lower left panel of Figure 16, are relatively small and consistent in the dry season, when precipitation decreases through both future periods. Monsoon and winter season precipitation show opposite trends, with monsoon-season precipitation increasing in the near future but decreasing in the far future and winter season precipitation decreasing slightly in the near future but increasing slightly in the far future (Figure 16 bottom left).

**Lower Santa Cruz River Basin Study
Hydroclimate Analysis**

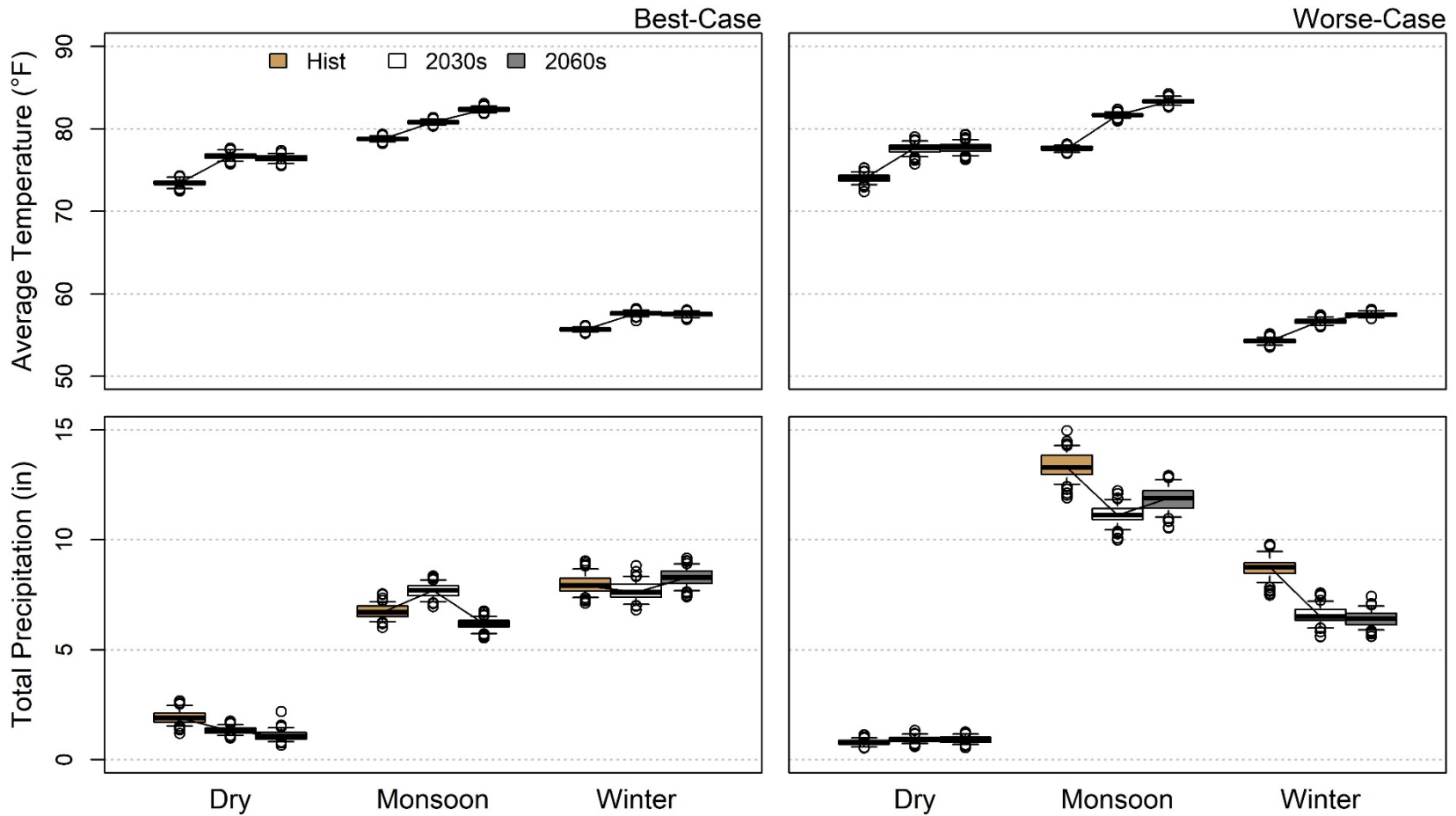


Figure 16 – Model simulated temperature averaged over the surface water model boundary area (top row) presented as a 30-year averaged seasonal mean and averaged precipitation for the same area presented as a 30-year averaged seasonal total (bottom row) for each period (colors), season (x-axis), and climate scenario (column). Boxplot distributions reflect the variability in the weather generator results from an ensemble that includes 100 sequences of 30 years each. The whiskers representing the 5th and 95th percentile of the ensemble.

Table 5 – Statistics of the Weather Generated Ensemble of Averaged Temperature for the surface water model boundary area. Top presents a 30-year averaged seasonal mean and basin-averaged precipitation. Bottom presents a 30-year averaged seasonal total for each period, season, and climate scenario.

		Mean Temperature (°F)					
		<u>Best-Case Simulation</u>			<u>Worse-Case Simulation</u>		
		Hist.	2030s	2060s	Hist.	2030s	2060s
Dry	5 th Percentile	72.8	76.1	75.8	73.2	76.6	76.8
	Mean	73.4	76.7	76.4	74.0	77.6	77.7
	Median	73.4	76.7	76.4	74.0	77.7	77.8
	Mode	72.5	75.8	75.6	72.4	75.8	76.3
	95 th Percentile	74.2	77.5	77.0	74.8	78.5	78.7
Monsoon	5 th Percentile	78.5	80.5	82.0	77.2	81.3	82.9
	Mean	78.8	80.8	82.4	77.6	81.7	83.4
	Median	78.8	80.8	82.4	77.6	81.7	83.3
	Mode	78.3	80.4	81.9	77.0	81.0	82.7
	95 th Percentile	79.2	81.2	82.8	78.0	82.1	84.0
Winter	5 th Percentile	55.4	57.2	57.1	53.8	56.2	57.1
	Mean	55.7	57.6	57.5	54.3	56.7	57.5
	Median	55.7	57.6	57.5	54.3	56.7	57.5
	Mode	55.2	56.7	56.9	53.5	56.0	57.0
	95 th Percentile	56.0	58.0	57.9	54.7	57.2	57.9

		Total Precipitation (inches)					
		<u>Best-Case Simulation</u>			<u>Worse-Case Simulation</u>		
		Hist.	2030s	2060s	Hist.	2030s	2060s
Dry	5 th Percentile	1.54	1.11	0.81	0.57	0.74	0.70
	Mean	1.92	1.33	1.09	0.79	0.93	0.92
	Median	1.89	1.31	1.05	0.77	0.92	0.91
	Mode	1.20	0.98	0.67	0.54	0.59	0.55
	95 th Percentile	2.46	1.59	1.44	0.99	1.17	1.16
Monsoon	5 th Percentile	6.28	7.19	5.73	12.5	10.5	11.0
	Mean	6.73	7.69	6.17	13.4	11.2	11.8
	Median	6.71	7.70	6.18	13.3	11.1	11.9
	Mode	6.02	6.96	5.55	11.9	10.0	10.5
	95 th Percentile	7.18	8.17	6.52	14.3	11.8	12.7
Winter	5 th Percentile	7.38	7.07	7.69	8.05	5.99	5.91
	Mean	7.95	7.67	8.29	8.72	6.57	6.41
	Median	7.92	7.62	8.28	8.75	6.51	6.42
	Mode	7.13	6.81	7.42	7.49	5.59	5.61
	95 th Percentile	8.67	8.33	8.91	9.46	7.20	6.99

**Lower Santa Cruz River Basin Study
Hydroclimate Analysis**

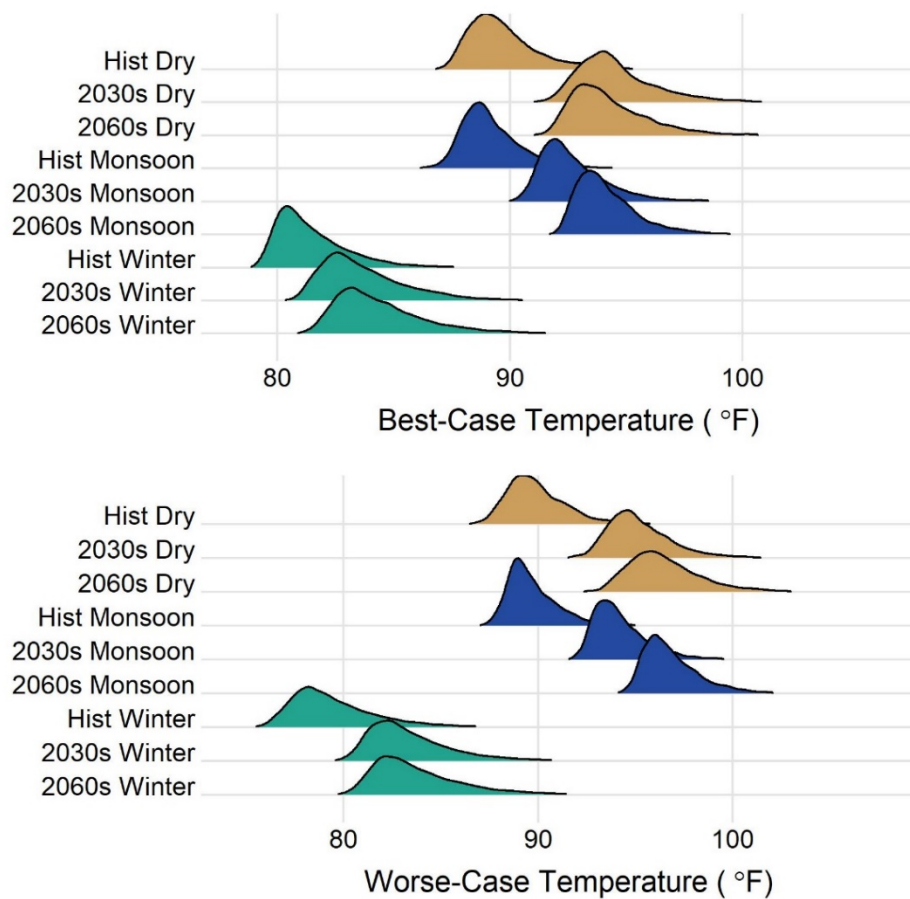


Figure 17 – Distributions of extreme daily temperatures, averaged over the surface water model boundary area, by period and season.

The weather generator was built around the assumption that the GCM and downscaling procedures adequately capture the seasonal and synoptic events. Here, the weather generator magnifies LOCA-MPI’s lack of larger monsoon events to sample from in the best-case. In contrast, the worse-case scenario, derived from WRF-MPI, contains high precipitation days (see Table 2) that may be larger than previously observed and provides a wider range for the weather generator to sample over.

For example, future precipitation in the worse-case scenario generally decreases in the monsoon and winter seasons and shows little change in the dry season (Figure 16 bottom right). The slight rebound in far future monsoon precipitation relative to the near future may reflect longer monsoon seasons in the far future or larger individual extreme events, indicated by the upward extension of the 2060s distribution in Figure 18. Greater variability in worse-case weather generated seasonal totals mirrors the greater variability in worse-case season lengths (see Figure 15).

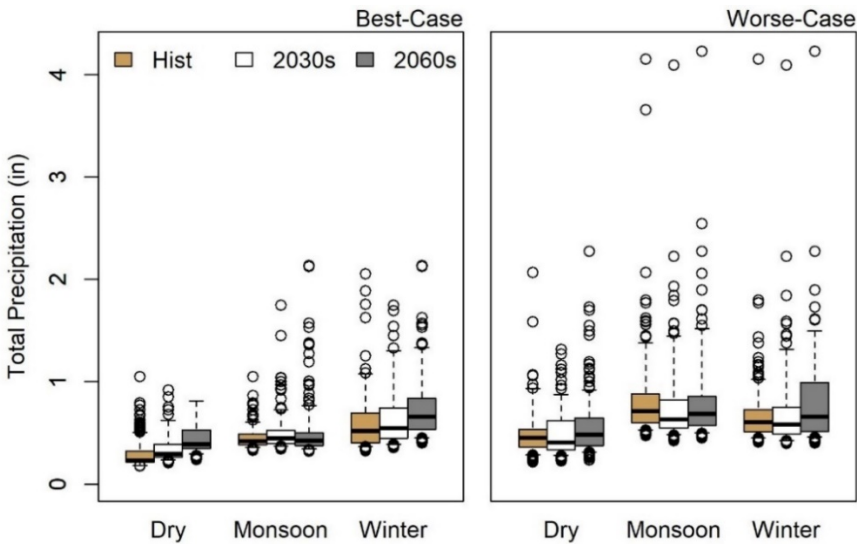


Figure 18 – Boxplot of extreme daily precipitation by season, period, and climate scenario.

Detection of changes in extreme precipitation events from daily, gridded modeled outputs is challenging because monsoon events are often short but intense, occur over small areas, and are highly variable in time and space. Rainfall observations in southeastern Arizona indicate an intensification of monsoon precipitation starting in the mid-1970s (Demaria et al., 2019), suggesting the historical period for this study has already experienced changes in climate processes.

Retrospective modeling using WRF at a convective permitting scale (about 3 km) since the 1990s also identified increased precipitable water and atmospheric instability typical of extreme monsoon events (Luong et al., 2017). This intensification is muted and the model processes simplified at the scale of the daily-averaged 25 km worse-case input data, similar to the smoothing noted at the Sac-SMA subbasin scale noted in Shamir et al. (2019). Limited observations or interpolation may also affect the intensification in the statistically downscaled simulations, although an increase in the largest monsoon events is apparent (Figure 18) but not necessarily tied to local physical properties.

Despite these limitations, both the weather generated best- and worse-case scenarios include changes in extreme precipitation events. Here, extreme precipitation is defined as daily rainy-day precipitation that exceeds the 90th percentile in that season, from all the years within a weather generated 30-year simulation. Statistics of the 30-year simulation represent shifts in climatology and the weather generated ensembles provide additional uncertainty in extreme precipitation between scenarios (Table 6).

**Lower Santa Cruz River Basin Study
Hydroclimate Analysis**

Table 6 – Statistics of Extreme Precipitation from the Weather Generator Ensemble

		Extreme Precipitation (inches)					
		Best-Case Simulation			Worse-Case Simulation		
		Hist.	2030s	2060s	Hist.	2030s	2060s
Dry	5 th Percentile	0.19	0.24	0.30	0.29	0.28	0.31
	Mean	0.28	0.34	0.44	0.50	0.49	0.53
	Median	0.23	0.30	0.39	0.45	0.41	0.49
	Mode	0.22	0.24	0.39	0.46	0.64	0.55
	95 th Percentile	0.51	0.62	0.82	0.94	0.88	0.92
Monsoon	5 th Percentile	0.36	0.37	0.34	0.53	0.48	0.50
	Mean	0.45	0.48	0.47	0.82	0.76	0.81
	Median	0.42	0.45	0.43	0.72	0.63	0.69
	Mode	0.40	0.41	0.51	1.56	0.67	1.90
	95 th Percentile	0.60	0.73	0.77	1.38	1.45	1.52
Winter	5 th Percentile	0.37	0.39	0.46	0.45	0.43	0.46
	Mean	0.60	0.66	0.74	0.66	0.67	0.80
	Median	0.52	0.55	0.66	0.61	0.59	0.66
	Mode	0.38	1.05	0.49	0.67	0.51	1.46
	95 th Percentile	1.08	1.30	1.34	1.02	1.32	1.50

Changes in the central tendency across the ensembles of extreme precipitation are not consistent, although increases in extreme winter precipitation are suggested by both the mean and the median statistics. The more severe ensemble extremes (that is, the 95th percentile) consistently increase through time in the both the monsoon and winter seasons. Maximum values represent less than 1% of extremes and can exceed 4 inches per hour in the worse-case scenario.

Figure 18 portrays these changes by illustrating the distribution of the precipitation values in the top 10 percent of each 30-year simulation. Changes in extremes are depicted by either a shift in the box and whiskers or by an upward spread of the box. A shift in the box is equivalent to changes in the central tendency of the data. For example, the winter season shifts upward under both cases, indicating a general increase in the magnitude of daily precipitation extremes. A spread upward indicates more isolated extreme events of greater magnitude, similar to the increase in monsoon and winter season events in the 95th percentile shown in Table 6 and Figure 19.

Increases in the general magnitude of extreme events is more apparent in the best-case scenario while the increase in larger individual events, particularly in the winter season, is more apparent in the worse-case scenario. This is consistent with the nature of the LOCA downscaling procedure, which may not be able to capture changes in individual events as well as the physically-based dynamically downscaled procedure used for the worse-case scenario.

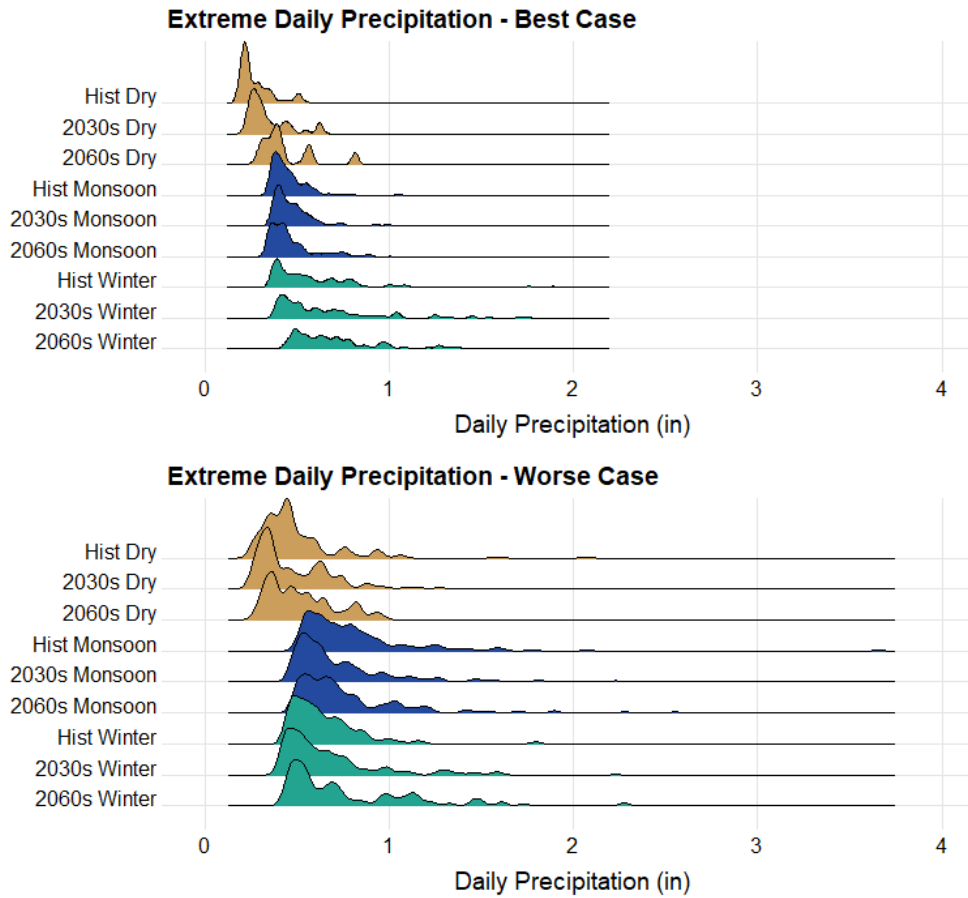


Figure 19 – Distribution of extreme daily precipitation by season, period, and climate scenario.

4. Surface Water Modeling

4.1. Sac-SMA Model

4.1.1. Description

The 100-projection ensembles of future temperature and precipitation created by the weather generator were used as input in a surface water model to derive a range of streamflows. Potential evapotranspiration (PET) is also needed for the Sacramento Soil Moisture Accounting surface water model. The method for estimating PET is described in Section 4.1.2.

The hydrologic simulation for this study uses the National Weather Service’s Colorado Basin River Forecast Center’s (CBRFC)⁸ calibrated Sac-SMA model of the Lower Santa Cruz River Basin and contributing watersheds, including the SNOW-17 model in elevation zones where snowfall is important. This model is part of the CBRFC’s operational streamflow modeling system, with a focus on simulating the antecedent soil conditions that drive the runoff response. The CBRFC calibrates the model by adjusting parameters for each subarea to match the daily-averaged observed streamflow at the basins’ outlets. The model available at the time of this study was calibrated from 1970-1999.

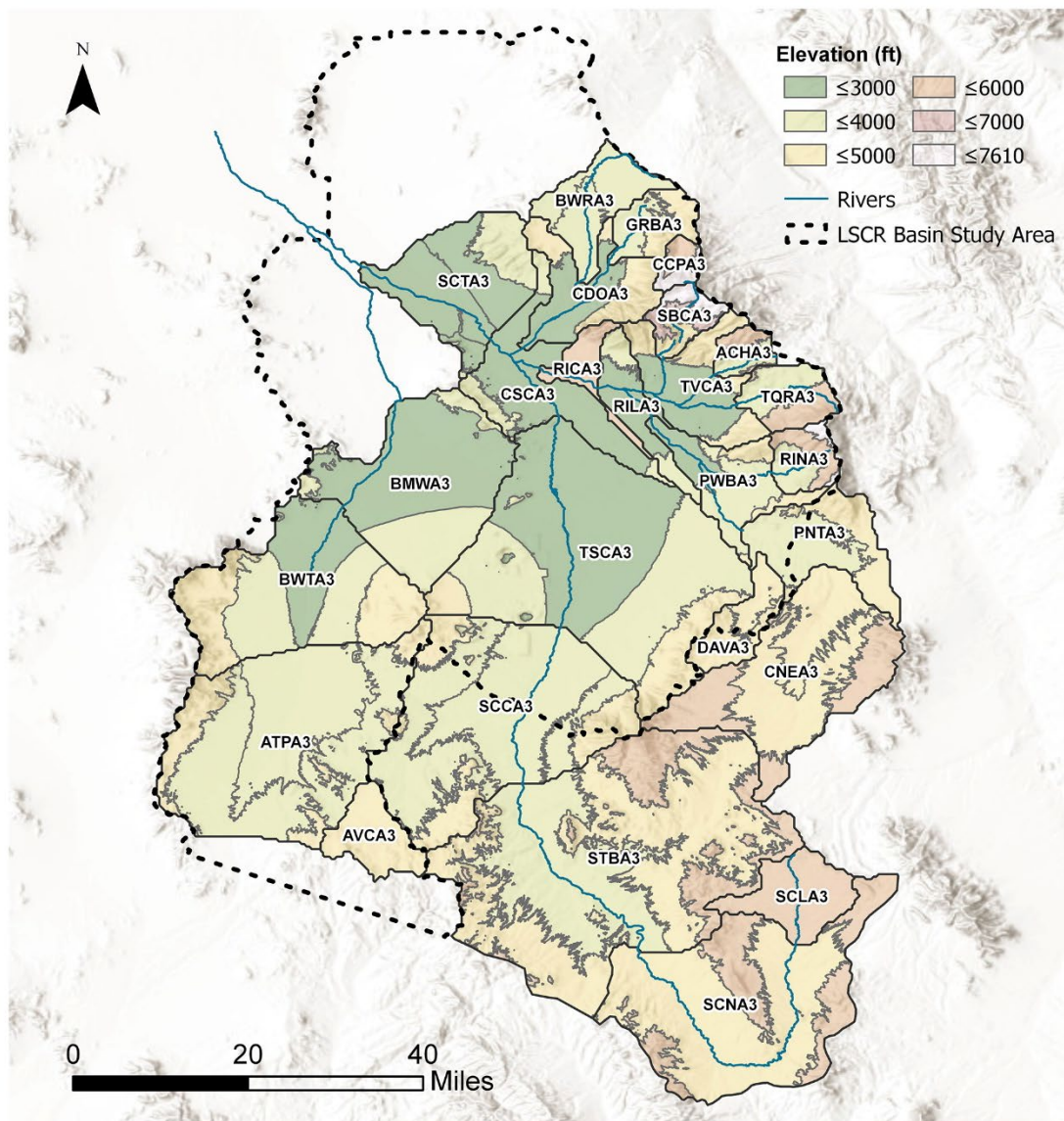
The Sac-SMA model simulates mechanisms that drive water movement through the soil column (surface runoff, infiltration, interflow, percolation, storage, evapotranspiration, and baseflow) while preserving the water balance. Additional information on how Sac-SMA calculates soil moisture and a diagram of the soil storage compartments and fluxes are provided in Section 4.3.

The Sac-SMA hydrologic model used by the CBRFC is run in a lumped framework, meaning parameters are averaged over elevation zones within the subbasins that make up a watershed. Each subbasin may include up to three elevation zones (Figure 20), depending on the topography, vegetation, and snowpack patterns in the basin. The surface water model boundary area used in this study has 26 subbasins divided into a total of 59 elevation zones, where the average size of an elevation zone is 79 square miles. Many subbasins are delineated to align outlets with available streamflow observations. Modeled streamflow for each subbasin is reported at the outlet where the river or stream leaves the subbasin.

The use of constant areal-averaged parameters—and perhaps more importantly, areal-averaged precipitation may limit a model’s ability to capture diverse streamflow responses. Areal averaging may dampen the response to intense local storms, characteristic of convective summer rainfall events in the region (Shamir et al., 2019). However, this is true of most hydrologic models that can be run operationally in this region, and the model used here has the added benefit of years of CBRFC development.

⁸ <https://www.cbrfc.noaa.gov/>

Lower Santa Cruz River Basin Study Hydroclimate Analysis



ID	DESCRIPTION	ID	DESCRIPTION
ACHA3	AGUA CALIENTE WASH - HOUGHTON RD	PWBA3	PANTANO WASH - BROADWAY BLVD.
ATPA3	ALTAR WASH - NR THREE POINTS AZ	RICA3	RILLITO CREEK - LA CHOLLA BLVD AT
AVCA3	ARIVACA CK AT ARIVACA AZ	RILA3	RILLITO CREEK - TUCSON AT DODGE BLVD.
BMTA3	BRAWLEY WASH - AT MILEWIDE RD	RINA3	RINCON CREEK - NR TUCSON
BWRA3	BIG WASH - CAÑADA DEL ORO	SBCA3	SABINO CREEK - NR TUCSON
BWTA3	BRAWLEY WASH - THREE POINTS	SCCA3	SANTA CRUZ - CONTINENTAL
CCPA3	CAÑADA DEL ORO - CORONADO CAMP	SCLA3	SANTA CRUZ - NR LOCHIEL
CDOA3	CAÑADA DEL ORO - BLO INA RD NR TUCSON	SCNA3	SANTA CRUZ - NR NOGALES
CNEA3	CIENEGA CK - NR SONOITA	SCTA3	SANTA CRUZ - TRICO RD AT MARANA NR
CSCA3	SANTA CRUZ - AT CORTARO	STBA3	SANTA CRUZ RIVER - AT TUBAC AZ
DAVA3	DAVIDSON CANYON	TQRA3	TANQUE VERDE - GUEST RANCH
GRBA3	CAÑADA DEL ORO - GOLDER ROAD BRIDGE	TSCA3	SANTA CRUZ - AT TUCSON
PNTA3	PANTANO WASH - NR VAIL	TVCA3	TANQUE VERDE - TUCSON

Figure 20 – Sac-SMA elevations by elevation zone for each labeled subbasin. The LSCR Basin Study area is shown using a thick black outline with subbasins outlined with a thinner gray line. Elevation zones are not always continuous across a subbasin.

4.1.2. Input Development

In addition to calibrated model parameters obtained from the CBRFC, the model requires subdaily mean areal precipitation (MAP at 1-hour time resolution), mean areal temperature (MAT at 6-hour time resolution), and mean areal monthly PET. The weather generator process with the space-time disaggregation described in Section 3.3 produces MAP and MAT files at the spatial (elevation zone) and temporal (subdaily) scale required to run Sac-SMA.

To account for the effect of warmer future temperatures on PET, future scenarios scale the existing monthly PET in the calibrated model by the ratio of the temperature-based PET calculated with the Hamon method (Hamon, 1963), using calibrated Sac-SMA and weather-generated temperatures. Temperature averaged over the surface water model boundary area is used for these PET calculations and the subbasin scalars used in the calibrated model are retained to provide consistent spatial variability in PET.

4.2. Future Surface Water Discharge

4.2.1. Change in Seasonal Streamflow

Changes in seasonal streamflow, presented as a fraction of the simulated historical period flow, are presented in Figures 21 – 23. Note that these figures have scales tailored to the range of model results. This has been done to highlight the detail within each season's range of values.

Historically, most surface water subbasins in the study area experience no flow conditions in the dry season, particularly those in the valley bottom (Figure 21, left panel). Long periods without rainfall continue to characterize the dry season under future scenarios. Thus, small changes in streamflow result in numerically large fractional increases and decreases in streamflow that are not particularly meaningful to water supply and water resources planning (Figure 21).

Changes in the total monsoon seasonal streamflow result from changes in the length of the season, intensity, and frequency of storms. In the near future, the best-case scenario has a consistently longer monsoon season (see Figure 12) resulting in more total flow over this season. Streamflow decreases in some subbasins in the far future, particularly in subbasins that experience larger increases in no flow days, as discussed in Section 4.2.2.

Under the worse-case scenario, the near future appears to be a transition time, with generally shorter, but highly variable monsoon season length. The changes in monsoon seasonality result in decreased ensemble median streamflow (Figure 22), but high variability in seasonal totals from year to year.

In the far future, the longer monsoon season results in an apparent recovery of streamflow; however, streamflow events are less frequent (Section 4.2.2) and likely more extreme, consistent with the increase in individual large precipitation events under this scenario (see Figure 18 and Table 6). Larger precipitation events can have a disproportionate change on streamflow, since proportionally less water can infiltrate under the SAC-SMA model configuration. Thus, small increases in seasonal precipitation may result in large modeled increases in seasonal streamflow when large runoff events occur.

**Lower Santa Cruz River Basin Study
Hydroclimate Analysis**

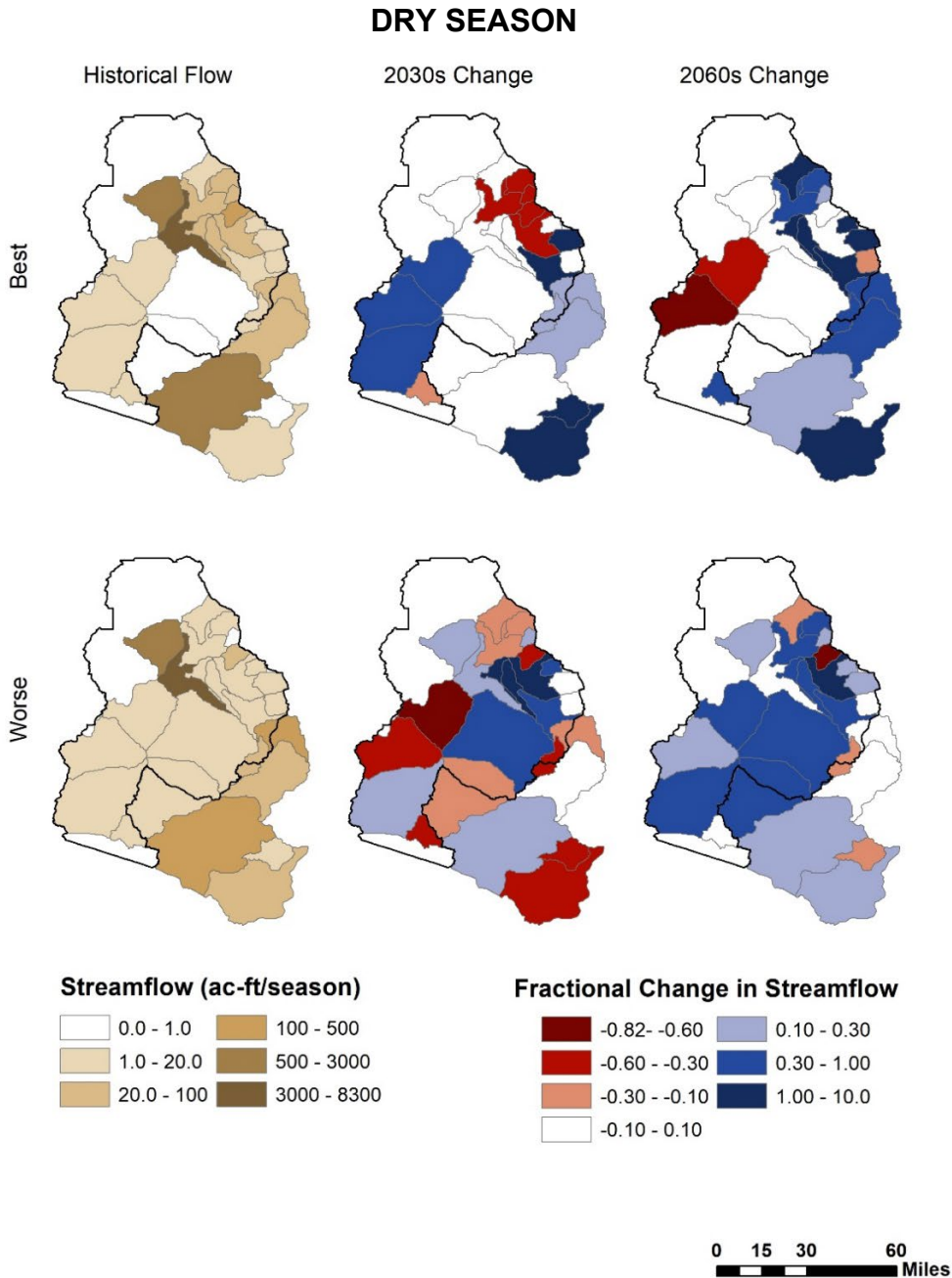


Figure 21 – Median of the ensemble 30-year average dry season total streamflow from the modeled historical period (tan) for each scenario, and projected change from historical (red for negative and blue for positive change respectively) in streamflow for the best- and worse-case climate scenarios. Note coverage is only over the areas identified as subbasins in Figure 20.

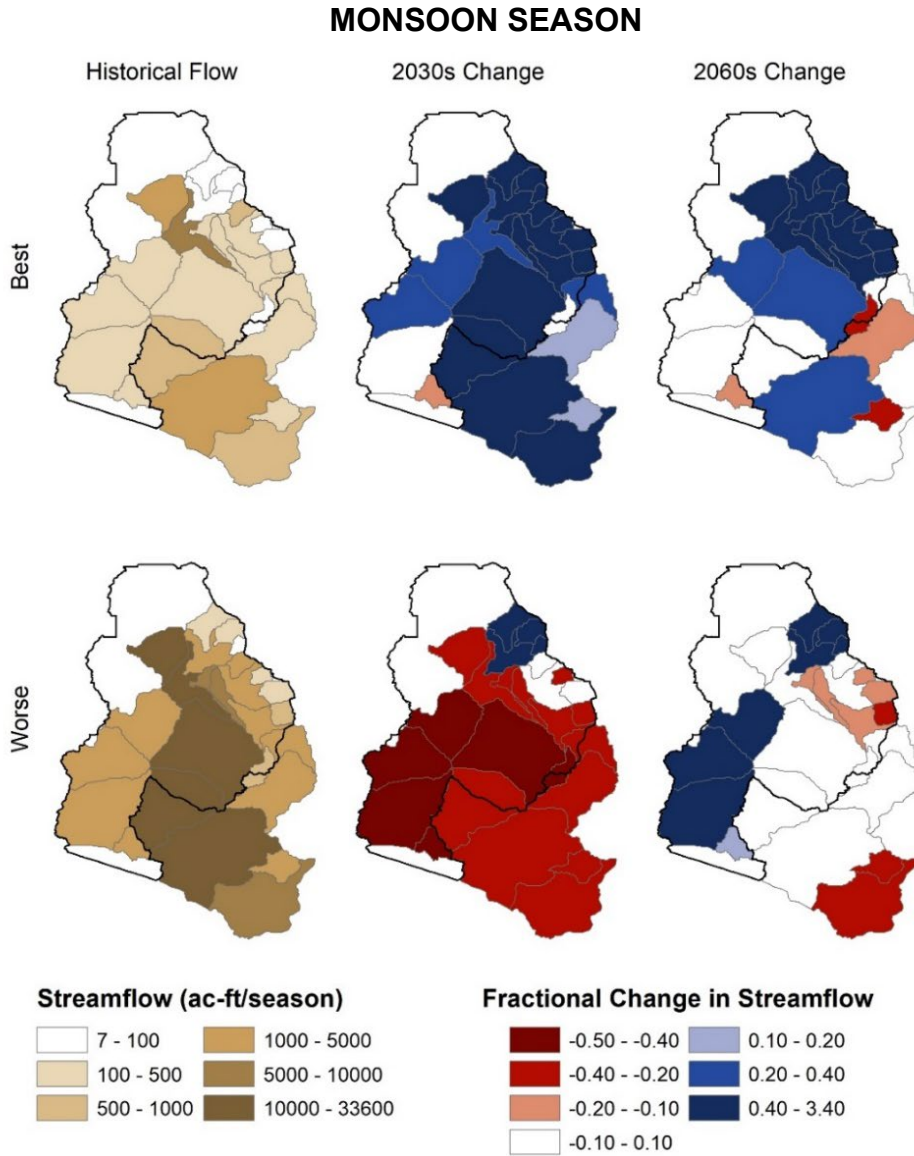


Figure 22 – Similar to Figure 21 but for the monsoon season.

The winter season shortens into the future under both scenarios. In the best-case scenario, the large events get consistently larger into the future (Figure 23), which compensates for the shortening of the season. In the worse-case scenario, total winter precipitation is consistently less under both future periods and this change in precipitation is reflected in reduced streamflow. Large precipitation events do not increase in the near future, resulting in little compensation for the shortening of the season; however, in the far future, more extreme precipitation likely results in some streamflow recovery.

**Lower Santa Cruz River Basin Study
Hydroclimate Analysis**

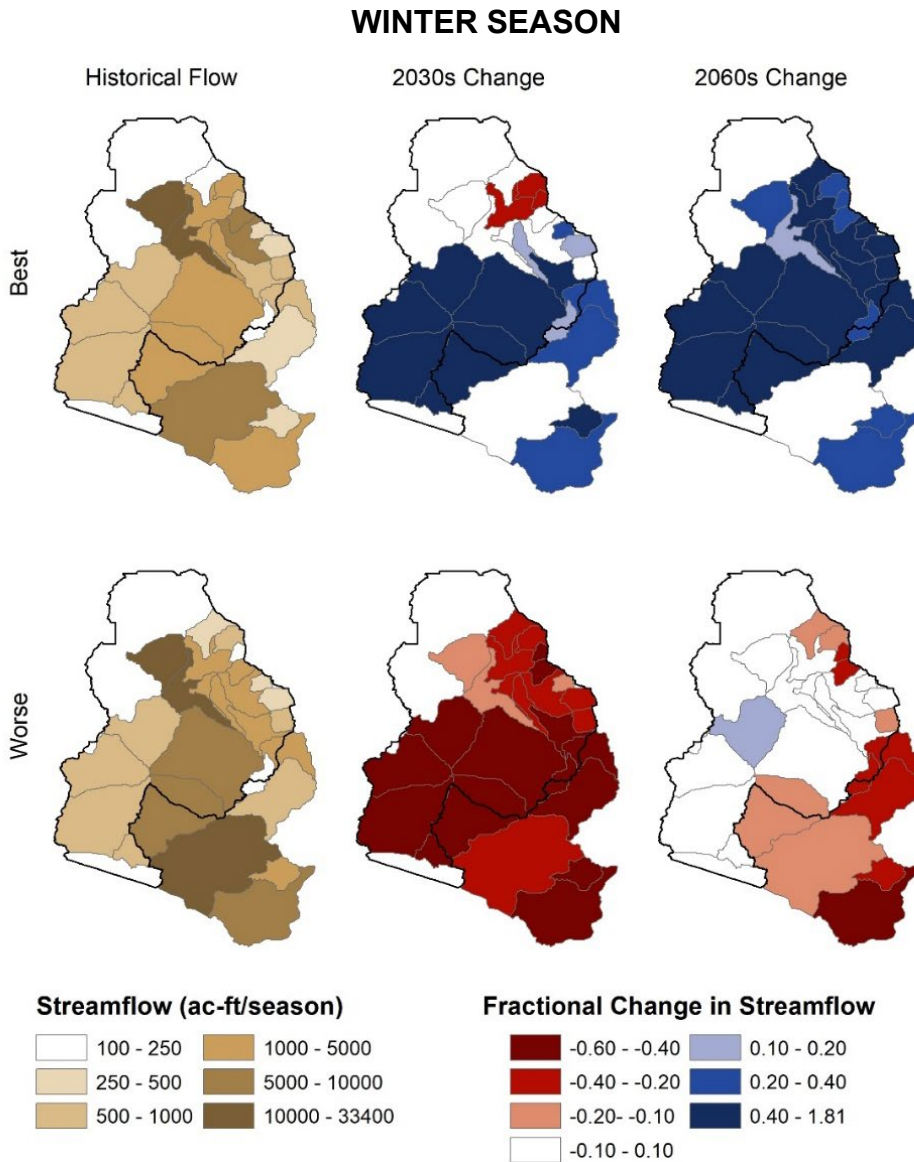


Figure 23 – Similar to Figure 21 but for the winter season.

Table 7 summarizes the ensemble statistics of historical streamflow and future change for select subbasins. The subbasins were selected to span a range of modeled flow regimes, ranging from year-round, or perennial, flow at Upper Cienega Creek (CNEA3), to streams that only flow in response to precipitation events during the dry season (ephemeral streams), to seasonal, or intermittent, flow that dries up in the spring at Rillito Creek at La Cholla (RICA3).

Note that the percent change under future scenarios is the change in that ensemble statistic. For example, Table 7 presents the change in the ensemble’s 95th percentile for the 30-year averaged seasonal total streamflow, not the 95th percentile of the change. CBRFC’s Sac-SMA modeled flows are also provided and represent the 30-year average of total acre-feet per season. The historical winter season is consistently higher and likely skewed by the 1983 flood that occurred during this period. This event may not have been well-captured in the LOCA and WRF historical period simulations.

**Lower Santa Cruz River Basin Study
Hydroclimate Analysis**

Table 7 – Statistics of Period-Averaged Seasonal Total Streamflow Ensembles for Each Scenario, Period, Season, and Selected Subbasins. Historical flows are in ac-ft/season and future periods are presented as the percent change from historical in the ensemble statistic.

Upper Cienega Creek (CNEA3)		<u>Sac-SMA</u>	<u>Best-Case Simulation</u>			<u>Worse-Case Simulation</u>		
		Hist	Hist	2030s	2060s	Hist	2030s	2060s
Dry	5 th Percentile	217	11.2	35%	72%	44.8	0.6%	-5.4%
	Mean		24.7	10%	46%	67.8	-6.2%	-2.3%
	Median		22.6	15%	54%	60.4	-3.8%	1.0%
	95 th Percentile		45.5	-12%	26%	147	-35%	-40%
Monsoon	5 th Percentile	1698	103	17%	-16%	1276	-43%	-12%
	Mean		163	13%	-17%	2183	-34%	7.8%
	Median		159	13%	-18%	2125	-32%	1.4%
	95 th Percentile		238	13%	-16%	3192	-25%	36%
Winter	5 th Percentile	2569	181	34%	60%	554	-37%	-27%
	Mean		282	37%	51%	887	-46%	-5.0%
	Median		268	39%	57%	869	-45%	-25%
	95 th Percentile		456	22%	24%	1319	-52%	35%

Rillito Creek-La Cholla (RICA3)		<u>Sac-SMA</u>	<u>Best-Case Simulation</u>			<u>Worse-Case Simulation</u>		
		Hist	Hist	2030s	2060s	Hist	2030s	2060s
Dry	5 th Percentile	537	1.20	-55%	-33%	0.09	69%	895%
	Mean		36.4	37%	97%	25.7	159%	24%
	Median		21.2	-10%	112%	6.90	214%	44%
	95 th Percentile		117	51%	106%	118	137%	23%
Monsoon	5 th Percentile	5812	161	248%	350%	3057	-50%	-8.8%
	Mean		451	165%	248%	8192	-29%	-12%
	Median		372	208%	286%	7540	-24%	-17%
	95 th Percentile		946	166%	194%	14846	-27%	-7.0%
Winter	5 th Percentile	18129	2640	12%	138%	2118	-29%	-8.7%
	Mean		5096	10%	101%	5129	-36%	3.1%
	Median		4539	9.1%	118%	4457	-31%	-2.1%
	95 th Percentile		9667	2.5%	50%	9493	-31%	3.8%

**Lower Santa Cruz River Basin Study
Hydroclimate Analysis**

Sabino Creek-Nr Tucson (SBCA3)		Sac-SMA Hist	Best-Case Simulation			Worse-Case Simulation		
			Hist	2030s	2060s	Hist	2030s	2060s
Dry	5 th Percentile	838	217	-32%	-6.6%	23.2	-65%	-74%
	Mean		388	-28%	-2.0%	48.0	-33%	-46%
	Median		368	-35%	-6.0%	42.4	-56%	-60%
	95 th Percentile		576	-4.2%	18%	86.5	57%	-6.4%
Monsoon	5 th Percentile	2281	379	66%	22%	667	-33%	-23%
	Mean		549	75%	44%	1067	-8.9%	-5.1%
	Median		528	73%	52%	1015	-6.0%	-2.9%
	95 th Percentile		732	114%	62%	1608	1.1%	-0.1%
Winter	5 th Percentile	10005	4581	-16%	44%	1362	-46%	-45%
	Mean		6435	-8.4%	32%	2070	-43%	-32%
	Median		6145	-5.5%	39%	2024	-45%	-34%
	95 th Percentile		8660	-6.1%	24%	2990	-43%	-23%

4.2.2. Change in Dry Days

Historically, the surface water systems in the surface water model boundary area are overwhelmingly ephemeral or intermittent, meaning that few locations in the area have streamflow all year long. A dry day is defined as any day with no flow modeled at the subbasin outlet. Figure 24 illustrates the ephemeral nature of the area, displaying the number of dry days at gaged concentration points calculated as average of the ensemble median over 30-year periods for the worse-case scenario. Thus, year-round flow, as seen for the Cienega Creek (CNEA3), may be a very small amount of modeled flow. It is also important to note that locations downstream of the wastewater treatment plants (CSCA3 and SCTA3) receive continuous recycled water contributions and thus also flow year-round.

The change in the number of streamflow dry days between the historical period and modeled future periods under the worse-case scenario are presented in Figure 25 for the 2030s and Figure 26 for the 2060s. The largest increases in no-flow days consistently occur in headwaters subbasins, such as the Sabino Creek and the Santa Cruz near Nogales. These increases tend to be largest where the modeled subbasins are not fully perennial streams but have at least some flowing days every month. This change suggests that these transitional basins may experience longer no-flow periods in the future. Larger increases consistently occur in the spring during the transition to the dry season, but also occur in August during the monsoon season. The later onset of the monsoon season in the 2030s relative to the 2060s is likely the reason why there are more dry days in these transition months in the near future.

The worse-case is provided here, showing larger changes as determined by this modeling effort. The corresponding best-case figures are provided in Appendix C.

Lower Santa Cruz River Basin Study Hydroclimate Analysis

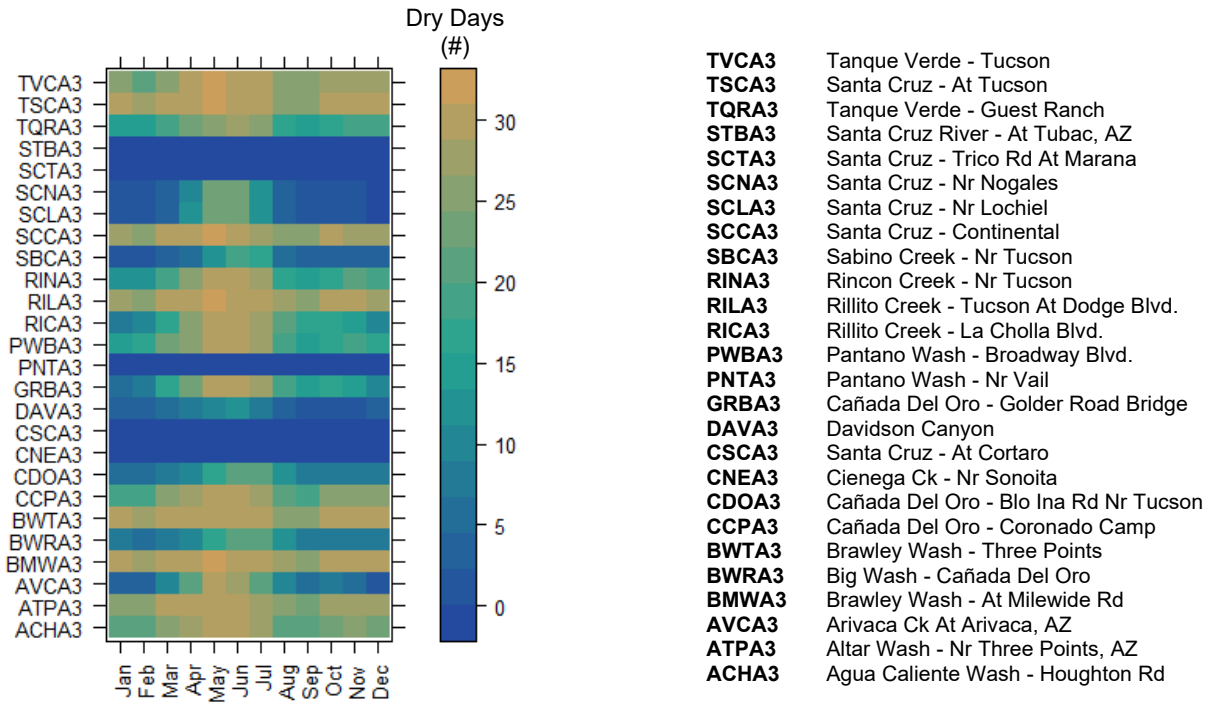
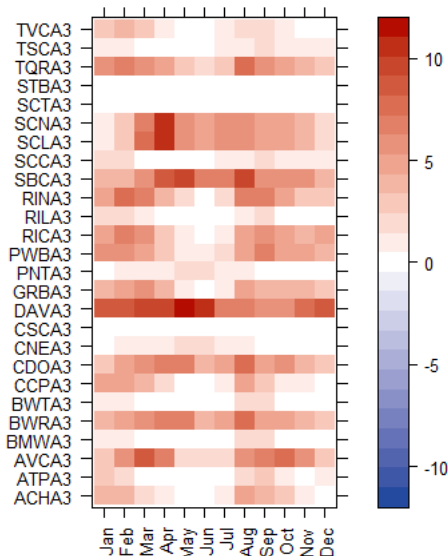


Figure 24 – The number of modeled historical dry days per month under the worse-case scenario for each Sac-SMA subbasin, abbreviated in the plot but defined on the right. Tan colors indicate months when the stream is dry the entire month, while the dark blue represents streams that flow the whole month.

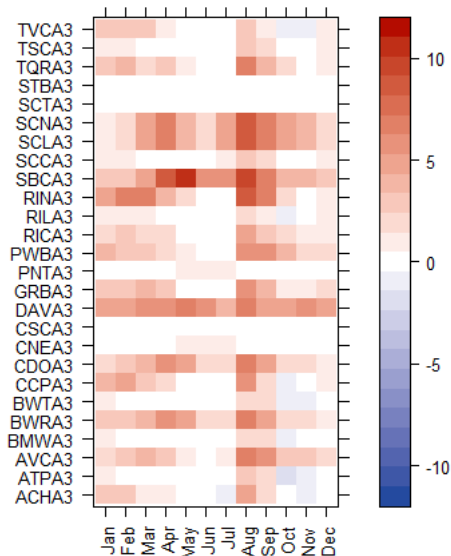


2030s - Top 5 increases in dry days month # days

Davidson Canyon (DAVA3)	May	12
Davidson Canyon (DAVA3)	June	11
Santa Cruz near Nogales (SCNA3)	April	10
Santa Cruz near Lochiel (SCLA3)	April	10
Sabino Creek (SBCA3)	May	10

Figure 25 – Change in the number of dry days per month in the near future for each subbasin under the worse-case climate scenario. The table to the right provides details on the subbasins and months with the top five increases in dry days under near future conditions.

Lower Santa Cruz River Basin Study Hydroclimate Analysis



2060s - Top 5 increases in dry days month # days

Sabino Creek (SBCA3)	May	10
Sabino Creek (SBCA3)	August	10
Sabino Creek (SBCA3)	April	9
Santa Cruz near Lochiel (SCLA3)	August	9
Santa Cruz near Nogales (SCNA3)	August	9

Figure 26 – Change in the number of dry days per month in the far future for each subbasin under the worse-case scenario. The table to the right provides details on the subbasins and months with the top five increases in dry days under far future conditions.

4.3. Soil Moisture

In addition to its role in streamflow generation, soil moisture supports upland vegetation communities and determines the amount of water needed for irrigation. Sac-SMA calculates sub-daily soil moisture for each elevation zone. Calculations include two soil layers: a fast-responding upper layer (about 20 centimeters) and a deeper (lower) layer that can extend to 60 inches, depending on the soil depth. Each layer is broken into tension and free water.

Free water is water controlled by gravity and can percolate to deeper soil layers. From the soil, it can return to the stream either as interflow from shallow layers or as baseflow from deeper layers. Tension water is held tightly in the soil by tension processes and can only be removed through evapotranspiration or diffusion. Storage and subsequent drainage from the deeper layer indicate a basin's antecedent conditions between runoff events. Deep storage is partitioned into fast (sub-daily to weeks) and slow (weeks to seasonally) draining reservoirs (Figure 27).

Changes in soil moisture generally mirror changes in precipitation under future climate scenarios. For the best-case scenario, soil moisture generally increases in the fall and winter, particularly in the far future, and decreases in the far future monsoon season months of July and August (see Appendix C, and for an example, Figure C2 for the Lower Cienega Creek subbasin).

The worse-case scenario is drier, with nearly all soil water zones indicating decreases in soil moisture in both the near and far future as exemplified by tension water in Figure 27. Model results indicate that more water is stored as tension water than free water; for an example see the moisture partitioning between free and tension water in both the upper and lower soil moisture layers in the Lower Cienega Creek subbasin depicted in Figure 27. This is consistent with the Arizona Department of Water Resources (ADWR) TAMA groundwater model inputs, which do

not include distributed recharge (from free drainage) but assume all soil water is lost through evapotranspiration.

The exceptions are the transitions to the dry season in May and the fall months in the far future, which suggest wetter soils during these periods. These soil moisture increases tend to occur in the lower-elevation, drier, portions of the area where large percentages of change may represent small increases in moisture. The higher elevation and wetter subbasins in the Santa Catalina and Rincon Mountains still decrease in soil moisture throughout the year. These high elevation subbasins are not located within the TAMA but contribute recharge to the basin through the lateral transfer of water through the mountain block to the basin boundaries, or via local return flow to streams. The subsequent changes in these mountain recharge processes warrant additional consideration and study, although existing studies of the nearby San Pedro watershed suggest mountain system recharge will decrease (summarized in Meixner et al., 2016).

Lower Santa Cruz River Basin Study
Hydroclimate Analysis

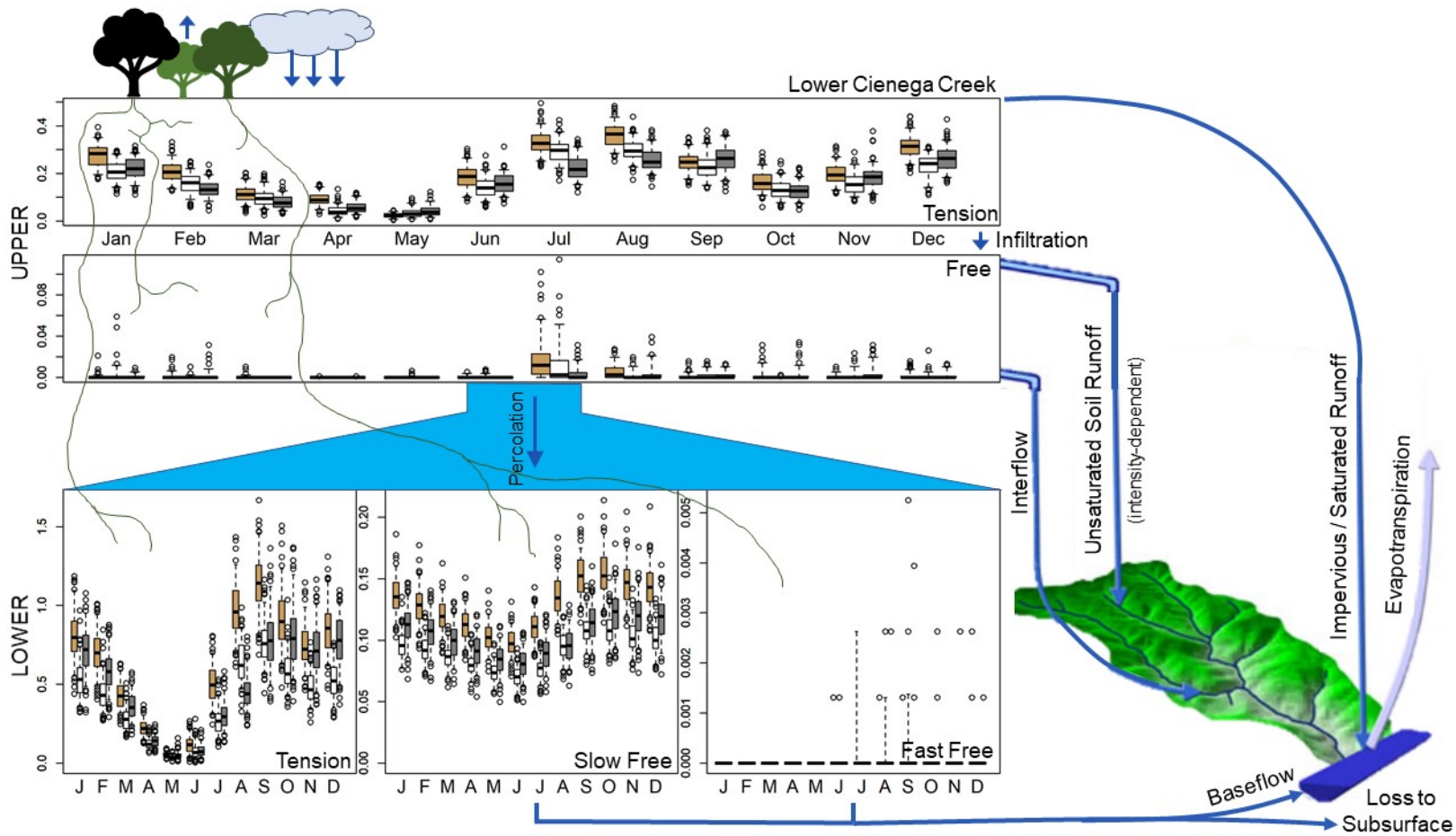


Figure 27 – Monthly averaged worst-case scenario soil moisture (inches) in each compartment of the Sac-SMA Cienega Creek lower elevation zone. Tan boxes are modeled historical distributions spanning the range of uncertainty from the weather generator simulations, white is near future, and gray is far future. Compartments include two in the upper layer (tension water and free water) and three in the deeper lower layer (tension water, and fast and slow draining free water). Graphics modified from https://www.cbrfc.noaa.gov/wsup/sac_sm/cbrfc_sacsma_101_20140731.pdf.

Lower Santa Cruz River Basin Study
Hydroclimate Analysis

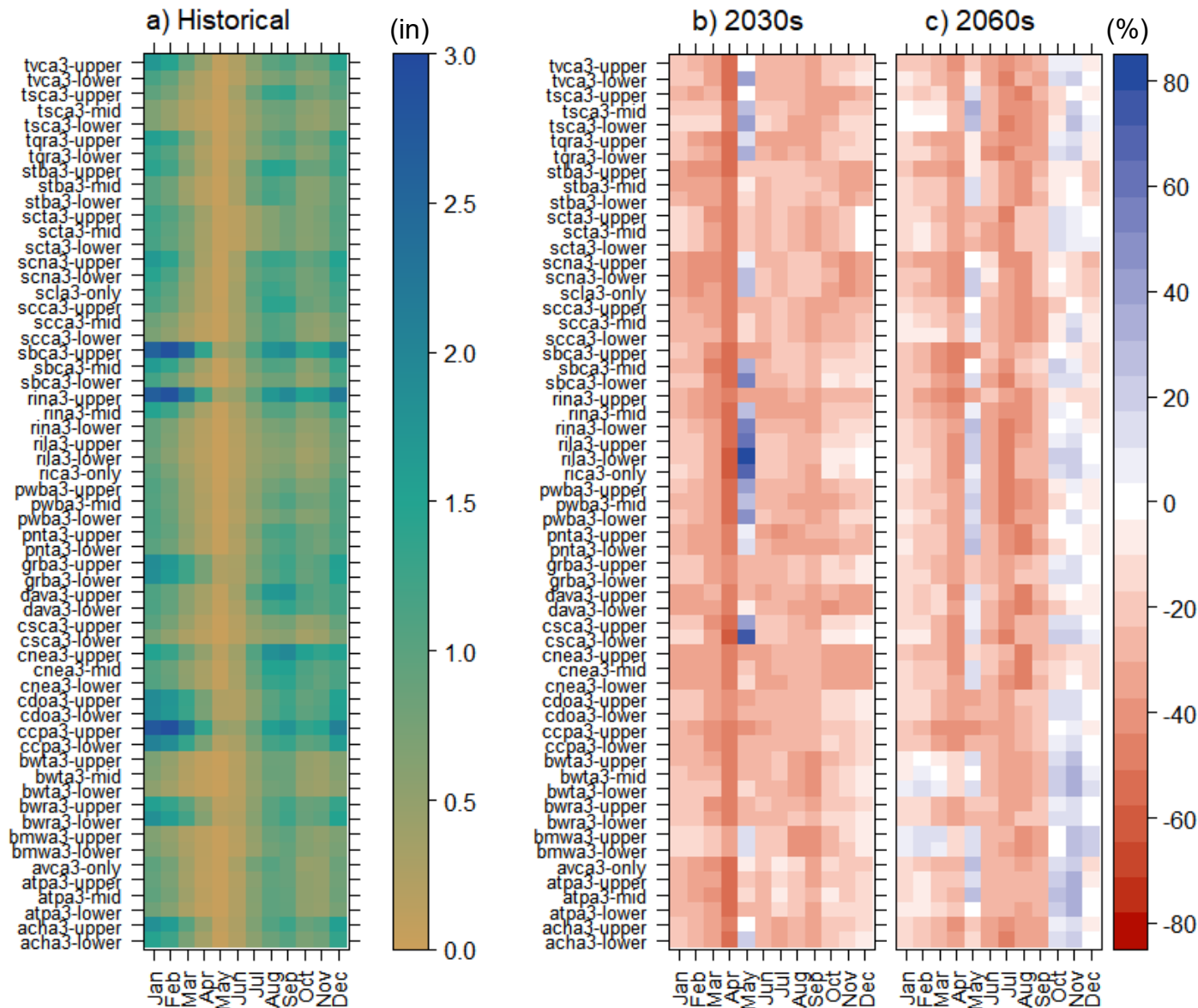


Figure 28 – Ensemble median, monthly average of the total tension water (sum of upper and lower soil zones) under the worse-case climate scenario for: a) modeled historical tension water in inches, b) near future change, and c) far future change as a percent relative to the historical period.

For soil moisture change, blue indicates an increase and red indicates a decrease. Results are presented for each elevation zone.

4.4. Evapotranspiration

Evapotranspiration (ET) is the movement of water from the ground, water surface, or vegetation to the air through evaporation or plant transpiration. In the LSCR basin, precipitation across the landscape rarely percolates deep enough to recharge the regional groundwater system before it is evaporated. The ADWR TAMA groundwater model, for example, does not include recharge from precipitation distributed across the landscape, assuming that the contribution is negligible relative to other sources of recharge (streamflow, mountain front, artificial recharge, etc.). Evapotranspiration is also expected to play a larger role in the water budget of the larger Colorado River system as the climate warms (e.g., Udall and Overpeck 2017).

Sac-SMA calculates actual ET by limiting PET to the amount of available water. Actual ET therefore reflects both changes in temperature (through adjusted PET) and changes in precipitation. Overall, the amount of water lost to the atmosphere through ET decreases in both the near and the far future (Figure 28). This trend follows the decreasing trend in soil moisture (Figure 27) which is consistent with the water-limited nature of southern Arizona.

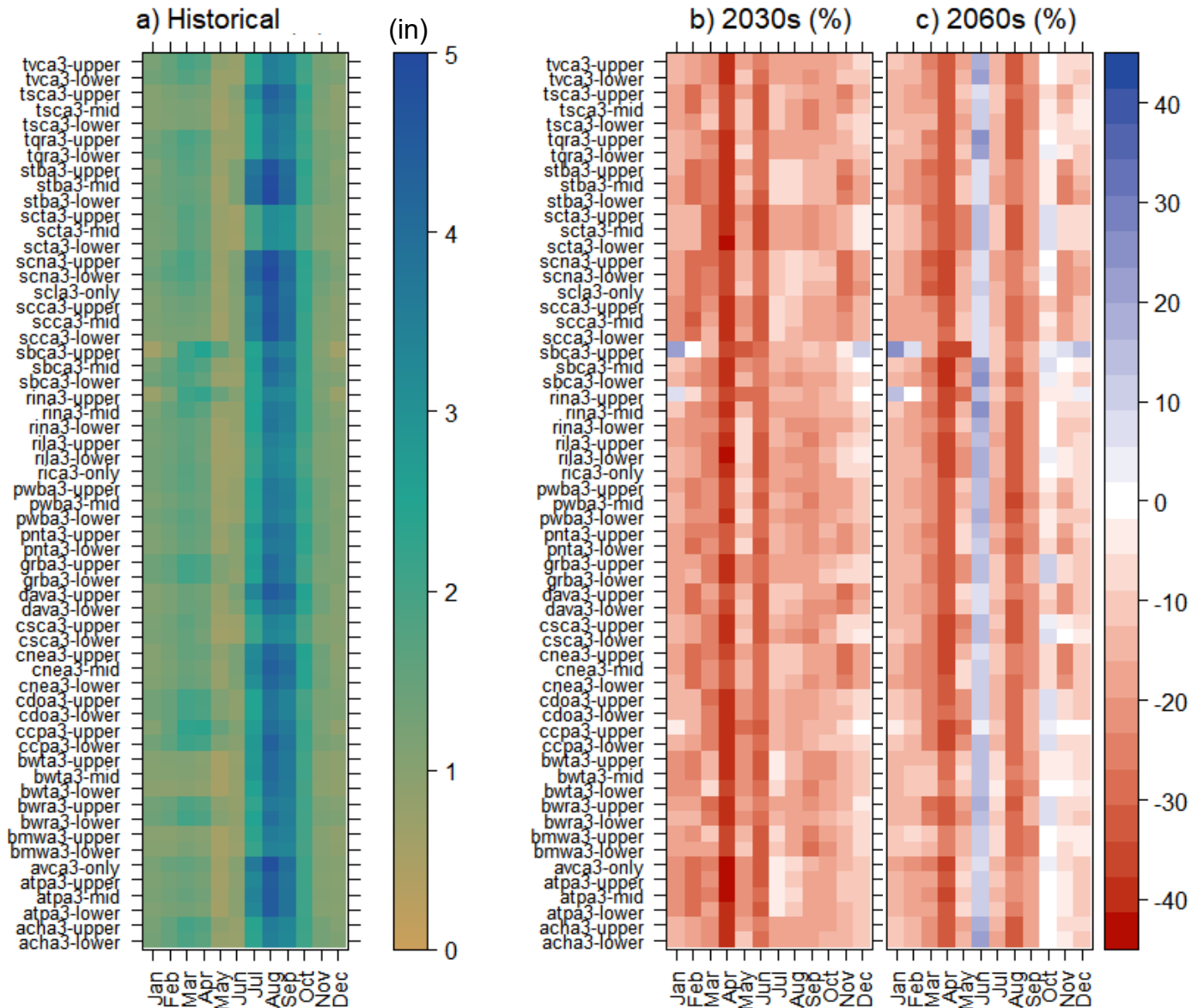


Figure 29 – Evapotranspiration (ET) under the worse-case climate scenario for a) modeled historical ET in inches, b) near future change, and c) far future change in ET as a percentage.

Blue indicates an increase and red indicates a decrease in ET.

5. Summary

This study investigated the potential range of climate and hydrologic changes in the SAC-SMA basins contributing to the Tucson Active Management Area, also referred to as the surface water model boundary area. It specifically examined changes in temperature, precipitation, streamflow, soil moisture and evapotranspiration for two thirty periods: 2020-2049 and 2050-2079. Reclamation and local stakeholders identified a “best-case”, lower emissions scenario (RCP 4.5) and a “worse-” (not “worst”) case emissions scenario (RCP 8.5).

To ensure that the study would fully reflect the impacts of climate change to the semi-arid climate, stakeholders selected a dynamically downscaled climate projection to represent the “worse-case”: the low-resolution Max-Planck-Institute Earth System Model MPI-ESM run downscaled using the Weather Research and Forecasting Model. A corresponding climate model, the medium resolution MPI-ESM-MR Global Climate Model, run with RCP 4.5 and downscaled using the statistical Localized Constructed Analogs (LOCA) method was selected for the “best-case”.

Changes over these thirty-year periods were evaluated for average annual area-wide temperature and precipitation and for the dry, monsoon and winter wet seasons. To reproduce the variability of the southeastern Arizona climate, a seasonal weather generator was used to produce an ensemble of 100 temperature and precipitation time-series for each case and future period.

These ensembles were then used as input to a surface hydrological model (the Sacramento Soil Moisture Accounting Model). This model was selected because it is part of the National Weather Service’s Colorado Basin River Forecast Center’s operational streamflow modeling system. The model available at the time of this study was calibrated over the water years 1971-1999.

This 1970-1999 Sac-SMA calibration set was used to provide a historical reference for model simulations of the same period. To identify projected changes while accounting for model biases, this study compares each simulated future period to a simulation of the period 1970-1999 using the same model configuration and inputs.

5.1. Results

Climate: Precipitation and Temperature by Season

All models and climate scenarios consistently identify increases in temperature through time. Increases are larger under the worse-case scenario, which represents higher future emissions. Seasonally, temperature increases in the monsoon and dry period were larger than in the winter wet season. Otherwise, seasonal temperature increases varied by scenario and time period.

Precipitation changes are more variable than temperature. The best-case provides a scenario with relatively minimal change in seasonal precipitation; in the worse-case scenario, total

precipitation decreases significantly in the monsoon and winter wet seasons. Precipitation also becomes increasingly variable under projected future conditions. Projected changes for the two future periods, relative to the simulated 1970-1999 historical period, are summarized in Table 4 in Section 2.5 as well as the executive summary.

5.1.1. Seasonal Length and Timing

The best-case scenario exhibited a slight advance in the date of monsoon onset, two days for each future period, to July 3 and July 1 for the 2030s and 2060s, respectively. The worse-case scenario does not show a single trend in monsoon onset date for the future periods, with a later median onset date of June 29 in the near future and returning to a median date of June 22 in the far future. This may be related to changes in the distribution of monsoon rainfall, with precipitation events becoming more intermittent, but more extreme, as documented in the historical record by Luong et al. (2017) and DeMaria et al. (2019). The worse-case climate scenario therefore does not provide earlier relief to the dry season, as in the best-case.

The best-case consistently shows a lengthening of the monsoon period and shortening of the winter wet period, but inconsistent changes in the length of the dry period. The worse-case has inconsistent trends over time for the monsoon and dry season, but does show a consistent trend toward a shorter winter season. In general, the worse-case scenario provides a greater range of seasonal lengths from year to year, representing a more variable future.

Extremes in both temperature and precipitation increased into the future. Increases in extreme temperature were consistently largest in the dry and monsoon season, when high heat is most dangerous for human health. Extreme temperatures increase over 7°F under the worse-case scenario in the far future, reflecting the largest change under unchecked emissions through the 2060s and beyond.

5.1.2. Surface Hydrology—Changes in 30-year Median Streamflow by Subbasin, Season, and Time Period

For the best-case monsoon season, a lengthening monsoon season and a slight increase in monsoon precipitation in the 2030s result in generally increasing streamflows for this period. In the 2060s, a slight decrease in monsoon precipitation negates some of these effects. Under the worse-case scenario, a decrease in monsoon rainfall by an average of 2.38 inches leads to decreased streamflow on the order of 20-50% for most of the sub-basins in the near future, but this trend is mostly reversed in the far future.

For the winter wet period, the best-case also predicts increases in streamflow over time. As the length of the winter season is predicted to shorten, this may be due to changes in storm size. The worse-case scenario predicts near future decreases in streamflow that are even more widespread than for the monsoon season, again moderating to some extent in the far future.

Other notable trends include:

- The number of no-flow days per month consistently increases in the worse-case, especially in April, May, and August.
- Soil moisture decreases are most pronounced in the months preceding the dry season, particularly in the worse-case scenario.

Lower Santa Cruz River Basin Study Hydroclimate Analysis

- In both future scenarios, evapotranspiration decreases due to soil moisture limitation despite rising temperatures that drive increases in the potential for evapotranspiration.

5.2. Conclusion

The goal of the Study is to identify where physical water resources are needed to mitigate supply-demand imbalances and to develop a strategy to improve water reliability for the municipal, industrial, agricultural, and environmental sectors. This memorandum delineates a range of potential changes in future temperature, precipitation, streamflow, soil moisture and evapotranspiration rates.

In southern Arizona, where the climate is already highly variable across space and time, the combination of these findings suggests a range of risks to the sustainability of groundwater, infrastructure, and environmental systems. In particular, projected changes may reduce the natural groundwater recharge that supports much of the municipal, industrial, agricultural, and environmental water use within the basin. In addition, alterations in the onset and length of the monsoon and winter wet seasons may require adaptation by water providers to maintain reliable deliveries throughout the year. Also of note are the projected changes in extreme temperature and precipitation and their implications for environmental and human health, as well as public safety and infrastructure investments.

The information and analysis in this report will be used as input to a groundwater model for the study area to identify water supply-demand imbalances for six growth/climate scenarios. The outcomes of these analyses will then be used to develop adaptation strategies for specific local sectors including municipal and industrial water supply, agriculture, and the environment.

6. References

- Burnash, R. J. C., Ferral, R. L., and McGuire, R.A. 1973. A Generalized Streamflow Simulation System—Conceptual Modeling for Digital Computers, U.S. Department of Commerce, National Weather Service and State of California, Department of Water Resources.
- Castro L. C., et al. 2017. Assessing climate change impacts for DoD Installations in the Southwest United States during the warm season. A Final Report to Strategic Environmental Research and Development Program (SERDP) Project Number RC-2205, 128pp.
- Chang , H. I. 2018. Dynamically Downscaled Climate Projections in the Lower Santa Cruz Basin Study. Final Report R17AC00061.
- Crimmins, M. 2018. Personal Communication from Michael Crimmins, Climate Science Extension Specialist, the University of Arizona, email.
- Demaria, E. M., Hazenberg, P., Scott, R. L., Meles, M. B., Nichols, M., and Goodrich, D. 2019. Intensification of the North American Monsoon rainfall as observed from a long-term high-density gauge network. *Geophys. Res. Lett.*, 46(12), 6839-6847.
- Ellis, A. W., Saffell, E. M., Hawkins, T. W., 2004. A method for defining monsoon onset and demise in the southwestern USA. *International Journal of Climatology: A Journal of the Royal Meteorological Society*, 24(2), 247-265.
- Gangopadhyay, S., Bearup L. A., Verdin, A., Pruitt, T., Halper, E., and Shamir, E., 2019. A collaborative stochastic weather generator for climate impacts assessment in the Lower Santa Cruz River Basin, Arizona. Abstract GC41G-1267 presented at 2019 Fall Meeting, AGU, San Francisco, CA, 9-13 Dec.
- Giorgetta, M. A., et al. 2013. Climate and carbon cycle changes from 1850 to 2100 in MPI-ESM simulations for the Coupled Model Intercomparison Project phase 5. *J. Adv Model Earth*, 5(3), 572-597.
- Hamon, W. R., 1963. Computation of direct runoff amounts from storm rainfall. *International Association of Scientific Hydrology Publication*, 63, 52-62.
- IPCC, 2014. *Climate Change 2014: Synthesis Report. Contribution of Working Groups I, II and III to the Fifth Assessment Report of the Intergovernmental Panel on Climate Change.* Core Writing Team, R.K. Pachauri and L.A. Meyer (eds.). IPCC, Geneva, Switzerland, 151 pp.

Lower Santa Cruz River Basin Study Hydroclimate Analysis

- Livneh, B., Bohn, T. J., Pierce, D. W., Munoz-Arriola, F., Nijssen, B., Vose, R., Cayan, D. R., and Brekke, L., 2015: A spatially comprehensive, hydrometeorological data set for Mexico, the U.S., and Southern Canada 1950-2013. *Scientific Data*, v. 2, article 150042.
- Luong, T. M., Castro, C. L., Chang, H. I., Lahmers, T., Adams, D. K., and Ochoa-Moya, C. A. 2017. The more extreme nature of North American monsoon precipitation in the southwestern United States as revealed by a historical climatology of simulated severe weather events. *J. Appl. Meteorol. Climatol*, 56(9), 2509-2529.
- Maurer, E. P., Brekke, L., Pruitt, T., and Duffy, P. B., 2007. Fine-resolution climate projections enhance regional climate change impact studies, *Eos Trans. AGU*, 88(47), 504.
- Meixner, T., et al., 2016. Implications of projected climate change for groundwater recharge in the western United States. *J. Hydrol*, 534, 124-138.
- Moss, R., Edmonds, J., Hibbard, K. et al, 2010. The next generation of scenarios for climate change research and assessment. *Nature* 463, 747–756.
- Mukherjee, R. 2016. Implications of statistical and dynamical downscaling methods on streamflow projections for the Colorado River Basin. University of Arizona Master's Thesis. Available at: https://repository.arizona.edu/bitstream/handle/10150/620708/azu_etd_14736_sip1_m.pdf?sequence=1.
- NOAA, 2020. Climate website. <https://www.climate.gov/maps-data/primer/climate-forcing>. Accessed 11/11/2020.
- Payne, J.T., Wood, A.W., Hamlet, A.F., Palmer, R.N., and Lettenmaier, D.P., 2004. Mitigating the effects of climate change on the water resources of the Columbia River basin. *Clim. Change*, 62(1.3):233.256.
- Pierce, D. W., Cayan, D. R., and Thrasher, B. L. 2014. Statistical downscaling using localized constructed analogs (LOCA). *J. Hydrometeorol*, 15(6), 2558-2585.
- Prein, A. F., Bukovsky, M. S., Mearns, L. O., Bruyère, C., and Done, J. M. 2019. Simulating North American Weather Types with Regional Climate Models. *Front. Environ. Sci.*, 7, 36.
- PRISM Climate Group, 2018. Oregon State University, <http://prism.oregonstate.edu>, created 4 Feb 2004. Data retrieved 2018.
- Reclamation. 2011. SECURE Water Act, Section 9503(c) Reclamation Climate Change and Water 2011. Report to Congress.
- _____. 2012. Colorado River Basin Water Supply and Demand Study: Study Report. December 2012, 95 pp. <https://www.usbr.gov/lc/region/programs/crbstudy.html>.
- _____. 2015. West-Wide Climate Risk Assessments: Irrigation Demand and Reservoir Evaporation Projections. Technical Memorandum No. 86-68210-2014-01.

- Riahi, K., 2011. RCP 8.5—A scenario of comparatively high greenhouse gas emissions. *Clim. Change*, 109, 33-57.
- Shamir, E and Halper, E., 2019. Estimating climatic change impacts on water resources in arid environments: the role of downscaling methodology, Research and Development Office, Science and Technology Program, Final Report ST-2019-9039-01. March 2019
- Shamir, E., Halper, E., Modrick, T., Georgakakos, K. P., Chang, H. I., Lahmers, T. M., and Castro, C. 2019. Statistical and dynamical downscaling impact on projected hydrologic assessment in arid environment: A case study from Bill Williams River basin and Alamo Lake, Arizona. *J. Hydrol X*, 2, 100019.
- Taylor, K. E., Stouffer, R. J., and G. A. Meehl. 2012. An Overview of CMIP5 and the experiment design. *Bull. Amer. Meteor. Soc.*, 93, 485-498.
- Thomson, A. M., et al. 2011. RCP4.5: a pathway for stabilization of radiative forcing by 2100. *Clim Change* 109:77-94.
- Thrasher, B., Maurer, E. P., McKellar, C., and Duffy, P. B. 2012. Technical Note: Bias correcting climate model simulated daily temperature extremes with quantile mapping, *Hydrol. Earth Syst. Sci.*, 16, 3309-3314.
- Udall, B. and Overpeck, J., 2017. The twenty-first century Colorado River hot drought and implications for the future. *Water Resour. Res.*, 53(3), 2404-2418.
- USAID, 2014. A review of downscaling methods for climate change projections. September 2014. African and Latin American Resilience to Climate Change Project. Prepared by Sylwia Trzaska and Emilie Schnarr, Center for International Earth Science Information Network. http://www.ciesin.org/documents/Downscaling_CLEARED_000.pdf.

Appendix A—Supporting Climate Figures

Combined time series and box plots of the best-case (left) and worse-case (right) climate scenario precipitation (Figure A1) and temperature (Figure A2), used as input to the weather generator. Bold timeseries lines are basin averages while the gray lines are subbasin values of seasonal totals (for precipitation) or averages (for temperature). Boxplots (located within the violin plots to the right of the time-series') are basin-averages with the whiskers representing the 5th/95th percentile of daily values and the remaining values indicated as points. The violin plots are subbasin values with the shaded area extending to the maximum and minimum daily values. Daily precipitation boxplots are for rainy days only, defined as precipitation values greater than 0.01 in/day.

Figure A3 depicts the annual total precipitation (top) and average temperature (bottom) for the three climate scenarios across three periods. Note the effects of bias correction in annual temperatures, which aligns the historical temperatures from the three scenarios.

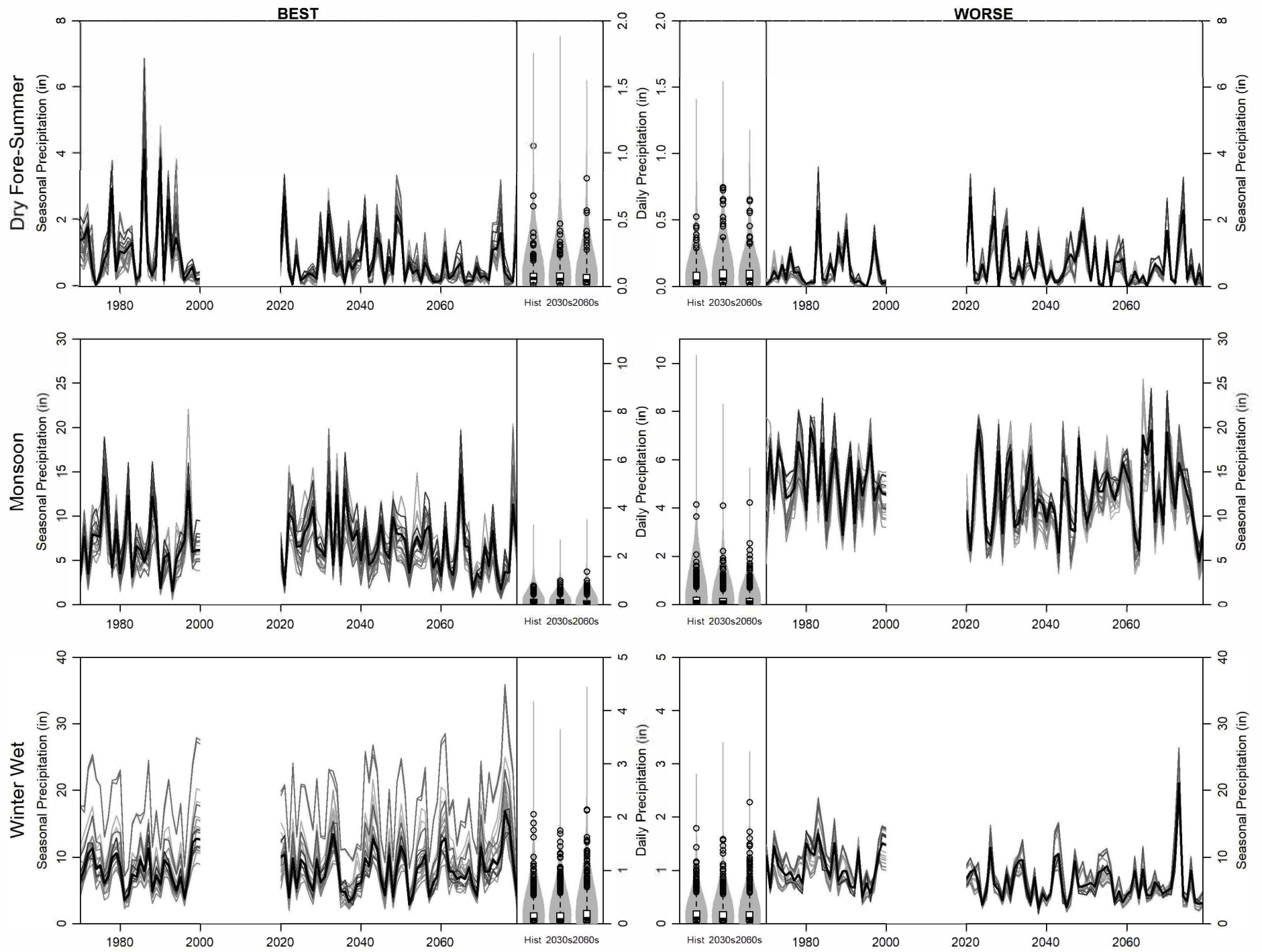


Figure A1 - Combined plot of climate scenario precipitation.

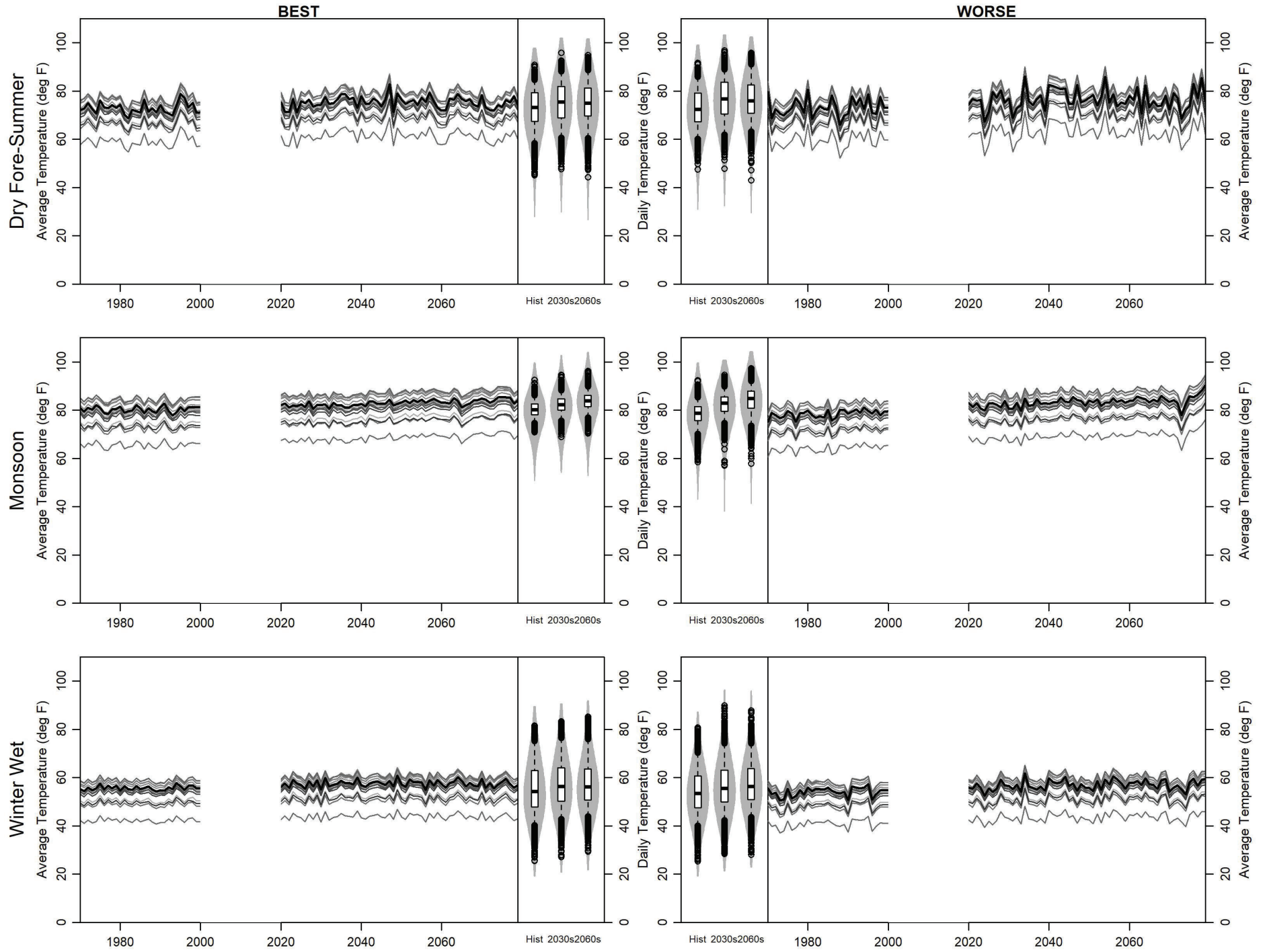


Figure A2 - Combined plot of climate scenario temperature.

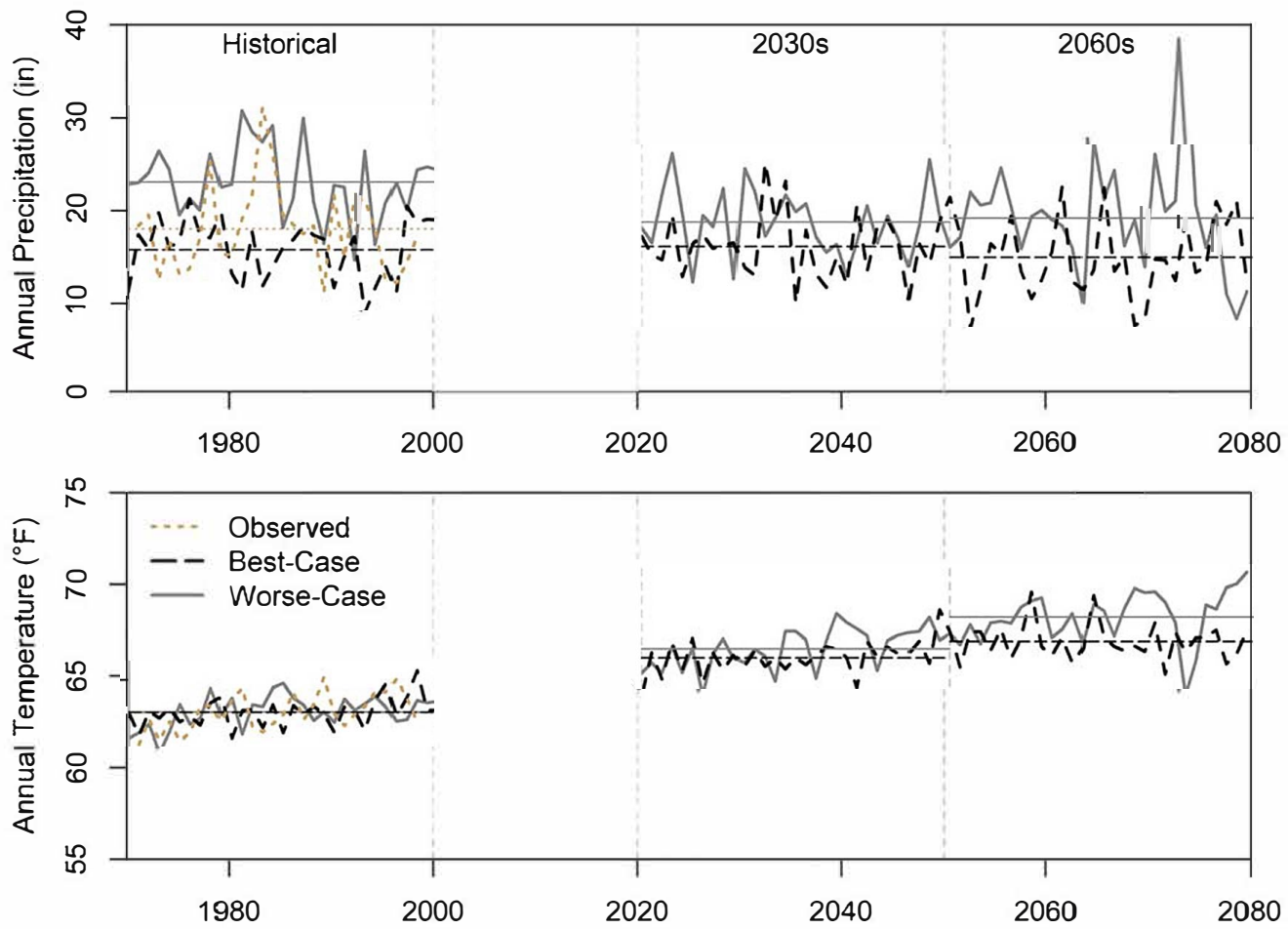


Figure A3 - Annual total precipitation (top) and average temperature (bottom) for the three climate scenarios across three periods.

Appendix B—Weather Generator Validation Figures

Statistics of basin-averaged weather generator outputs relative to inputs (or the training dataset).

Figure B1 – Validation of daily statistics of weather generator-derived precipitation.

Figure B2 – Validation of daily statistics of weather generator-derived temperature.

Figure B3 – Validation of monthly statistics of weather generator-derived dry spell length. Red lines are the statistics of the inputs dataset while the boxplots represent statistics from the weather generated ensemble. Month 1 is January.

Figure B4 – Validation of monthly statistics of weather generator-derived precipitation. Red lines are the statistics of the inputs dataset while the boxplots represent statistics from the weather generated ensemble. Month 1 is January.

Figure B5 – Validation of monthly statistics of weather generator-derived temperature. Red lines are the statistics of the inputs dataset while the boxplots represent statistics from the weather generated ensemble. Month 1 is January.

Figure B6 – Validation of seasonal statistics of weather generator-derived precipitation. Red lines are the statistics of the inputs dataset while the boxplots represent statistics from the weather generated ensemble. Season 1 is the dry season, 2 is the monsoon season, and 3 is the winter.

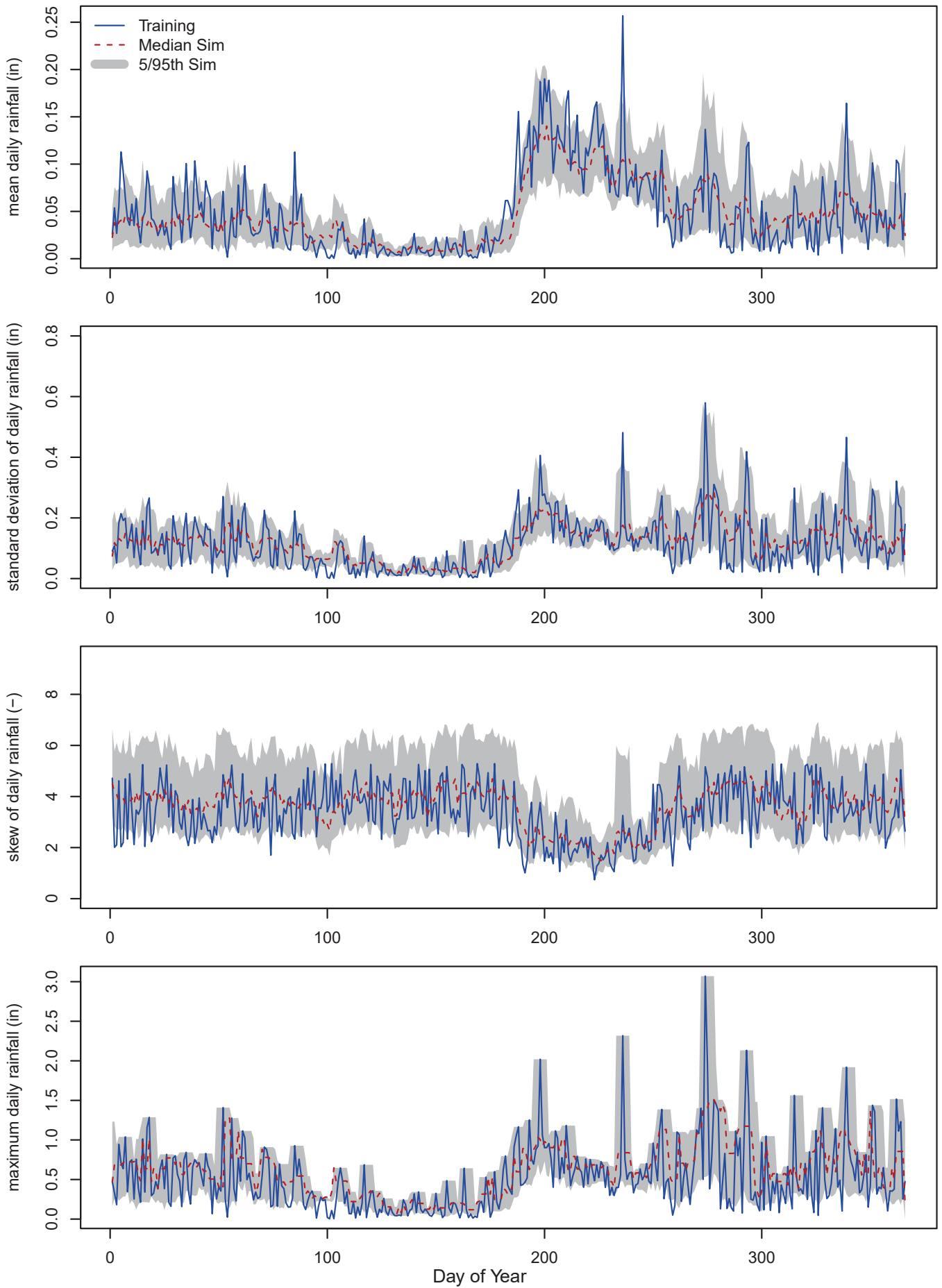


Figure B1 - Validation of daily statistics of weather generator-derived precipitation.

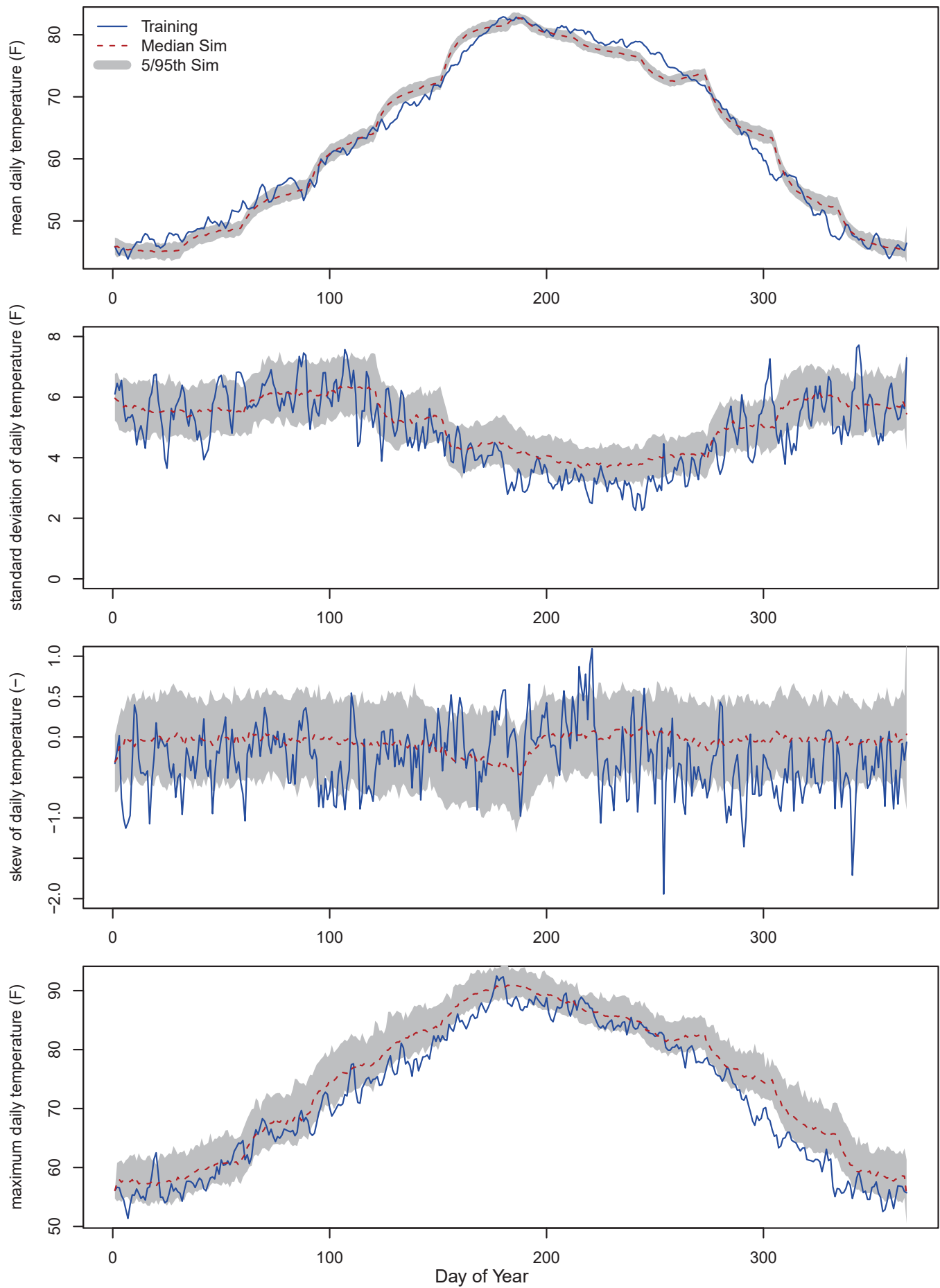


Figure B2 - Validation of daily statistics of weather generator-derived temperature.

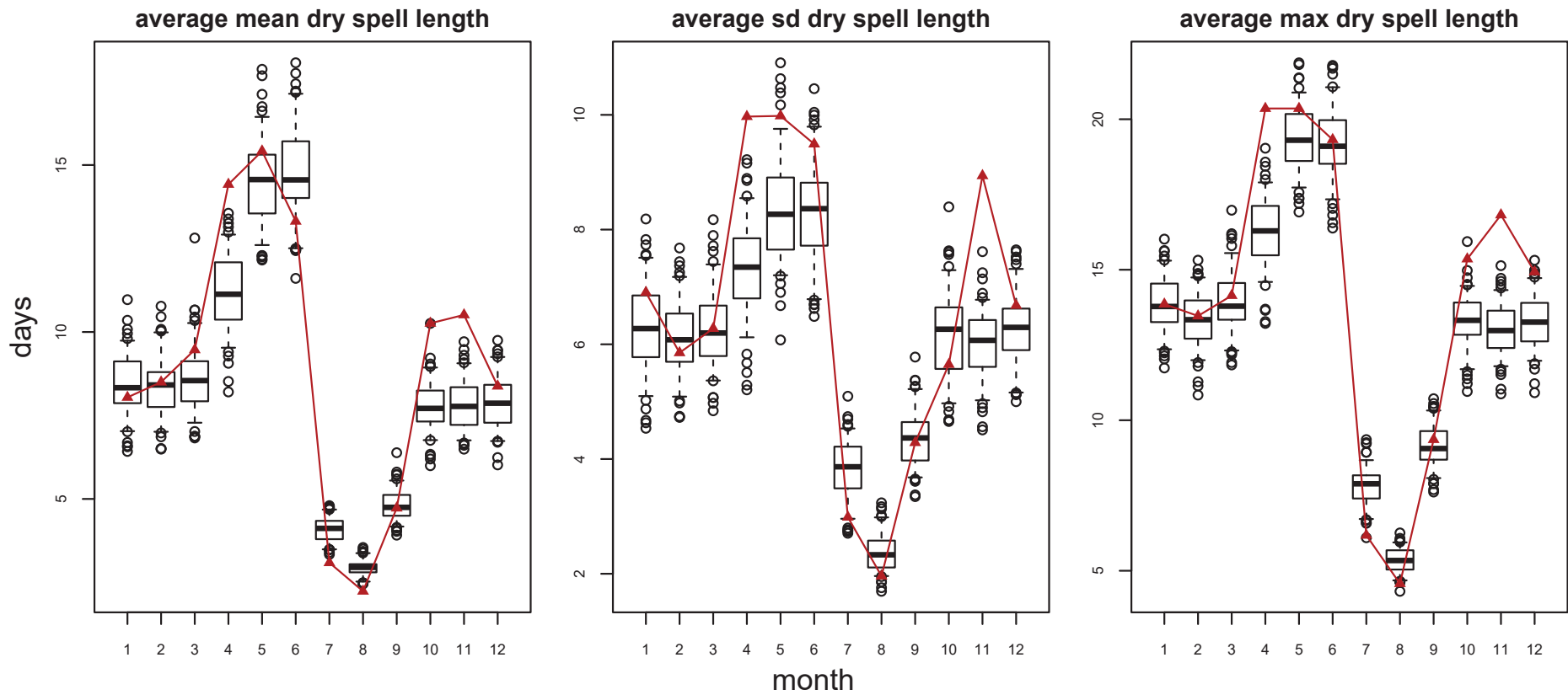


Figure B3 - Validation of monthly statistics of weather generator-derived dry spell length. Redlines are the statistics of the inputs dataset while the boxplots represent statistics from the weather generated ensemble. Month 1 is January.

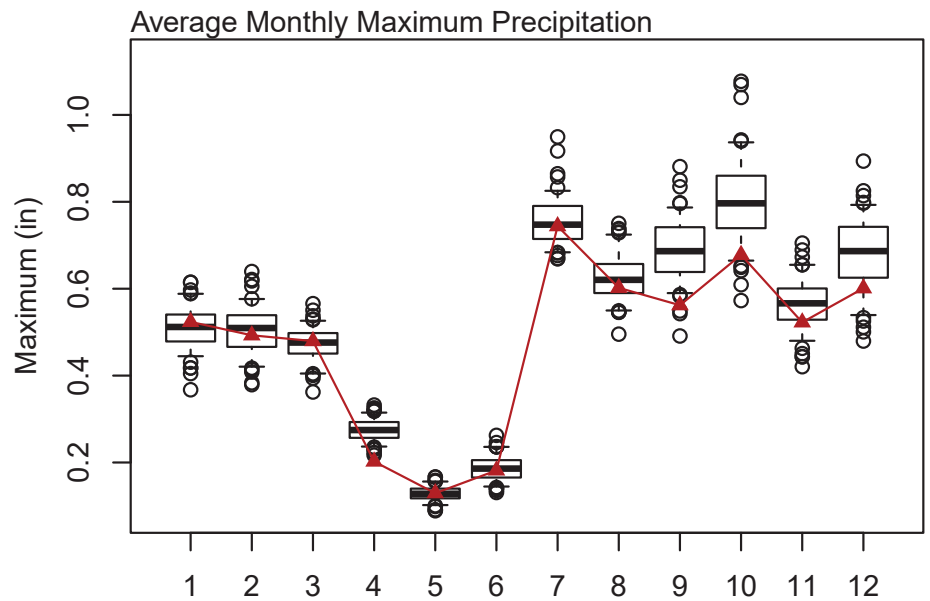
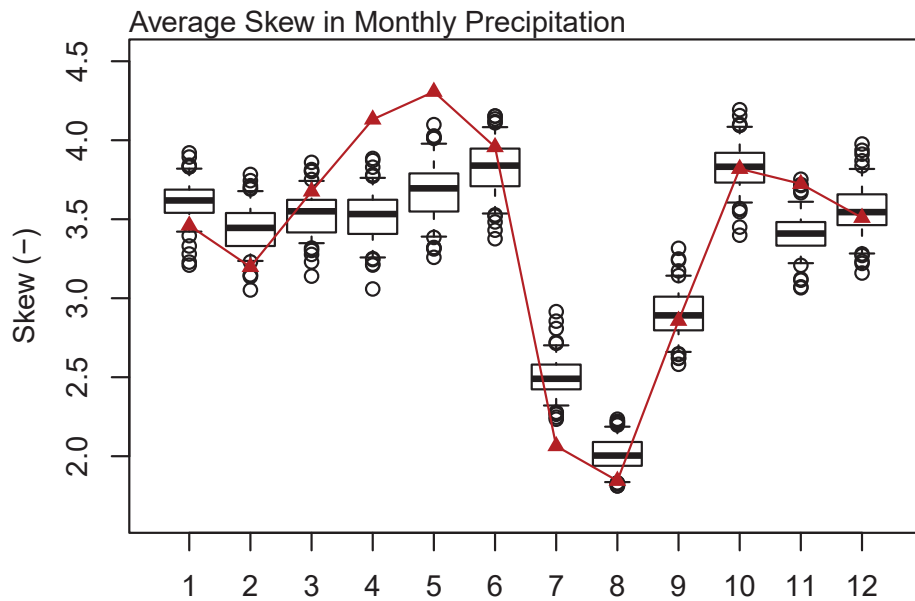
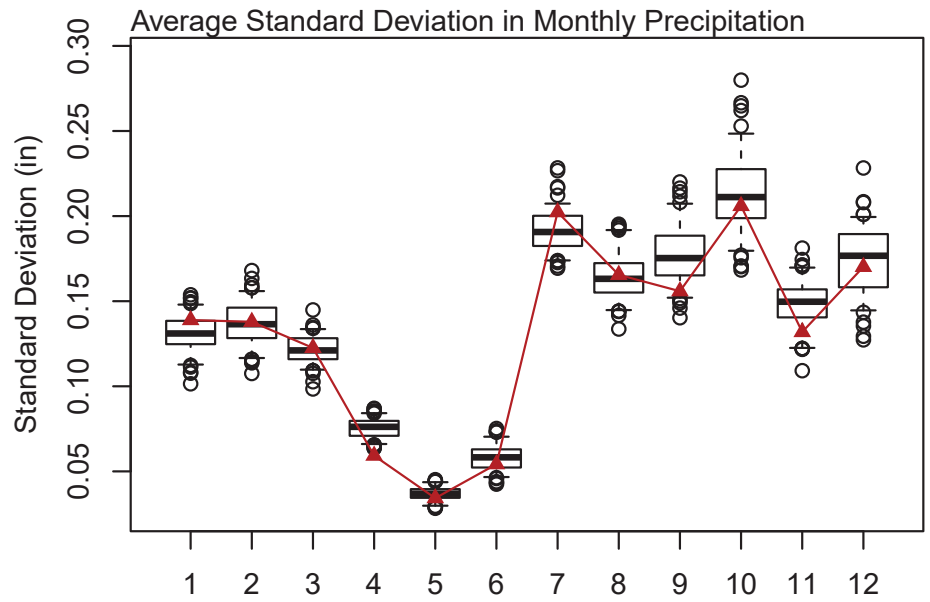
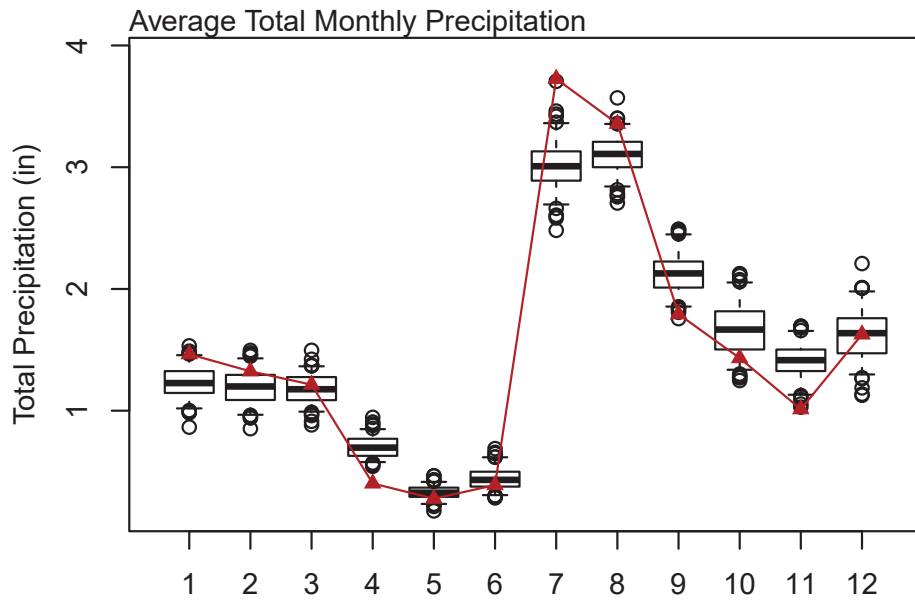


Figure B4 - Validation of monthly statistics of weather generator-derived precipitation. Redlines are the statistics of the inputs dataset while the boxplots represent statistics from the weather generated ensemble. Month 1 is January.

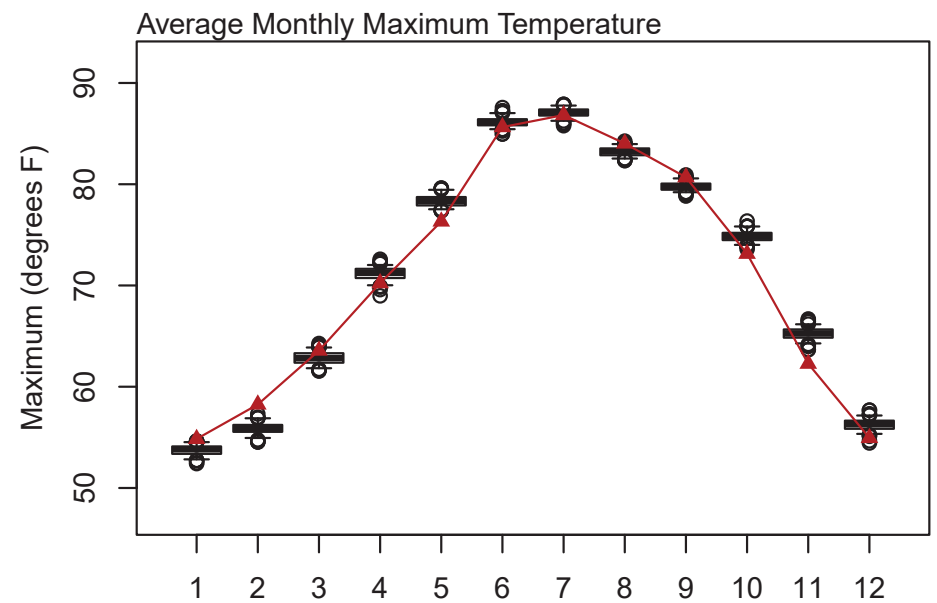
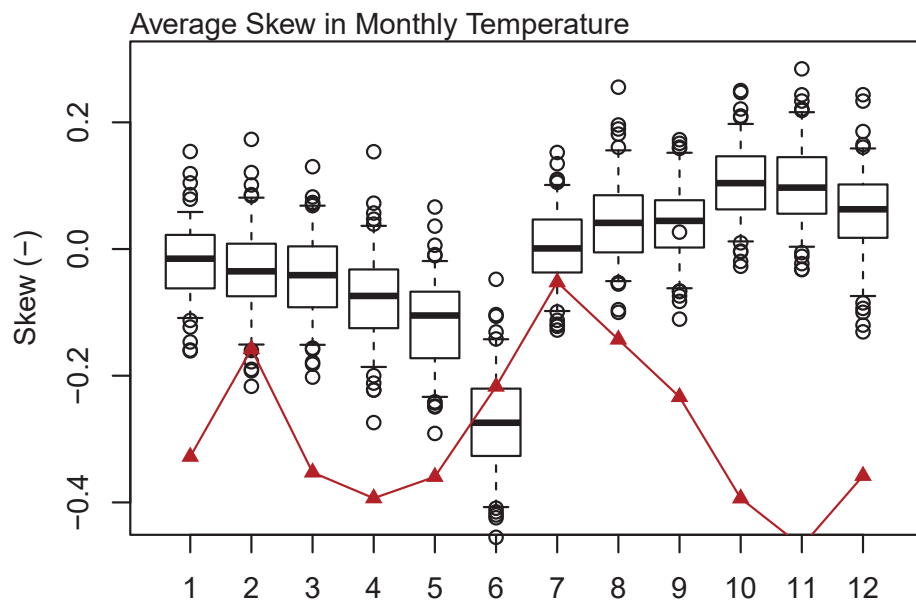
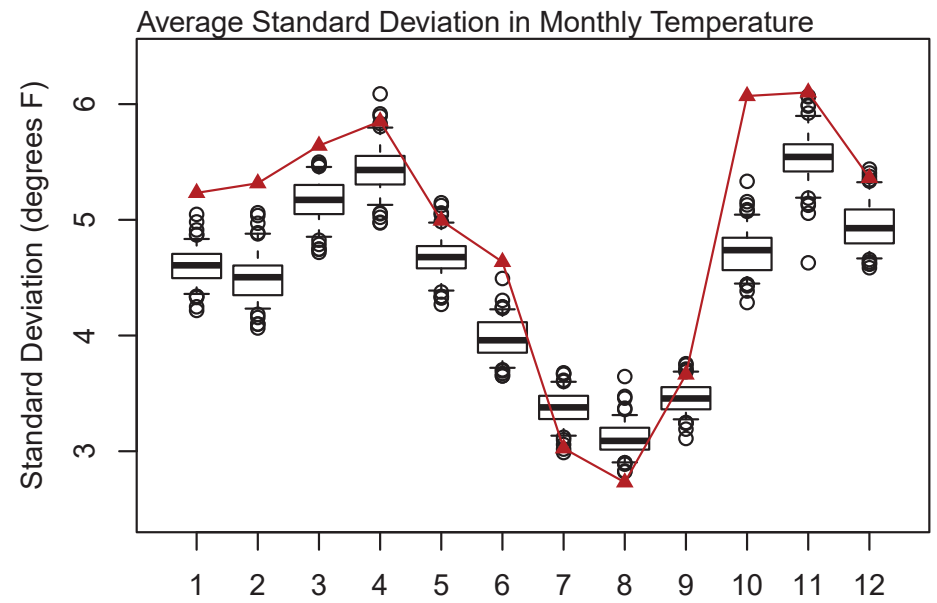
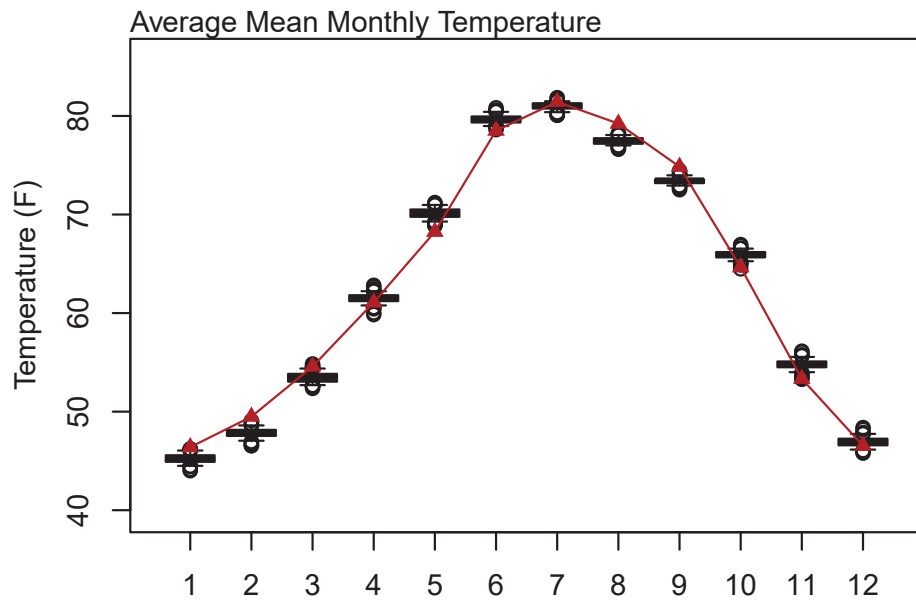


Figure B5 - Validation of monthly statistics of weather generator-derived temperature. Redlines are the statistics of the inputs dataset while the boxplots represent statistics from the weather generated ensemble. Month 1 is January.

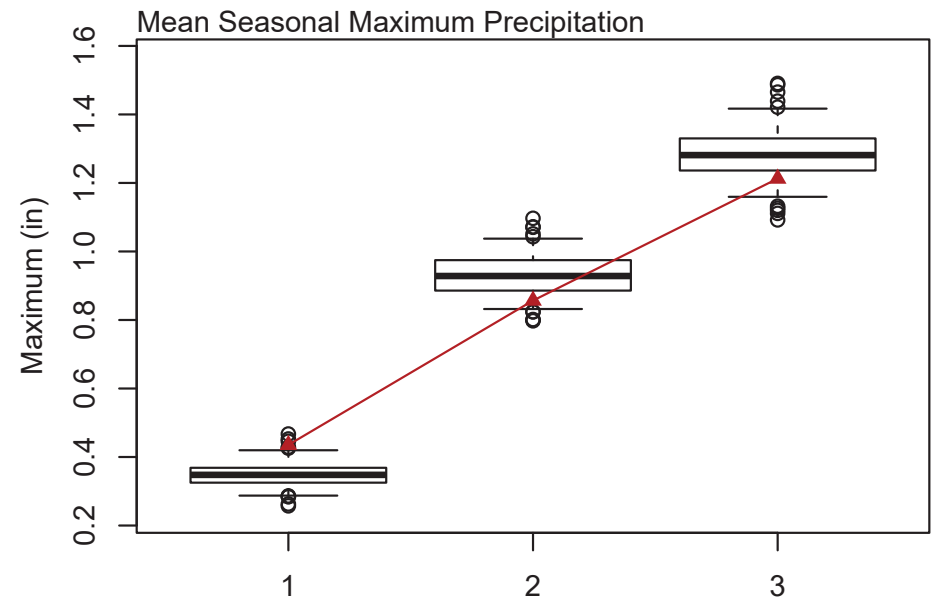
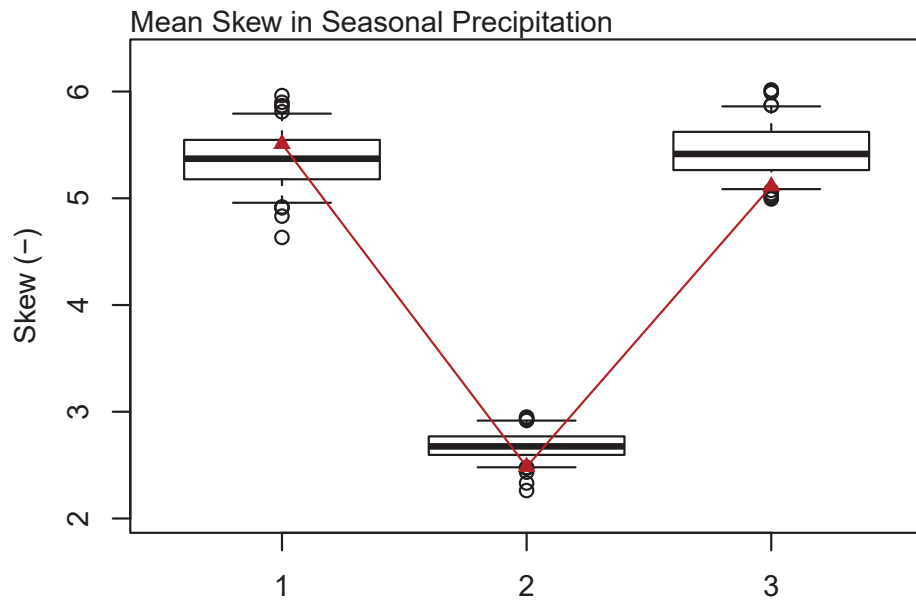
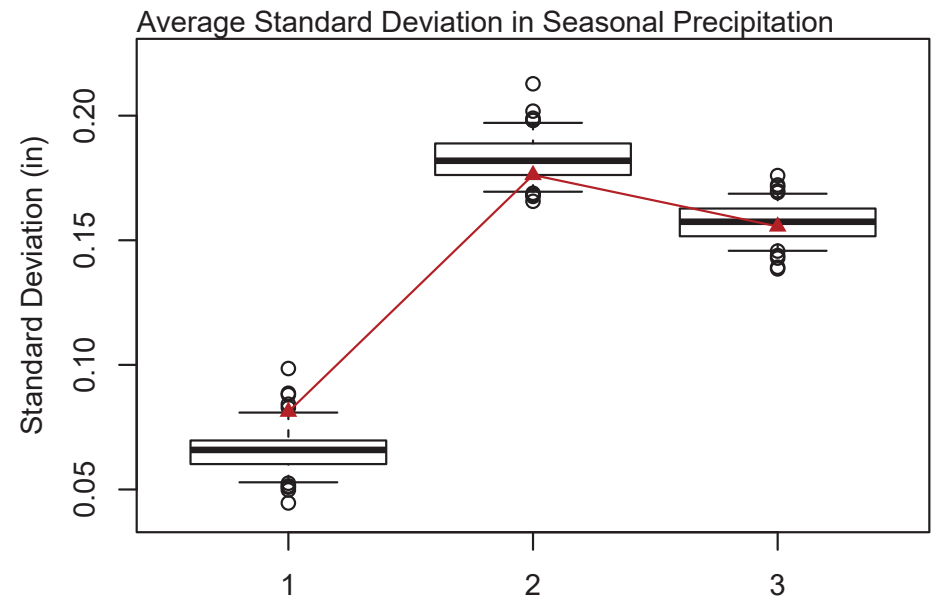
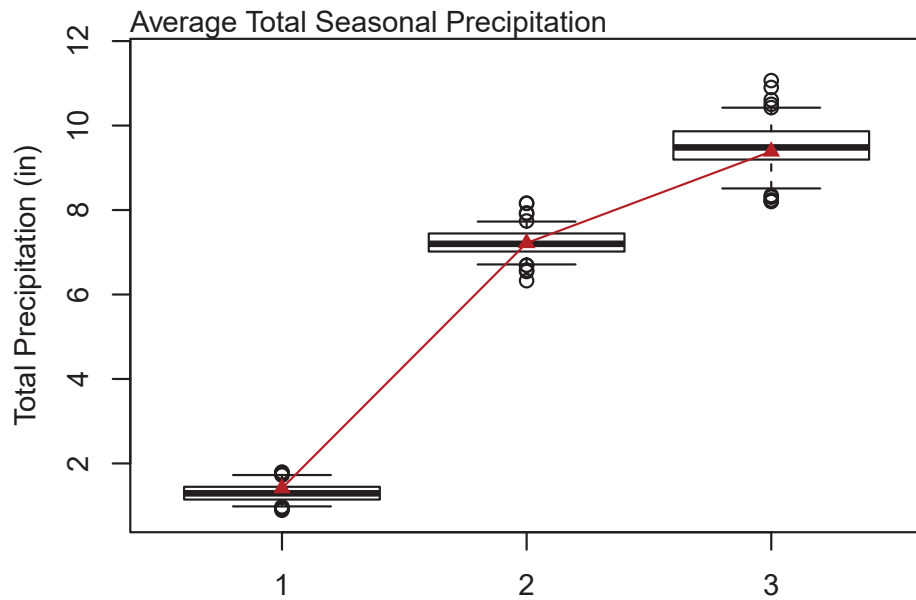


Figure B6 - Validation of seasonal statistics of weather generator-derived precipitation. Redlines are the statistics of the inputs dataset while the boxplots represent statistics from the weather generated ensemble. Season 1 is the dry season, 2 is the monsoon season, and 3 is the winter.

Appendix C—Supporting Surface Water Modeling Figures

Additional figures of surface water modeling outputs for the best-case scenario.

Figure C1 – Best-case scenario model results for each Sac-SMA subbasin, including a) modeled historical dry days per month where tan colors indicate months when the stream is dry the entire month and dark blue represents streams that flow the whole month and change in the number of dry days per month in the b) near future and c) far future.

Figure C2 – Best-case scenario soil moisture (inches) in each compartment of the Sac-SMA Lower Cienega Creek elevation zone. Tan boxes are modeled historical distributions spanning the range of uncertainty from the weather generator simulations, white is near future, and gray is far future. Compartments include two in the upper layer (tension water and free water) and three in the deeper lower layer (tension water, and fast and slow draining free water).

Figure C3 – Ensemble median, monthly average of the total tension water (sum of upper and lower soil zones) under the best-case climate scenario for a) modeled historical tension water in inches and b) near future change and c) far future change as a percent relative to the historical period. For soil moisture change, blue indicates an increase and red indicates a decrease. Results presented for each elevation zone.

Figure C4 – Evapotranspiration (ET) under the best-case climate scenario for a) modeled historical ET in inches, b) near future change and c) far future change in ET as a percent. Blue indicates an increase and red indicates a decrease in ET.

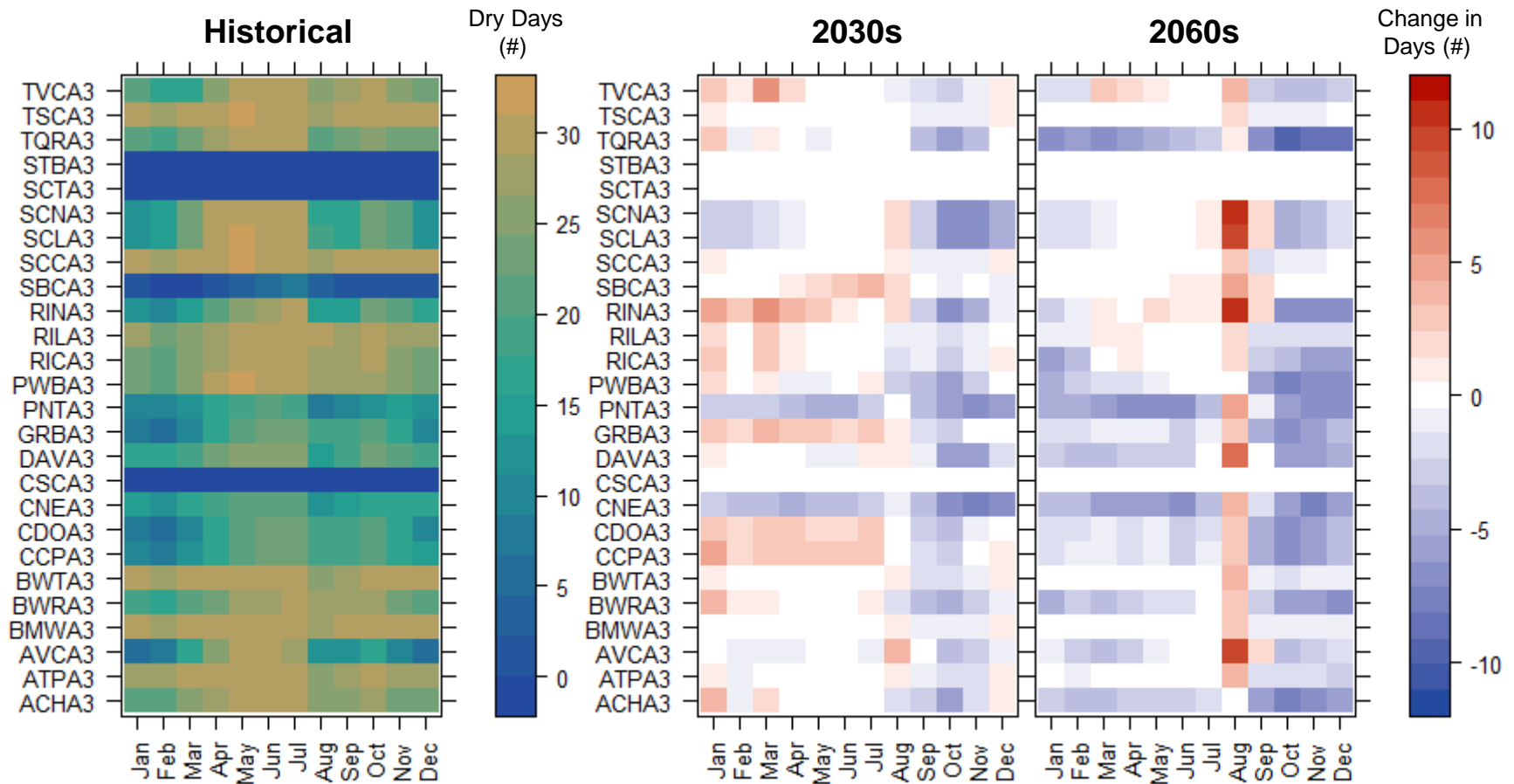


Figure C1 – Best-case scenario model results for each Sac-SMA subbasin, including a) historical dry days per month where tan colors indicate months when the stream is dry the entire month and dark blue represents streams that flow the whole month and change in the number of dry days per month in the b) near future and c) far future.

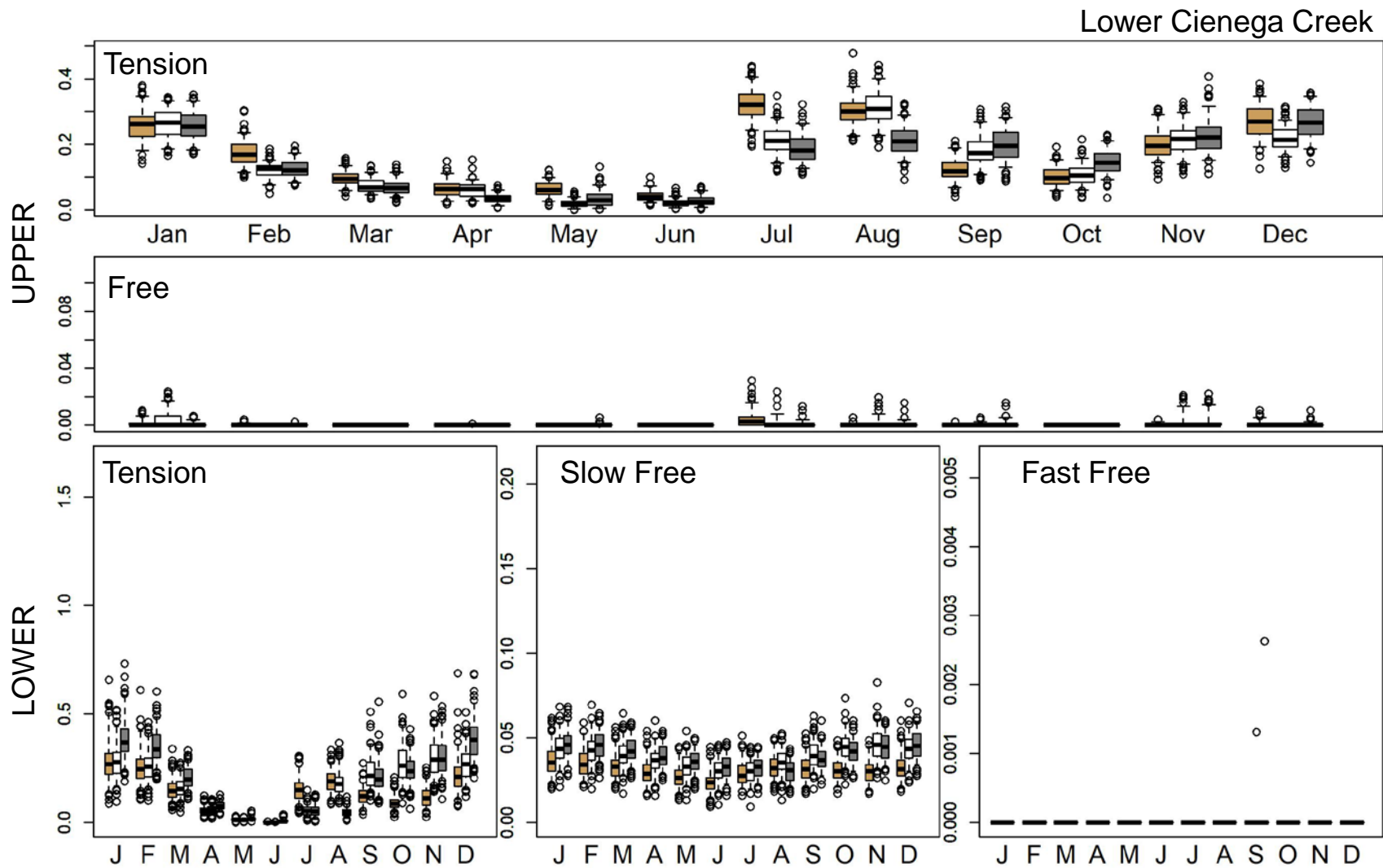


Figure C2 - Best-case scenario soil moisture (in) in each compartment of the Sac-SMA Lower Cienega Creek elevation zone. Tan boxes are historical distributions spanning the range of uncertainty from the weather generator simulations, white is near future, and gray is far future. Compartments include two in the upper layer (tension water and free water) and three in the deeper lower layer (tension water, and fast and slow draining free water).

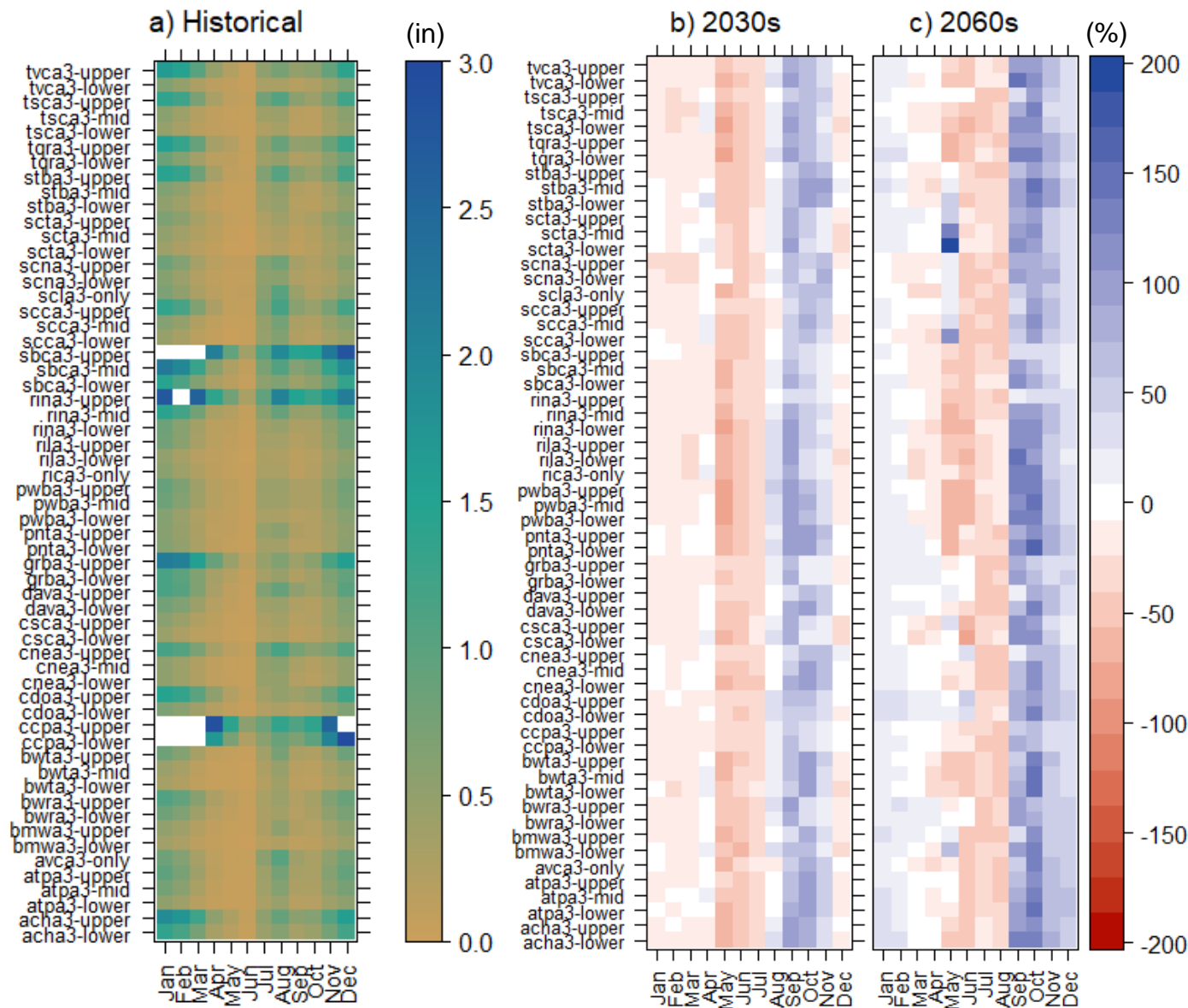


Figure C3 - Ensemble median, monthly average of the total tension water (sum of upper and lower soil zones) under the best-case climate scenario for a) modeled historical tension water in inches and b) near future change and c) far future change as a percent relative to the historical period. For historical results, white values indicate total tension water that exceeds 3 in with a maximum of 5.7 in. For soil moisture change, blue indicates an increase and red indicates a decrease. Results presented for each elevation zone.

